Supplementary Information

Influence of counterion on the formation of supramolecular ruthenium, rhodium and iridium complexes containing pyridyl thioamide derivatives and their reactions with azide: Antioxidants and antimicrobial studies

Lincoln Dkhar[a], Hrishikesh Gupta[b], Krishna Mohan Poluri [b], Paige M Gannon[c], Werner Kaminsky[c], Mohan Rao Kollipara[a]*

[a]Centre for Advanced Studies in Chemistry, North-Eastern Hill University, Shillong 793 022, India

[b]Department of Biosciences and Bioengineering, Indian Institute of Technology Roorkee, Roorkee 247 667, India

[c]Department of Chemistry, University of Washington, Seattle, WA 98195, USA

E mail: mohanrao59@gmail.com

Contents: -

Table S5: Selected bond lengths (Å) and bond angles (°) of binuclear complexes

Table S6: Antibacterial activity (Agar well) of tested compounds

Table S7: DPPH radical scavenging activity of tested compounds

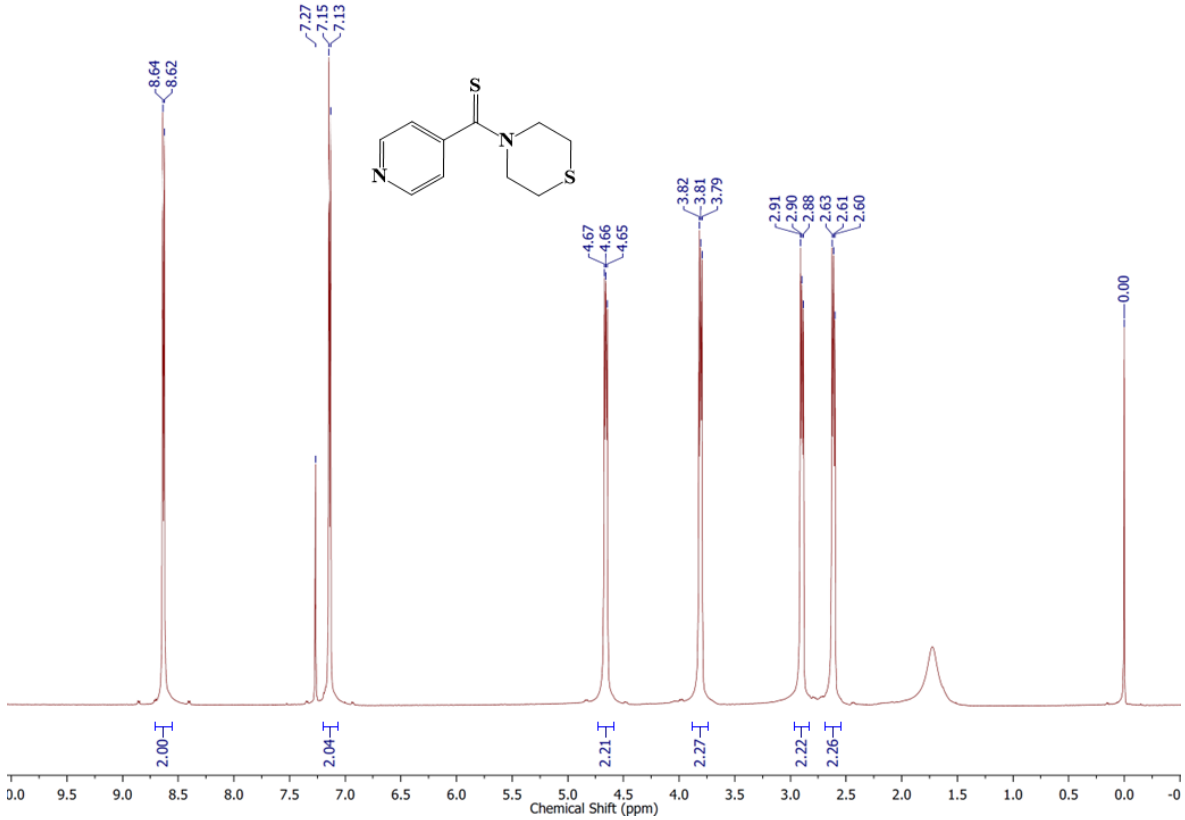

Figure S1: ^{1}H NMR spectrum of Ligand (**L3**) in CDCl3

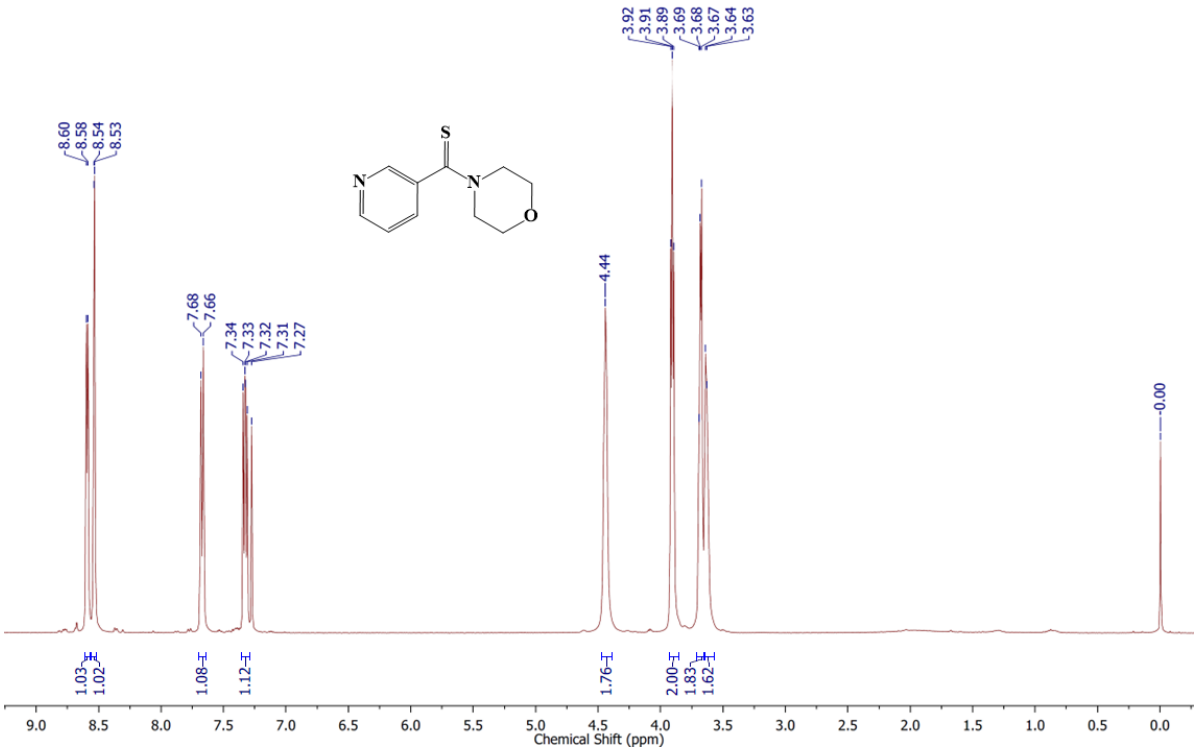

Figure S2: ^{1}H NMR spectrum of Ligand (**L5**) in CDCl3

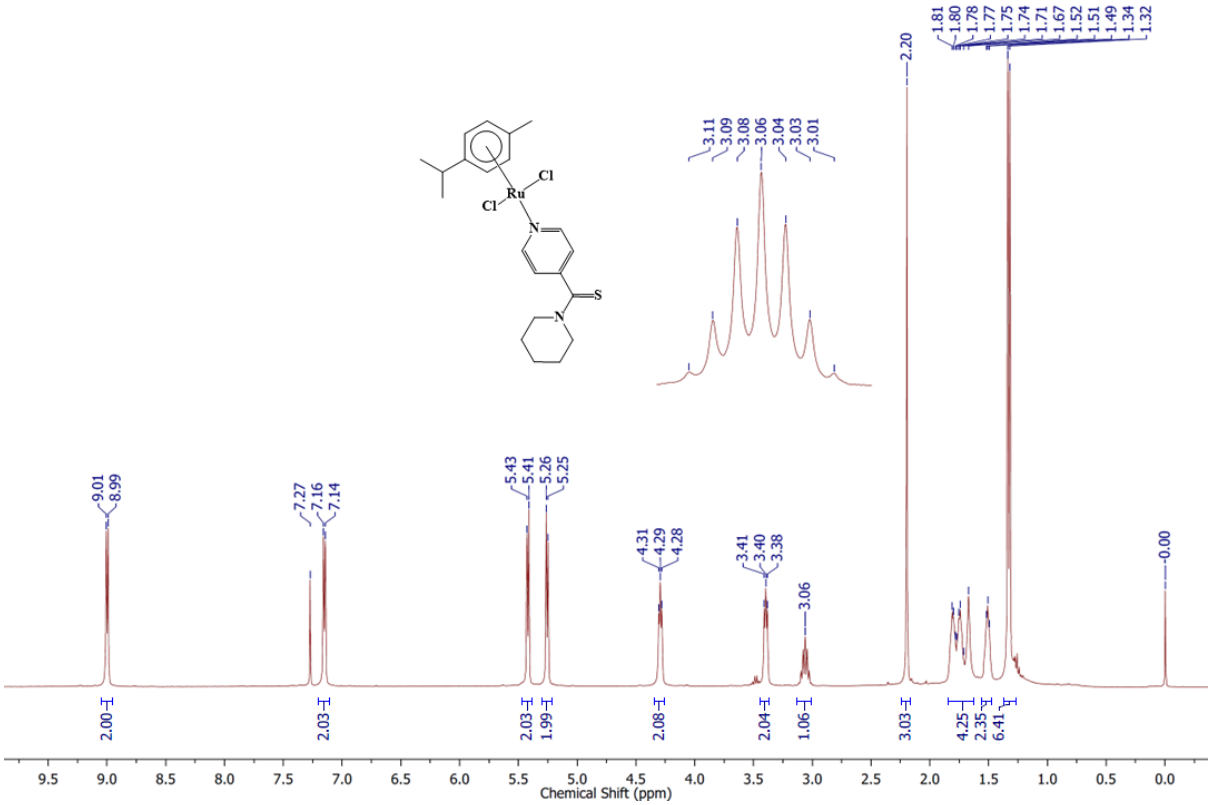

Figure S3: ^{1}H NMR spectrum of complex (**1**) in CDCl3

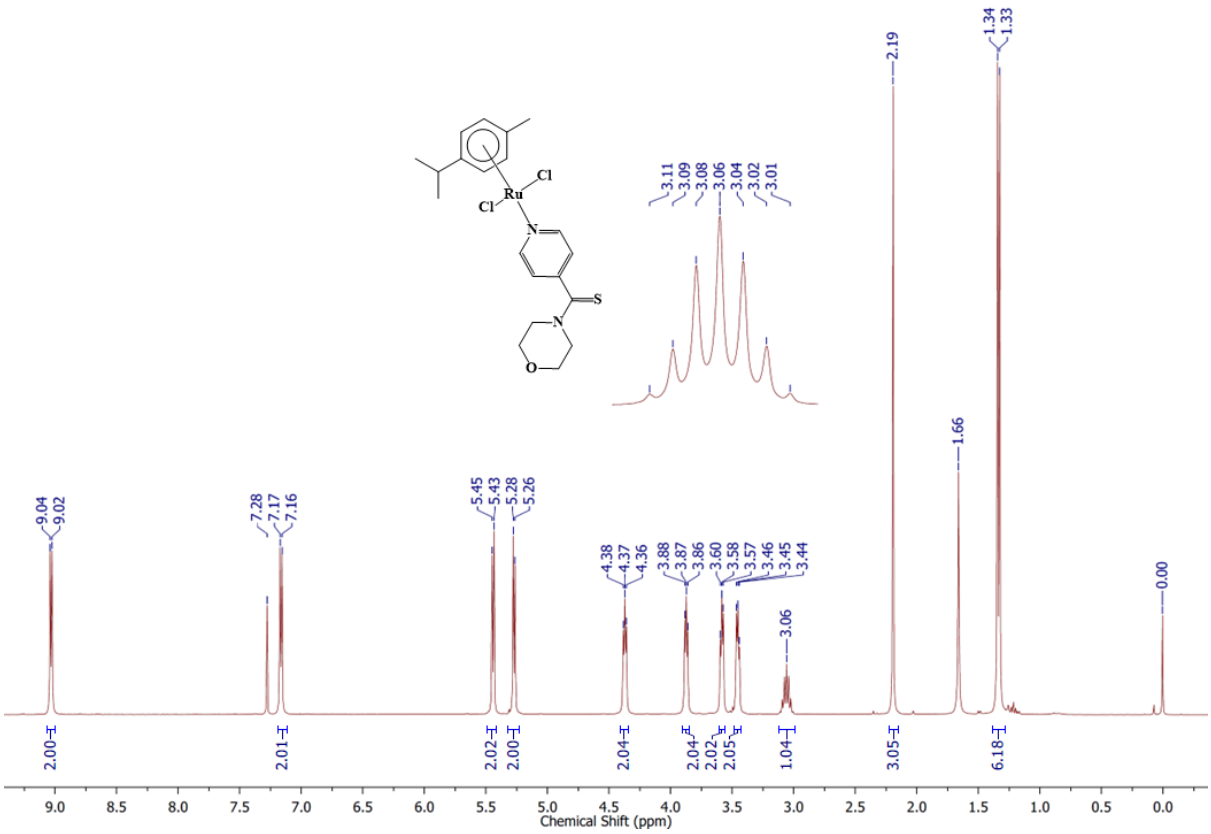

Figure S4: ^{1}H NMR spectrum of complex (**2**) in CDCl3

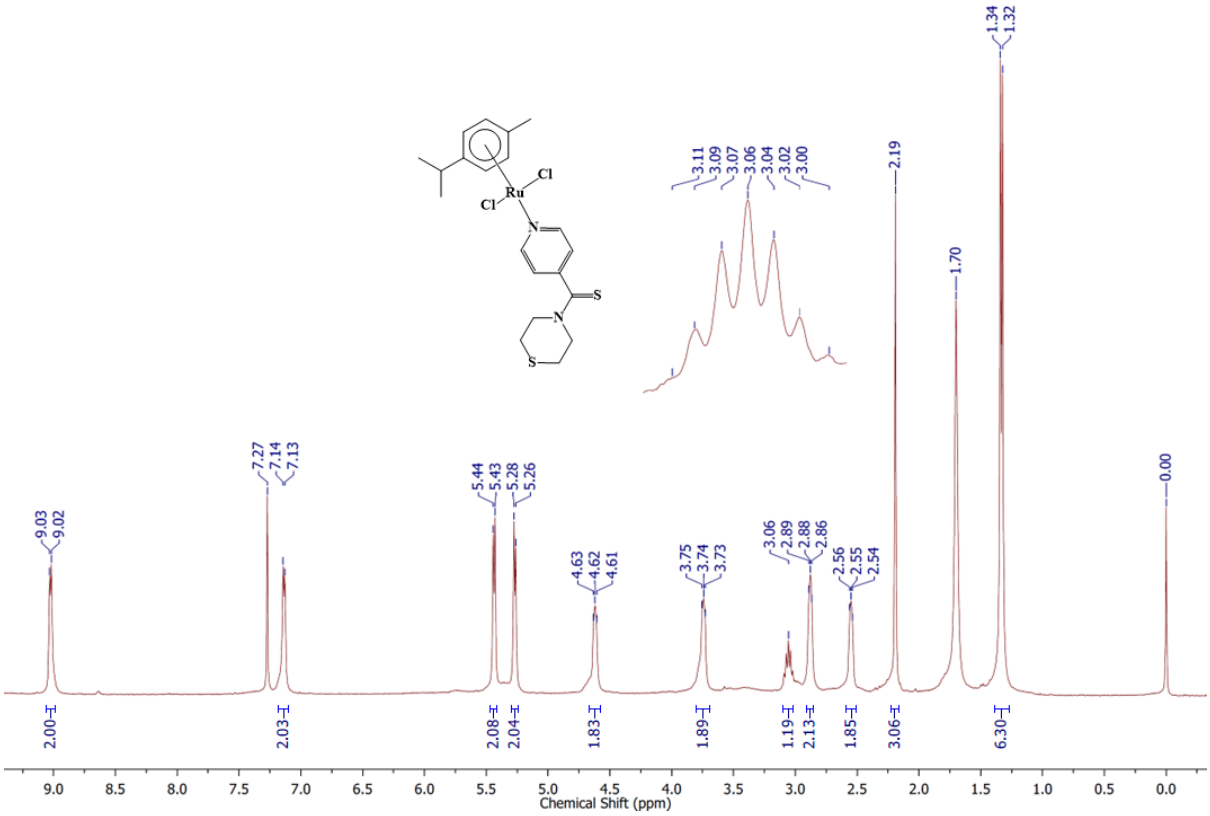

Figure S5: ^{1}H NMR spectrum of complex (**3**) in CDCl3

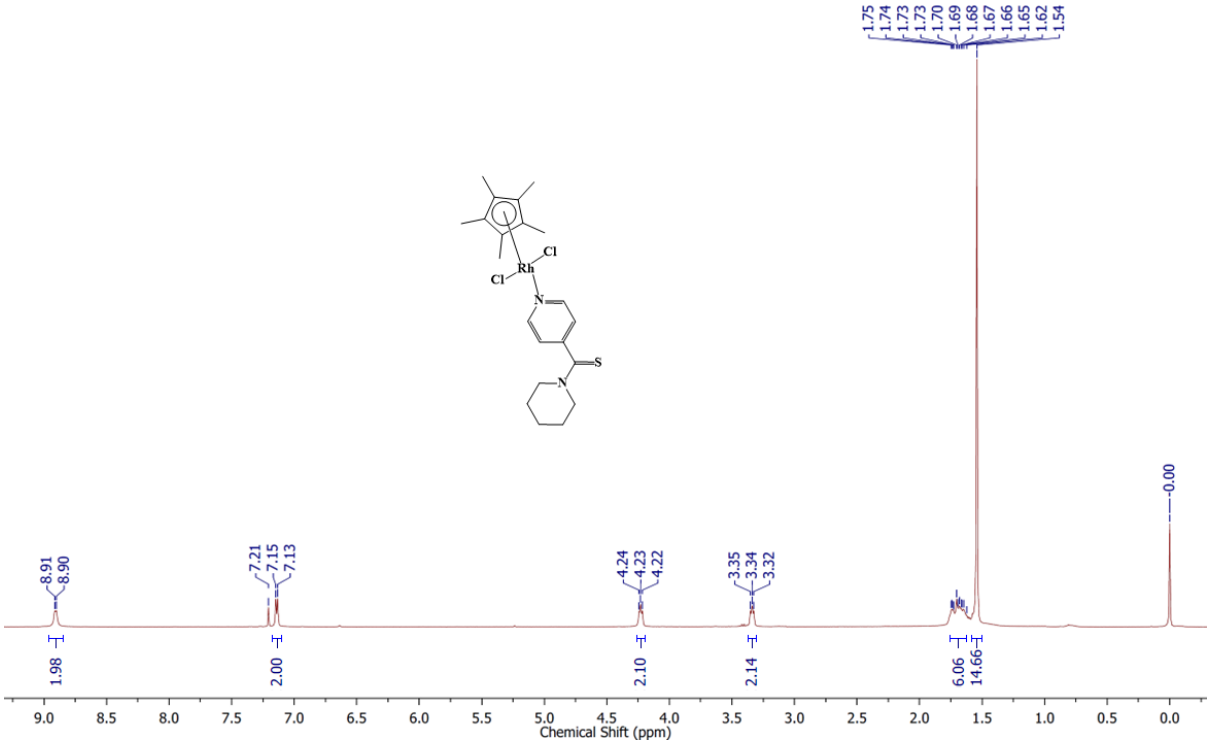

Figure S6: ^{1}H NMR spectrum of complex (**4**) in CDCl3

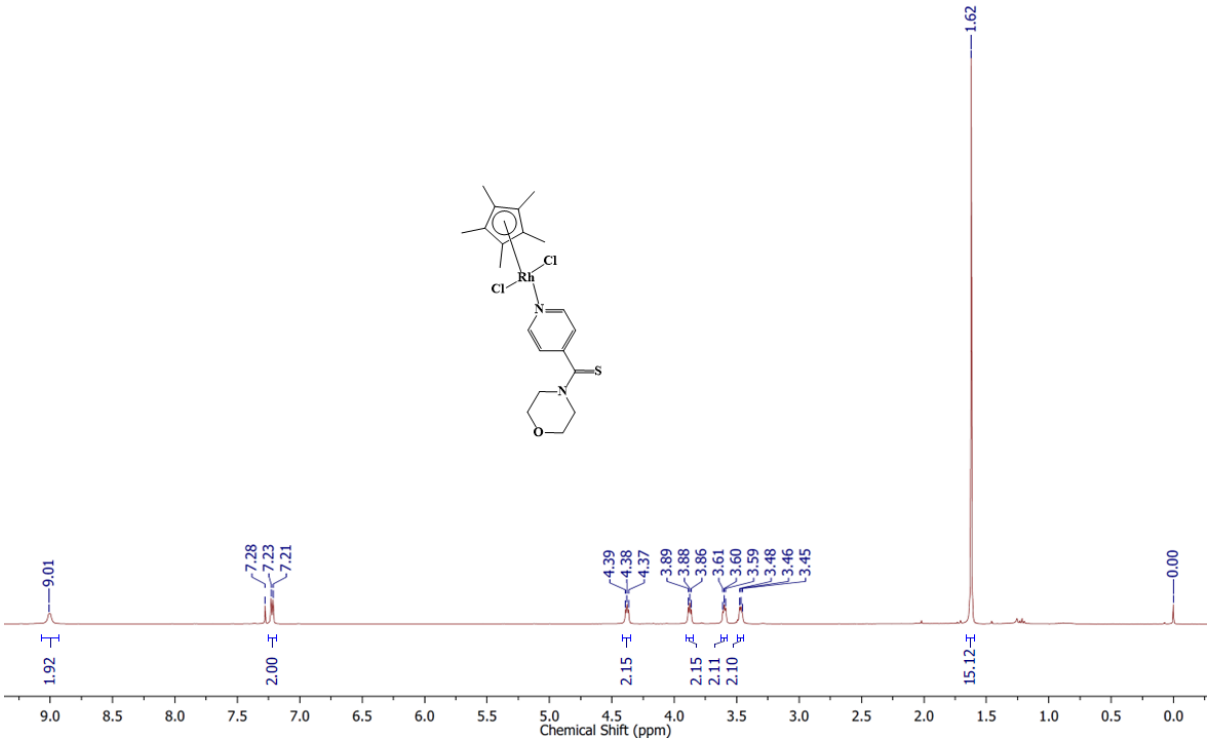

Figure S7: ^{1}H NMR spectrum of complex (**5**) in CDCl3

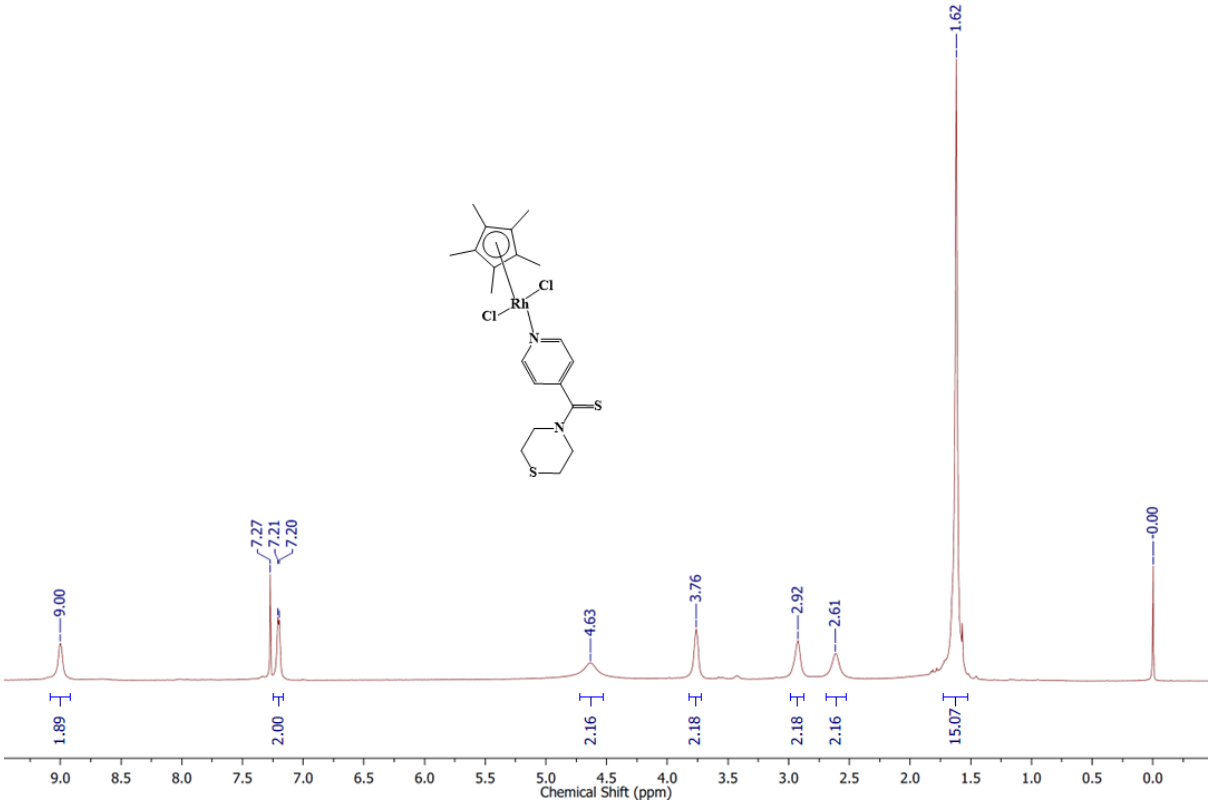

Figure S8: ^{1}H NMR spectrum of complex (**6**) in CDCl3

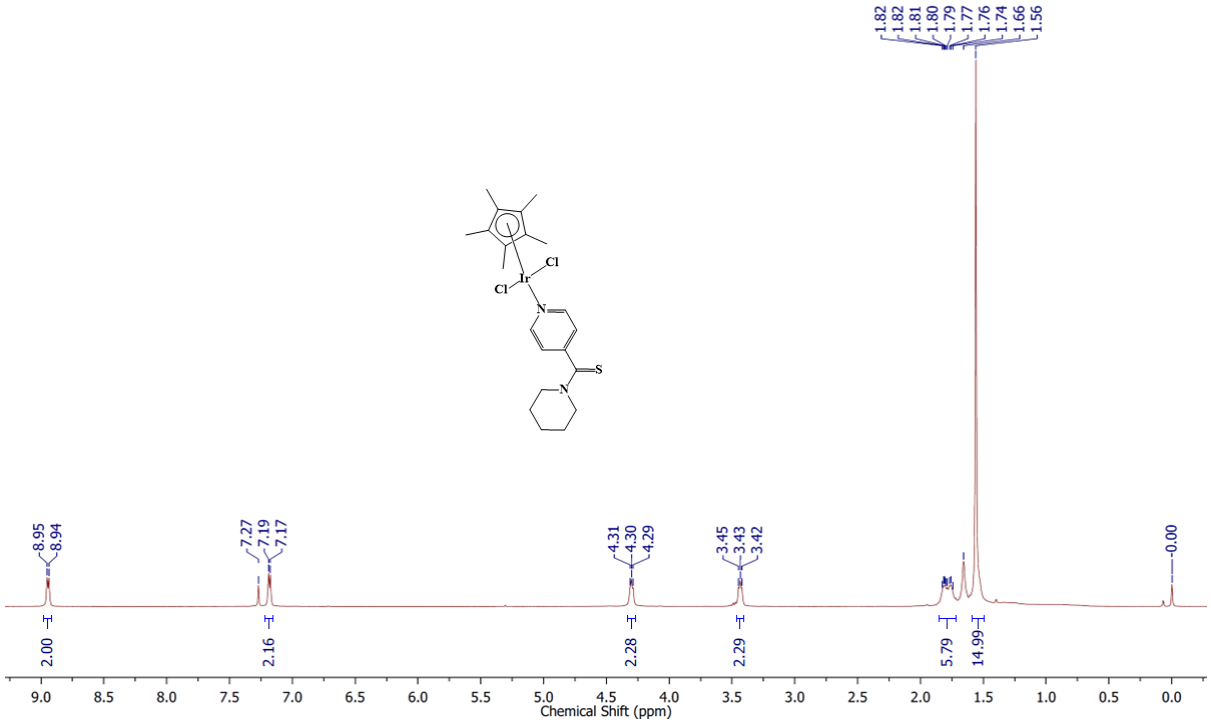

Figure S9: ^{1}H NMR spectrum of complex (**7**) in CDCl3

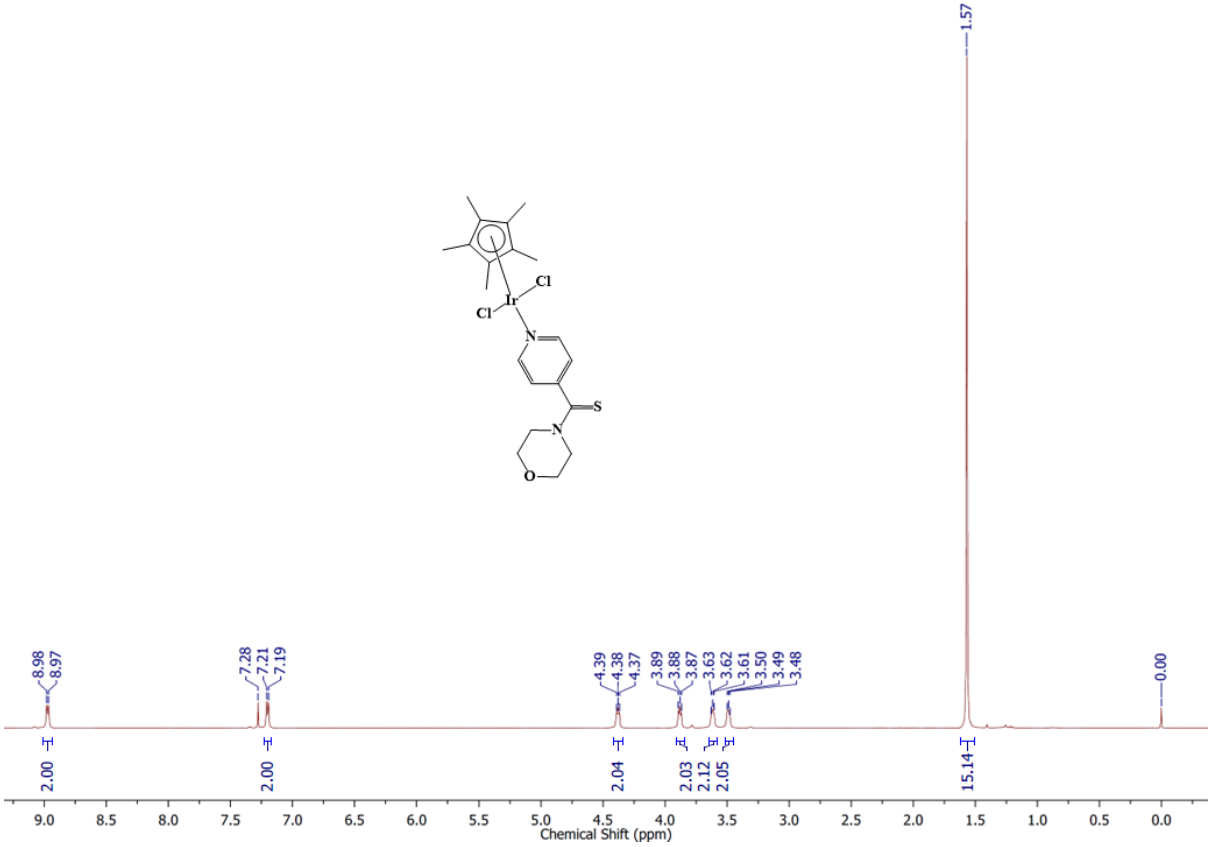

Figure S10: ^{1}H NMR spectrum of complex (**8**) in CDCl3

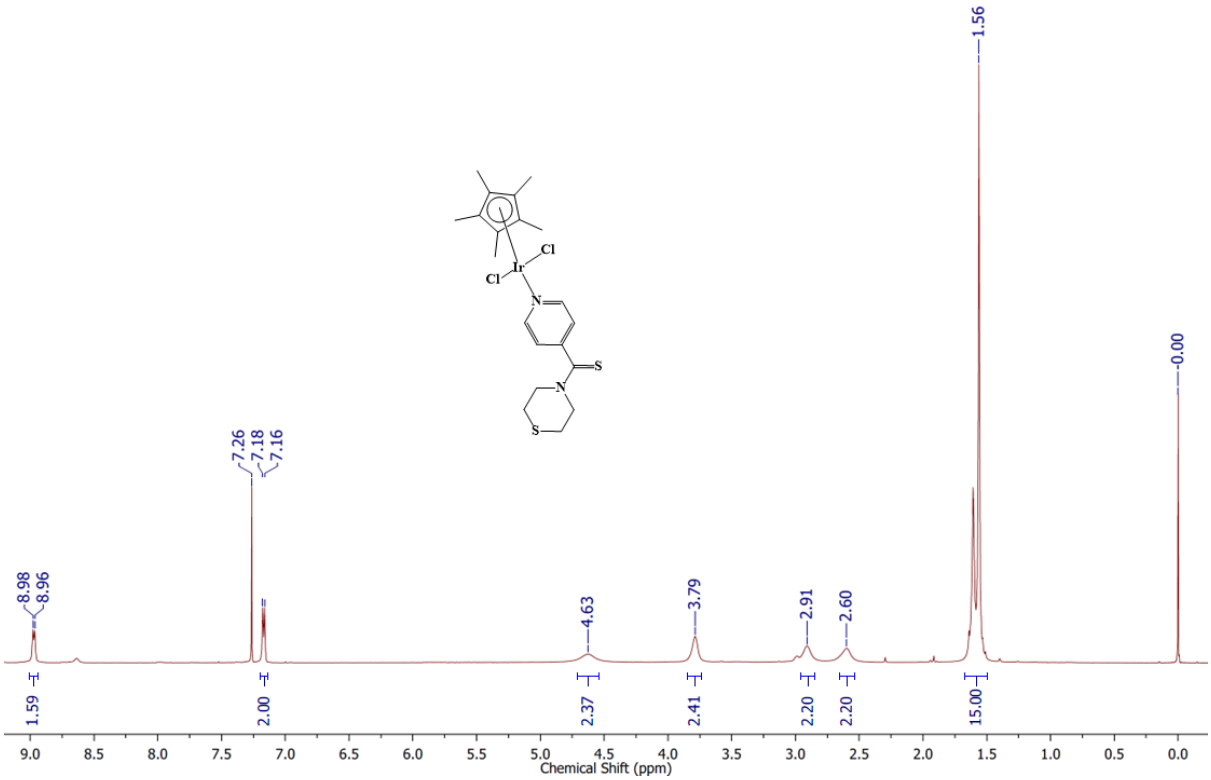

Figure S11: ^{1}H NMR spectrum of complex (**9**) in CDCl3

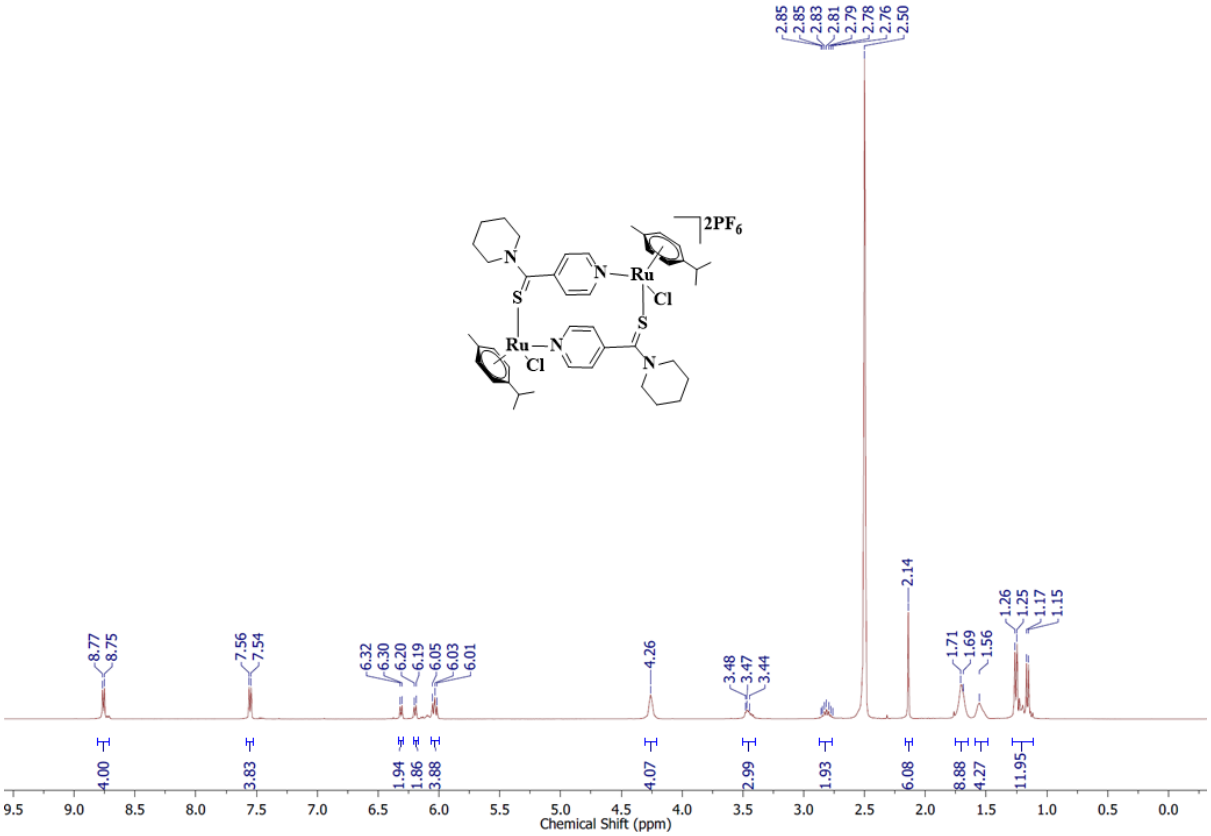

Figure S12: ^{1}H NMR spectrum of complex (**10**) in DMSO-d6

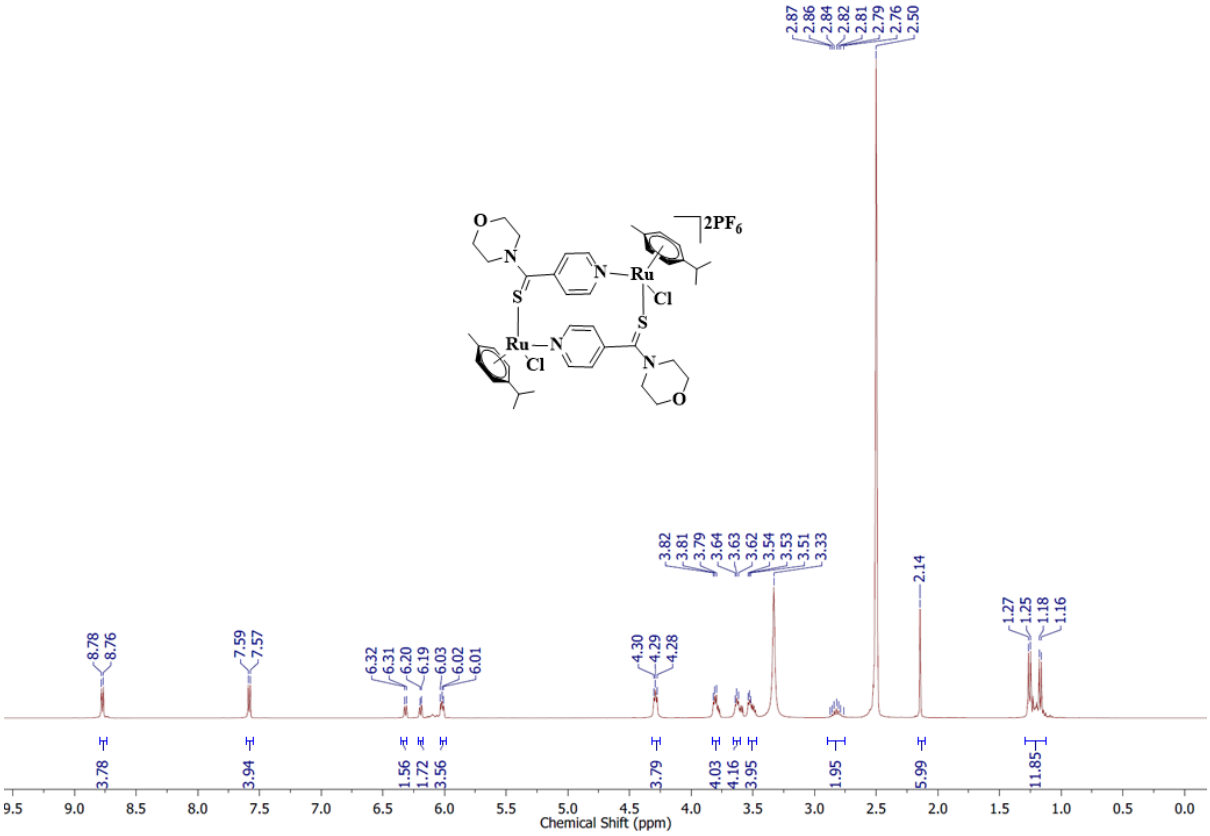

Figure S13: ^{1}H NMR spectrum of complex (**11**) in DMSO-d6

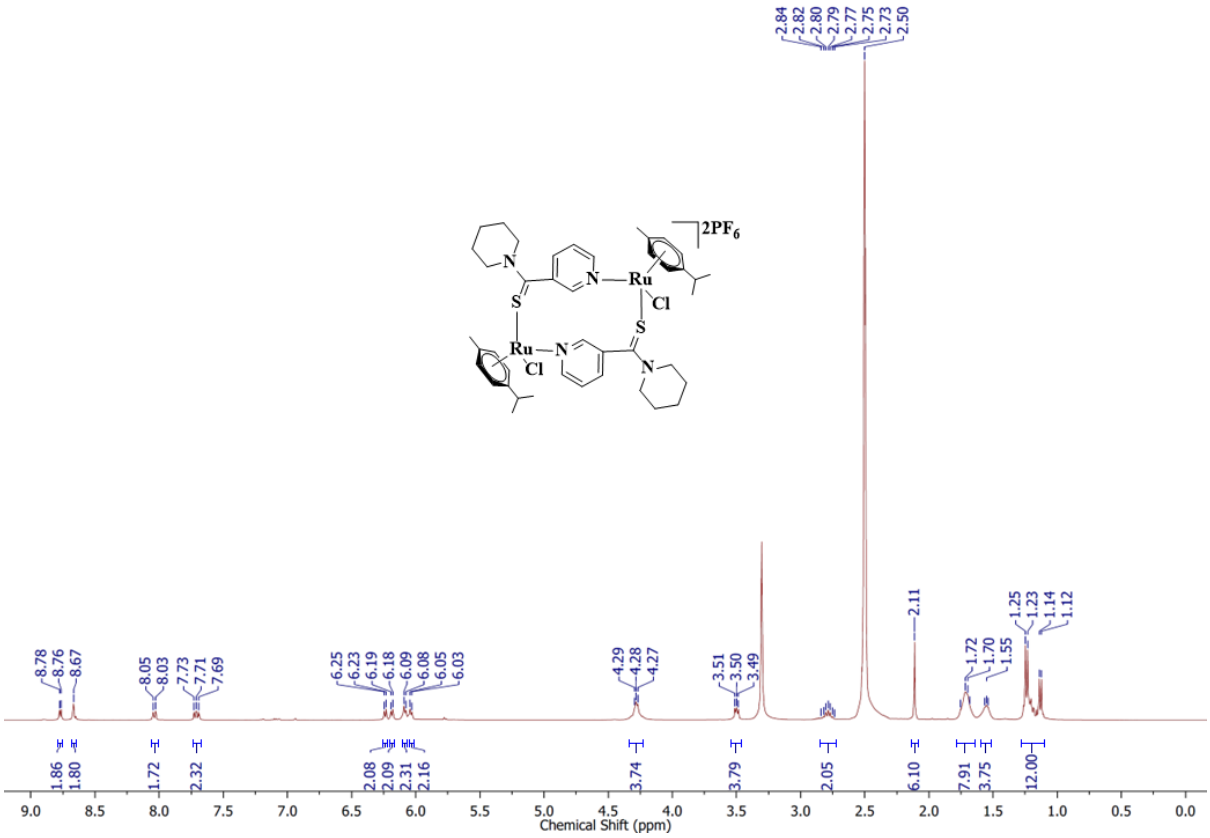

Figure S14: ^{1}H NMR spectrum of complex (**12**) in DMSO-d6

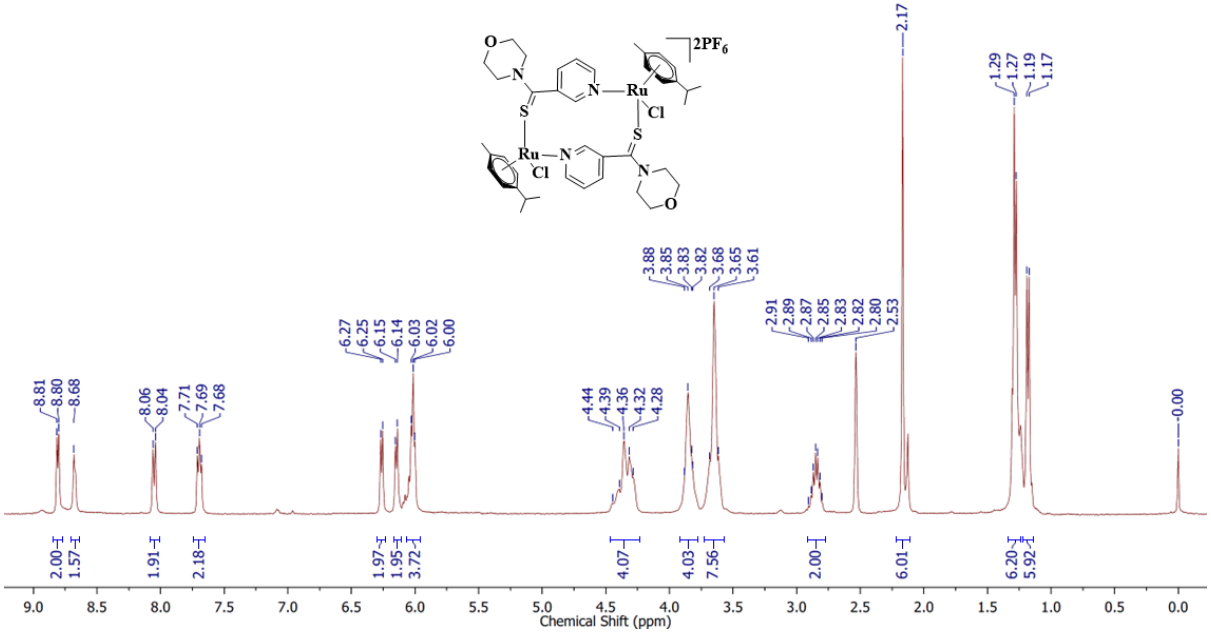

Figure S15: ^{1}H NMR spectrum of complex (**13**) in DMSO-d6

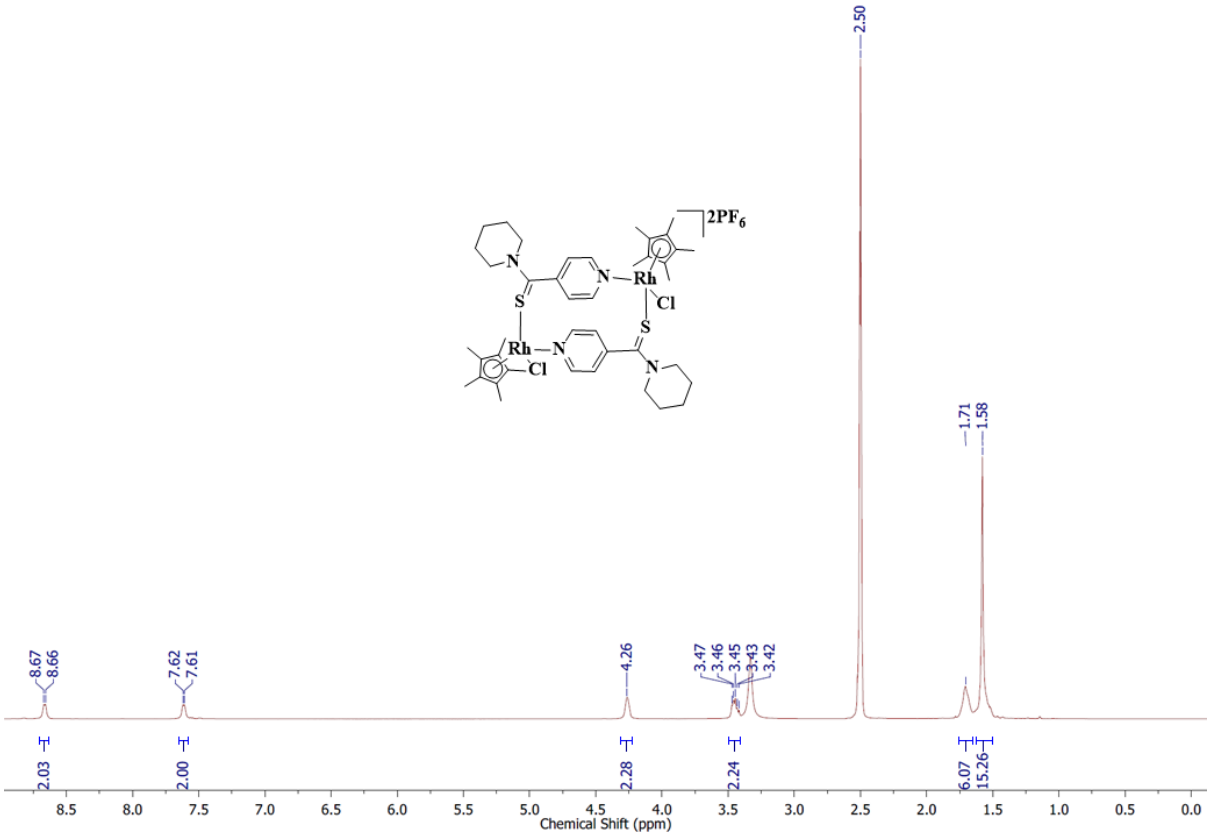

Figure S16: ^{1}H NMR spectrum of complex (**14**) in DMSO-d6

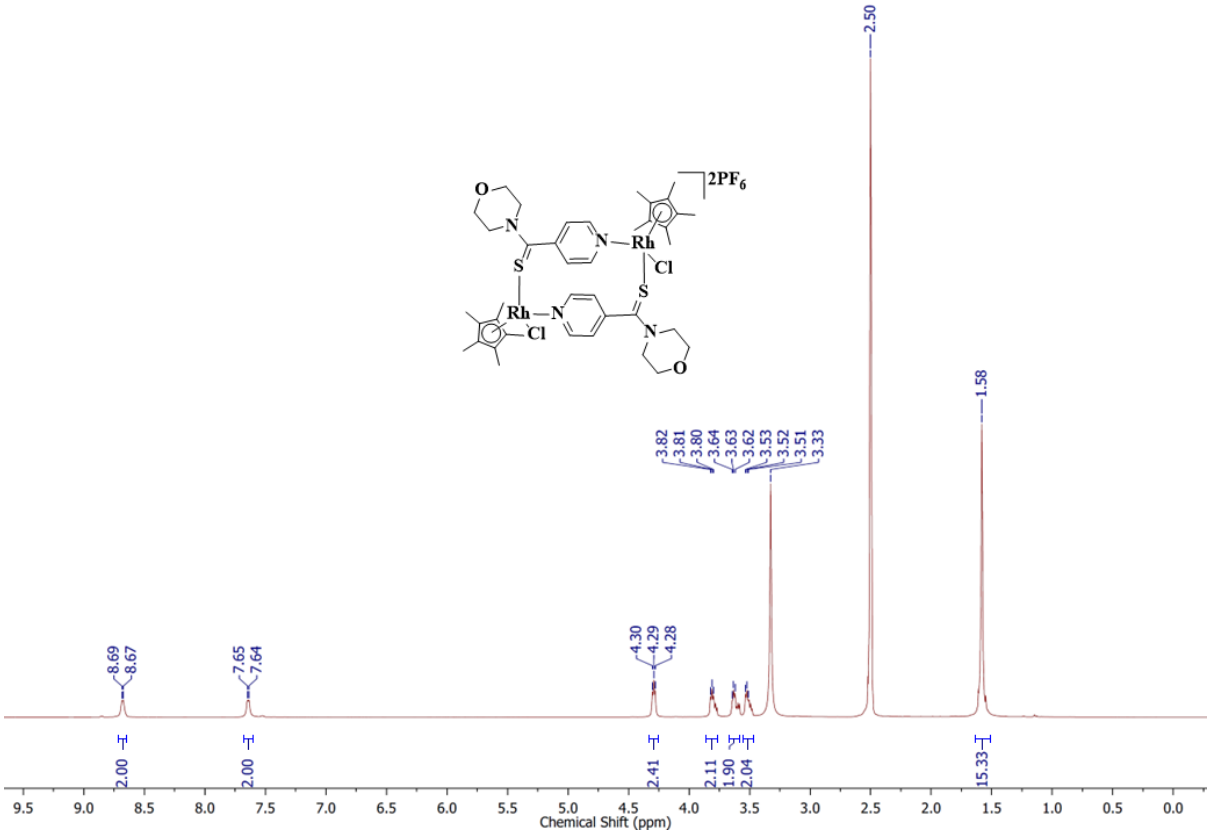

Figure S17: ^{1}H NMR spectrum of complex (**15**) in DMSO-d6

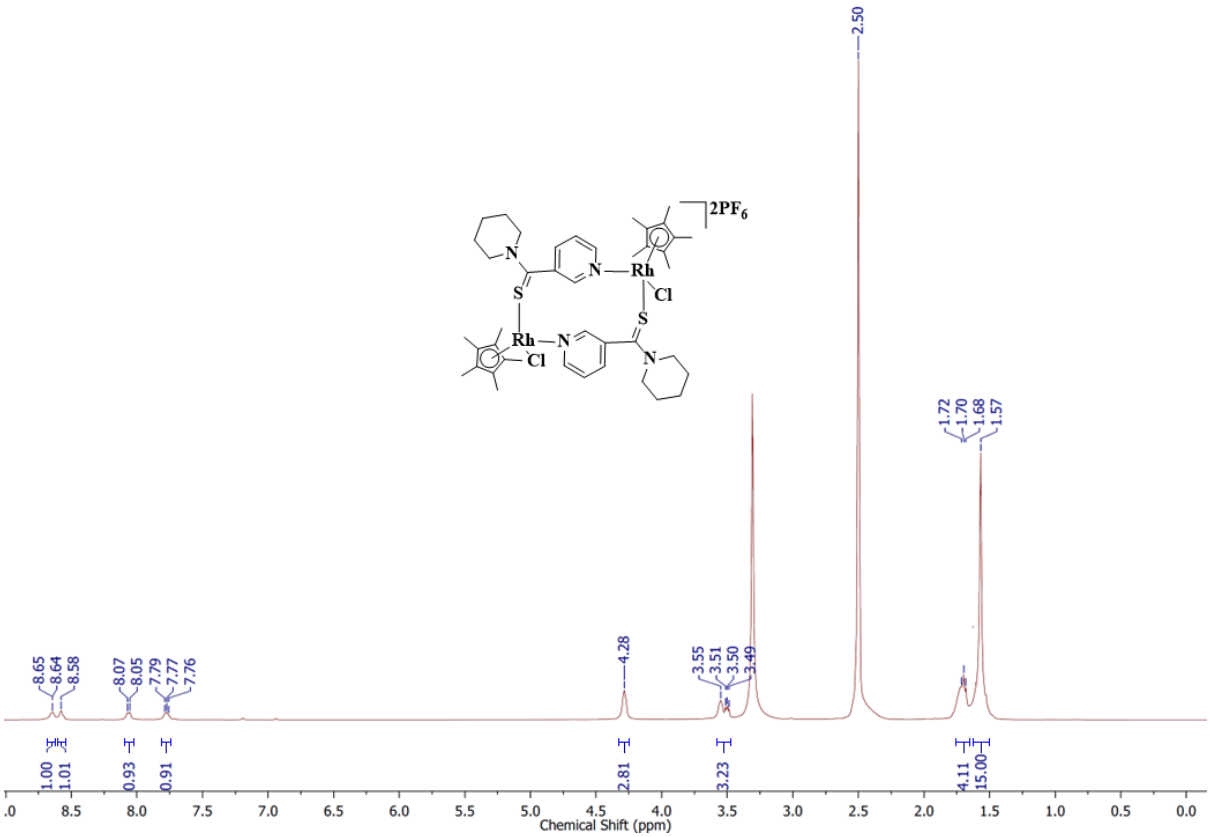

Figure S18: ^{1}H NMR spectrum of complex (**16**) in DMSO-d6

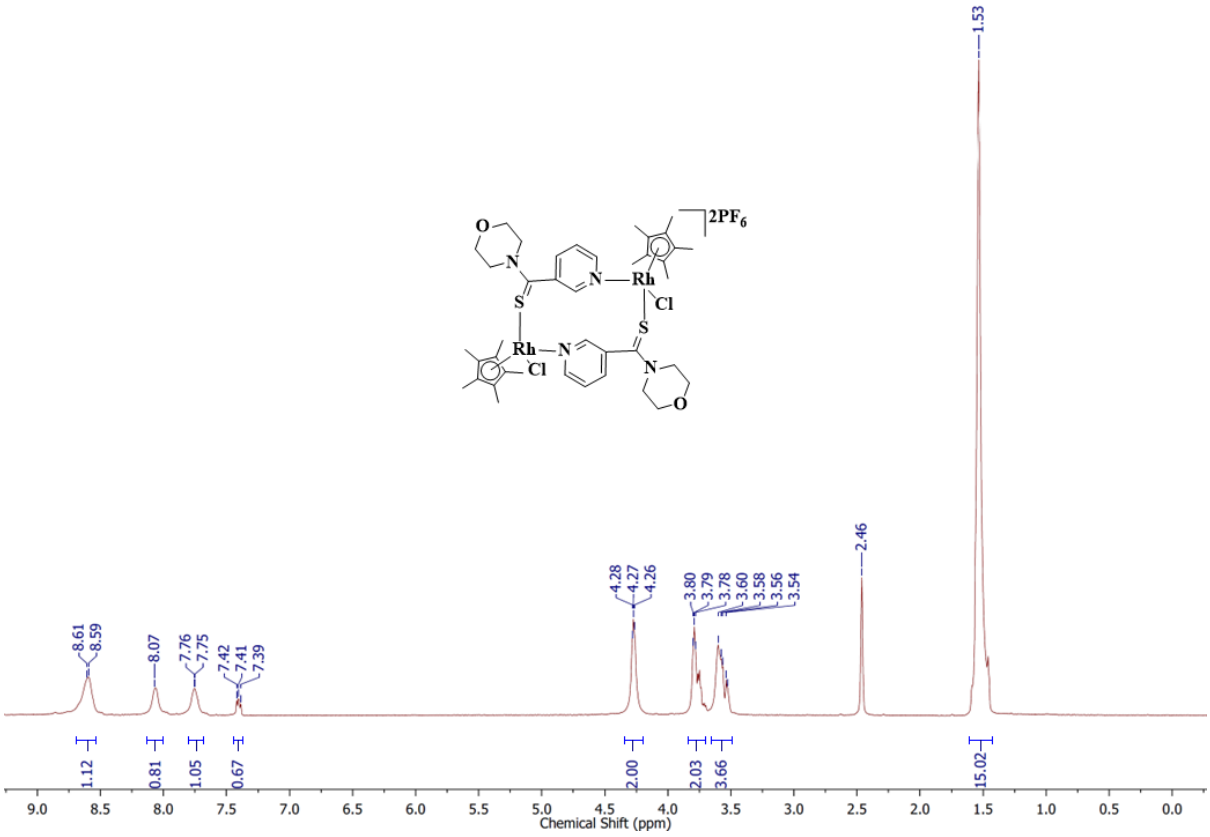

Figure S19: ^{1}H NMR spectrum of complex (**17**) in DMSO-d6

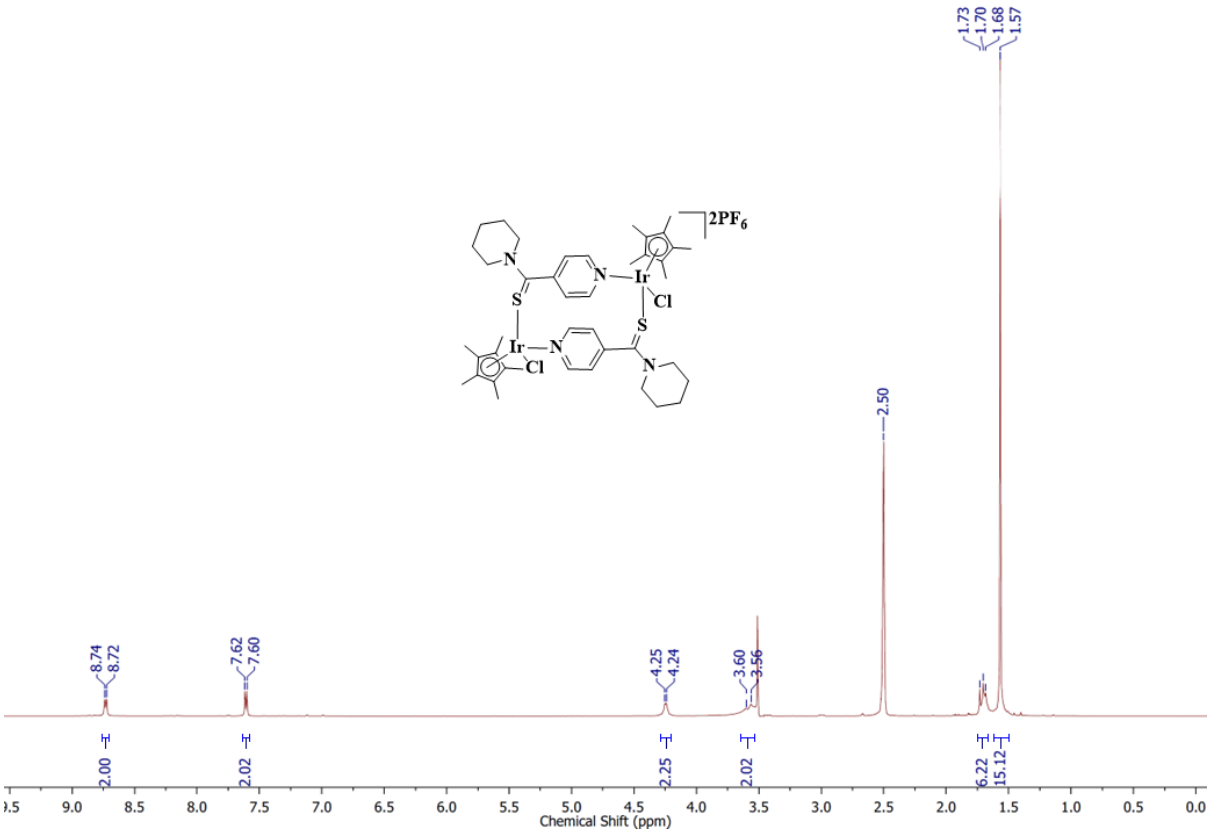

Figure S20: ^{1}H NMR spectrum of complex (**18**) in DMSO-d6

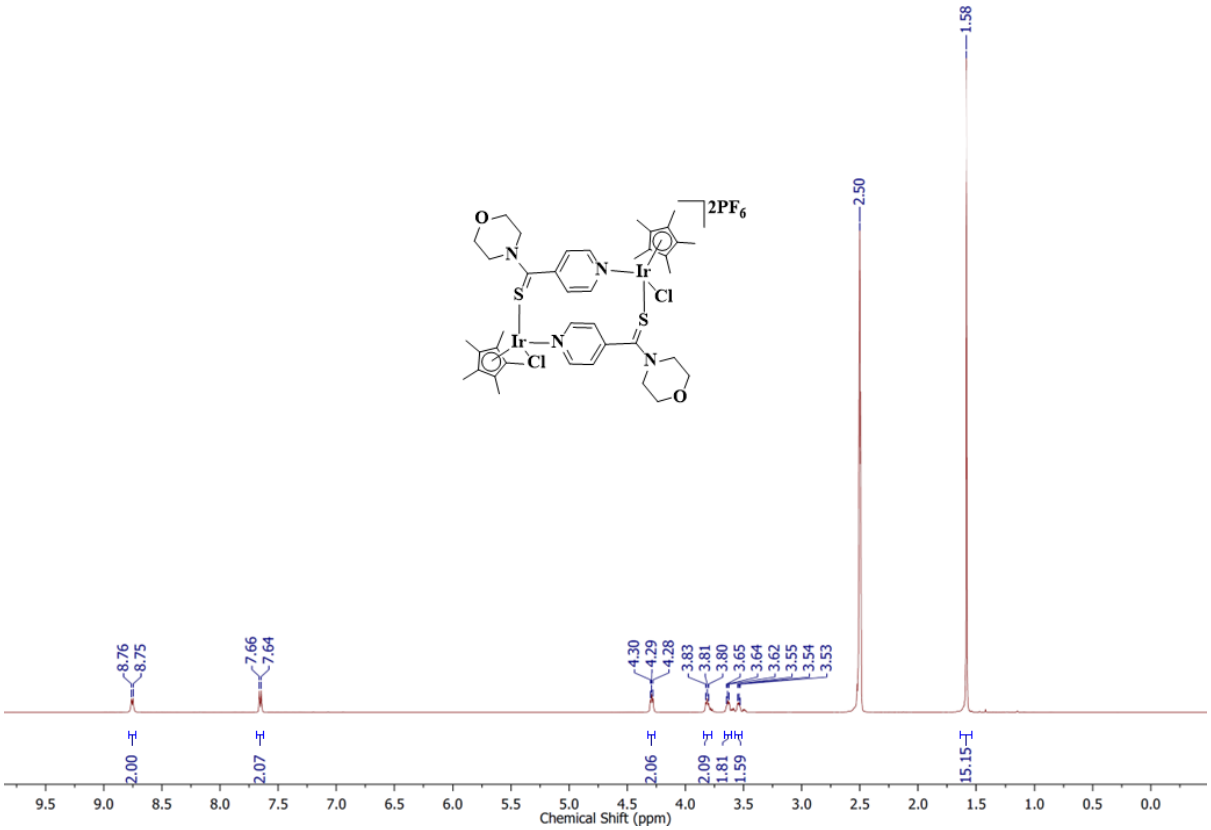

Figure S21: ^{1}H NMR spectrum of complex (1**9**) in DMSO-d6

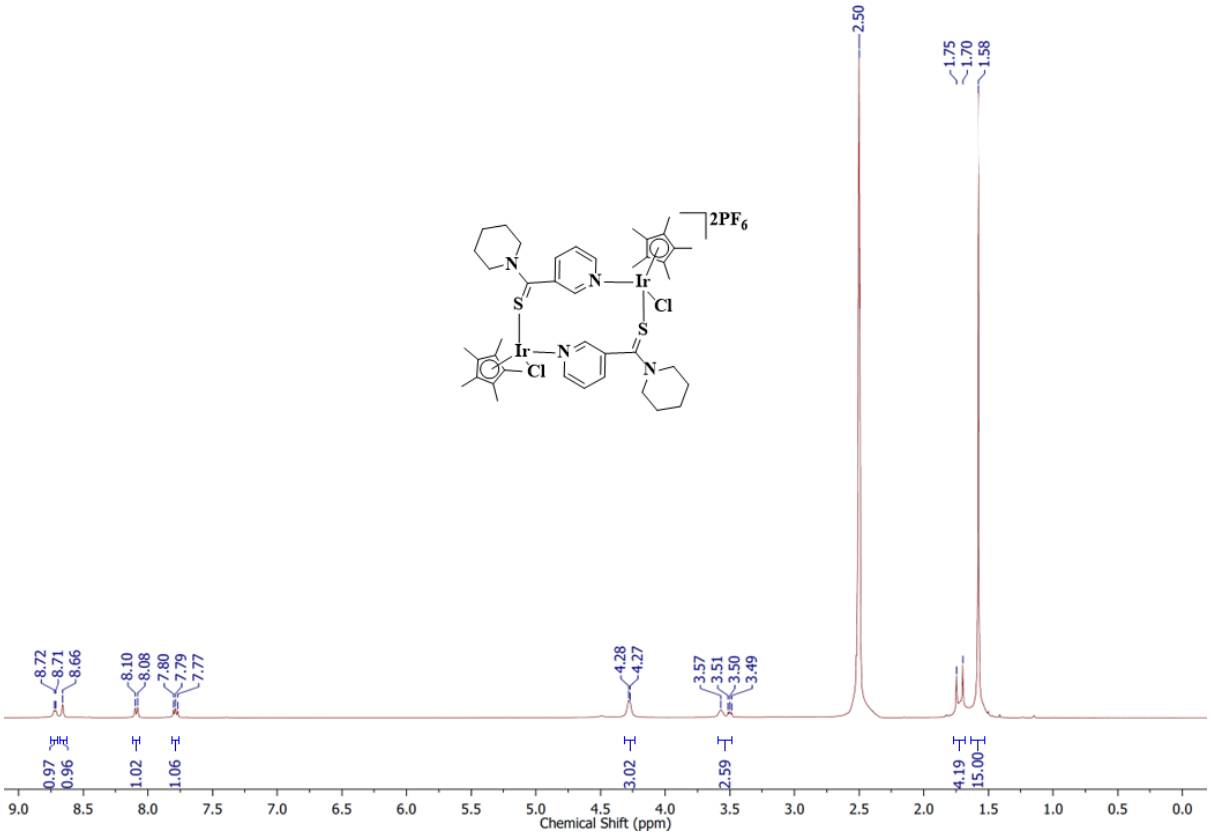

Figure S22: ^{1}H NMR spectrum of complex (**20**) in DMSO-d6

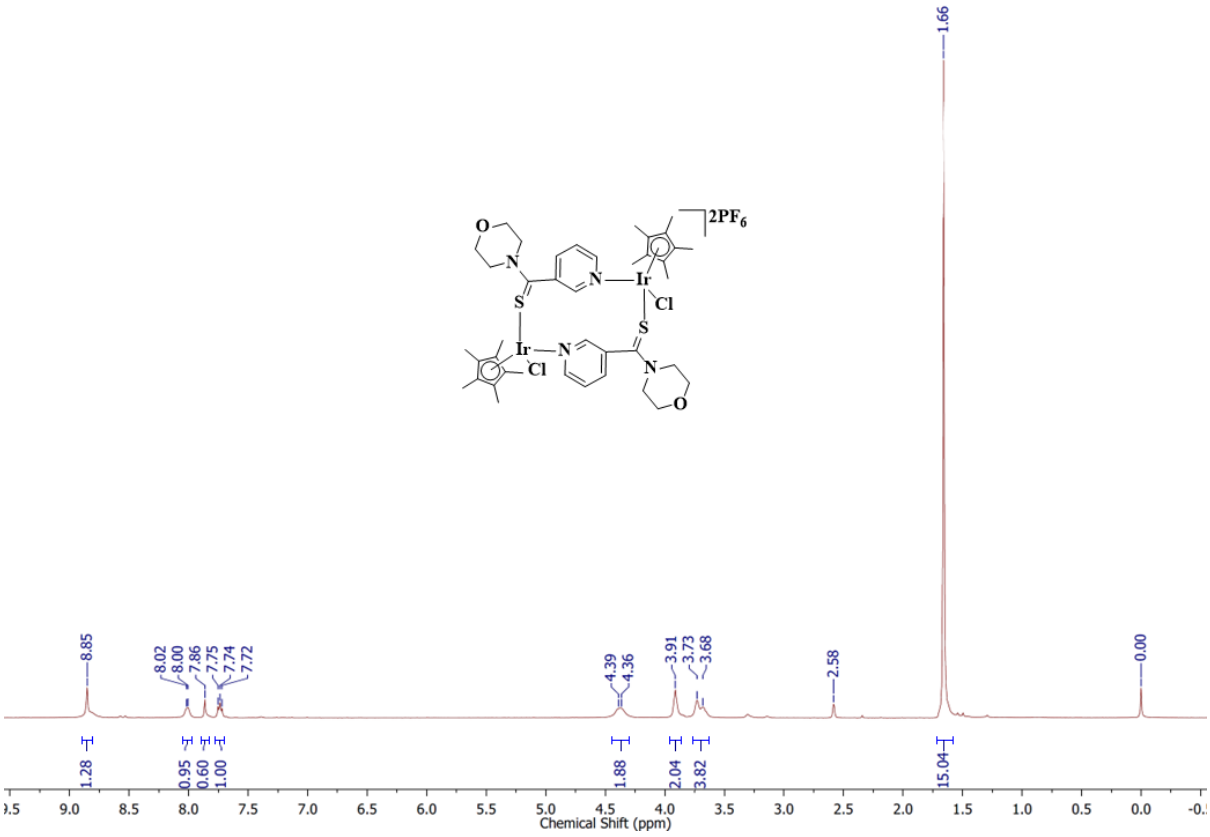

Figure S23: ^{1}H NMR spectrum of complex (**21**) in DMSO-d6

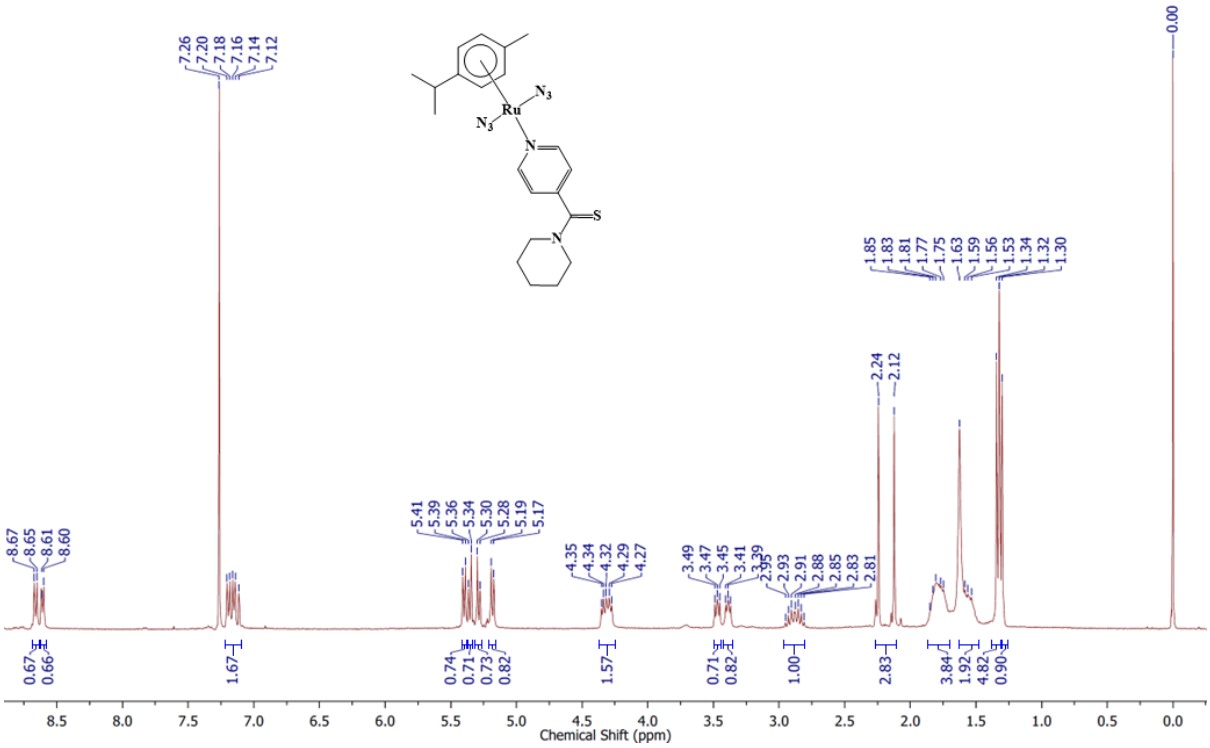

Figure S24: ^{1}H NMR spectrum of complex (**22**) in CDCl3

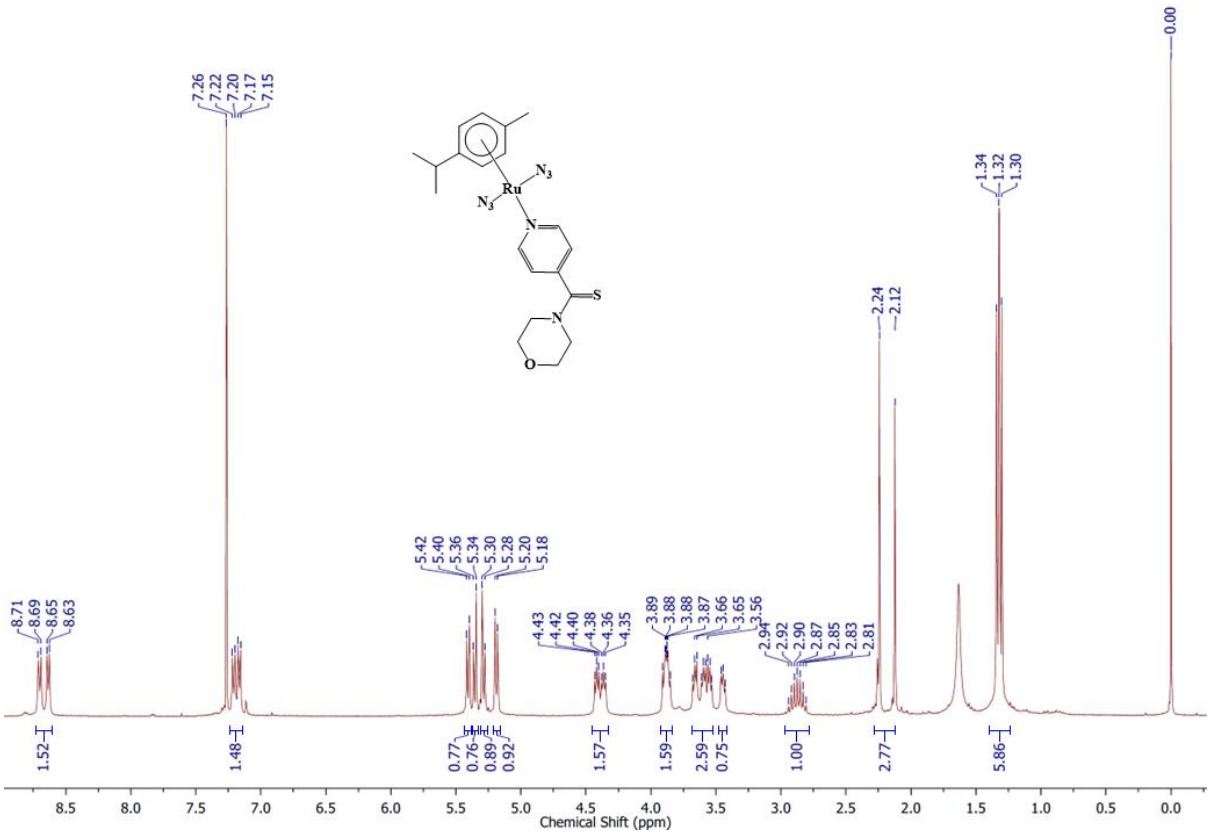

Figure S25: ^{1}H NMR spectrum of complex (**23**) in CDCl3

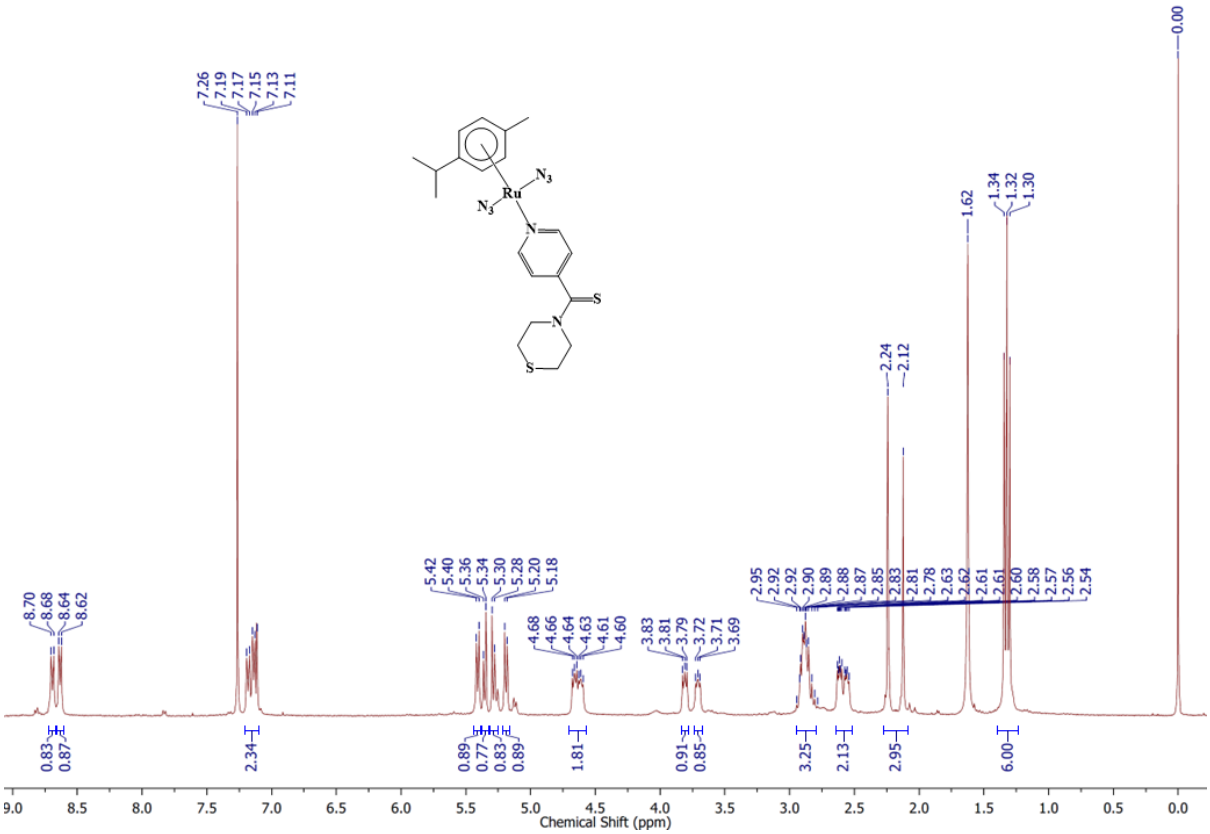

Figure S26: ^{1}H NMR spectrum of complex (**24**) in CDCl3

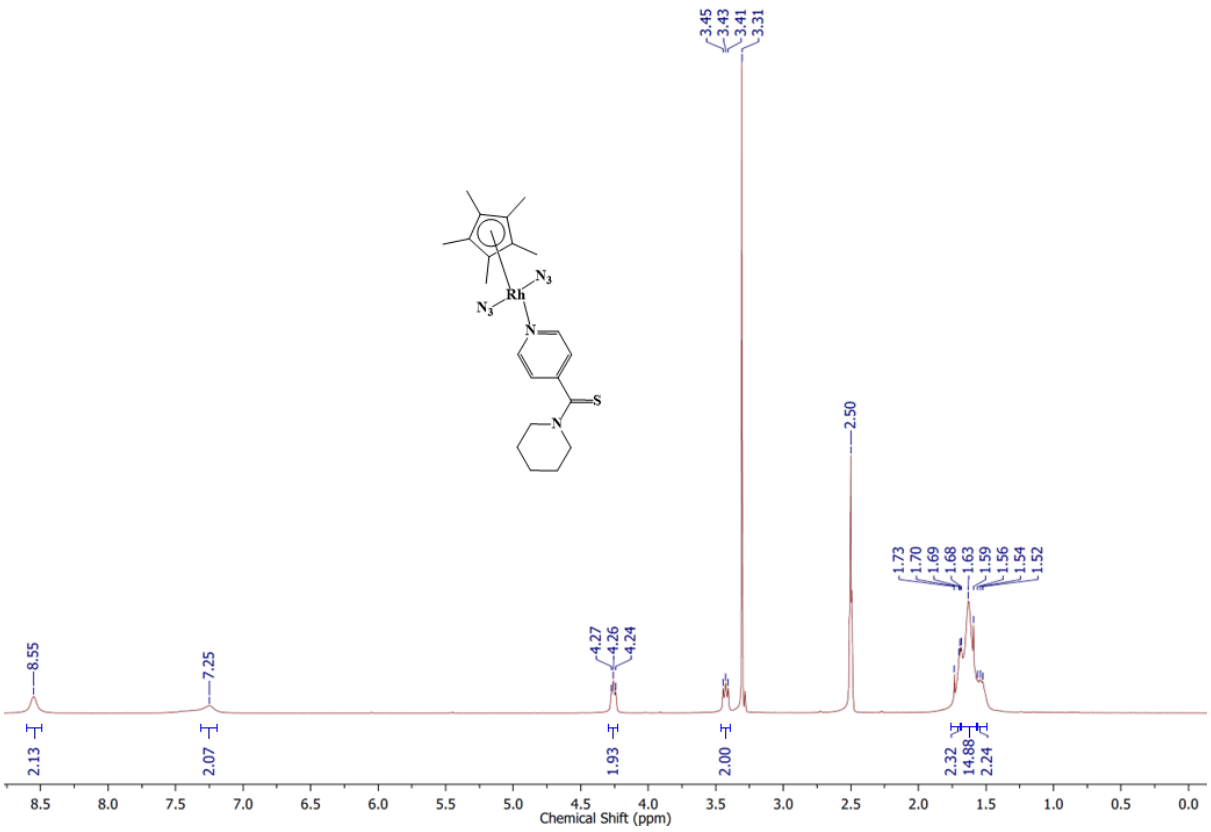

Figure S27: ^{1}H NMR spectrum of complex (**25**) in DMSO-d6

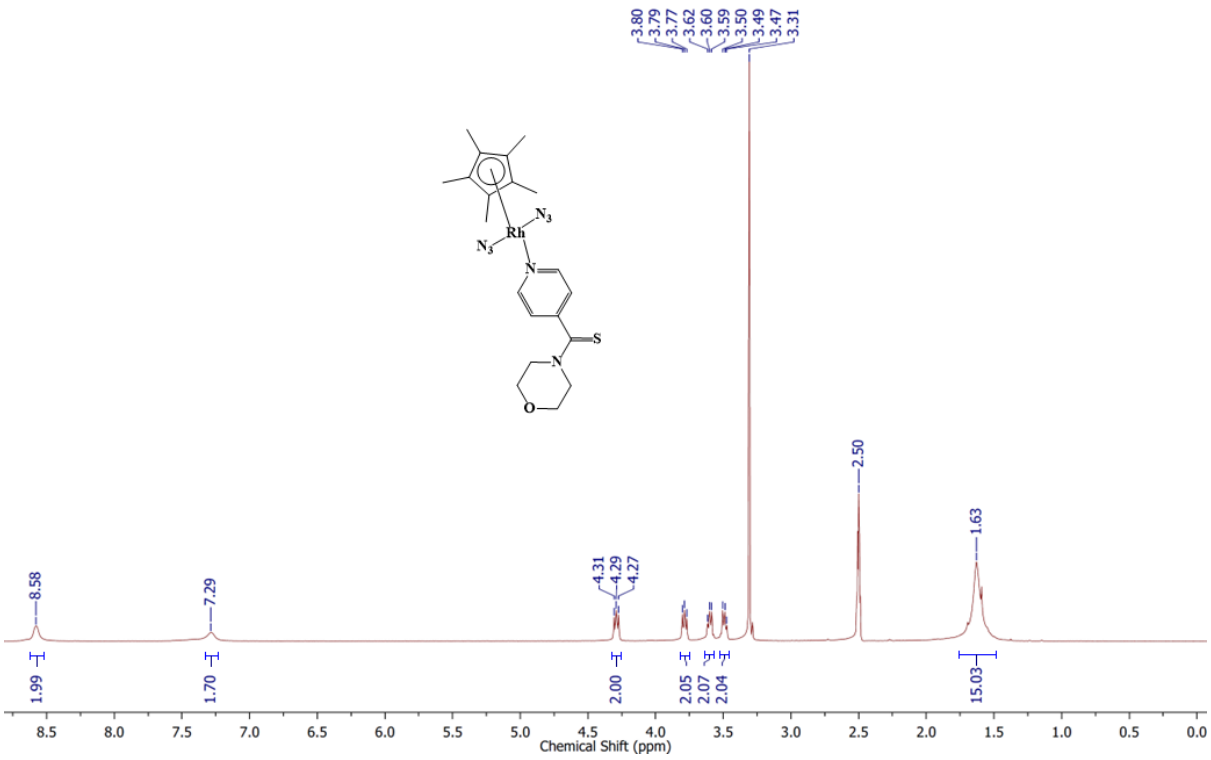

Figure S28: ^{1}H NMR spectrum of complex (**26**) in DMSO-d6

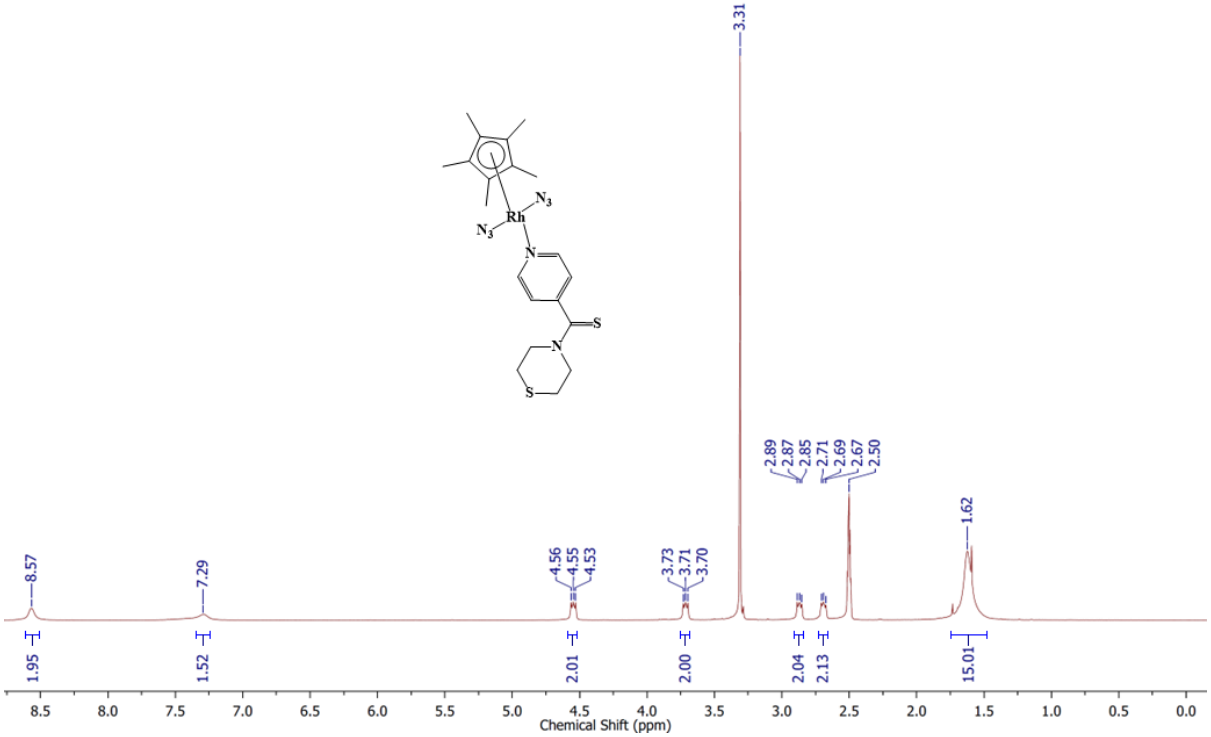

Figure S29: ^{1}H NMR spectrum of complex (**27**) in DMSO-d6

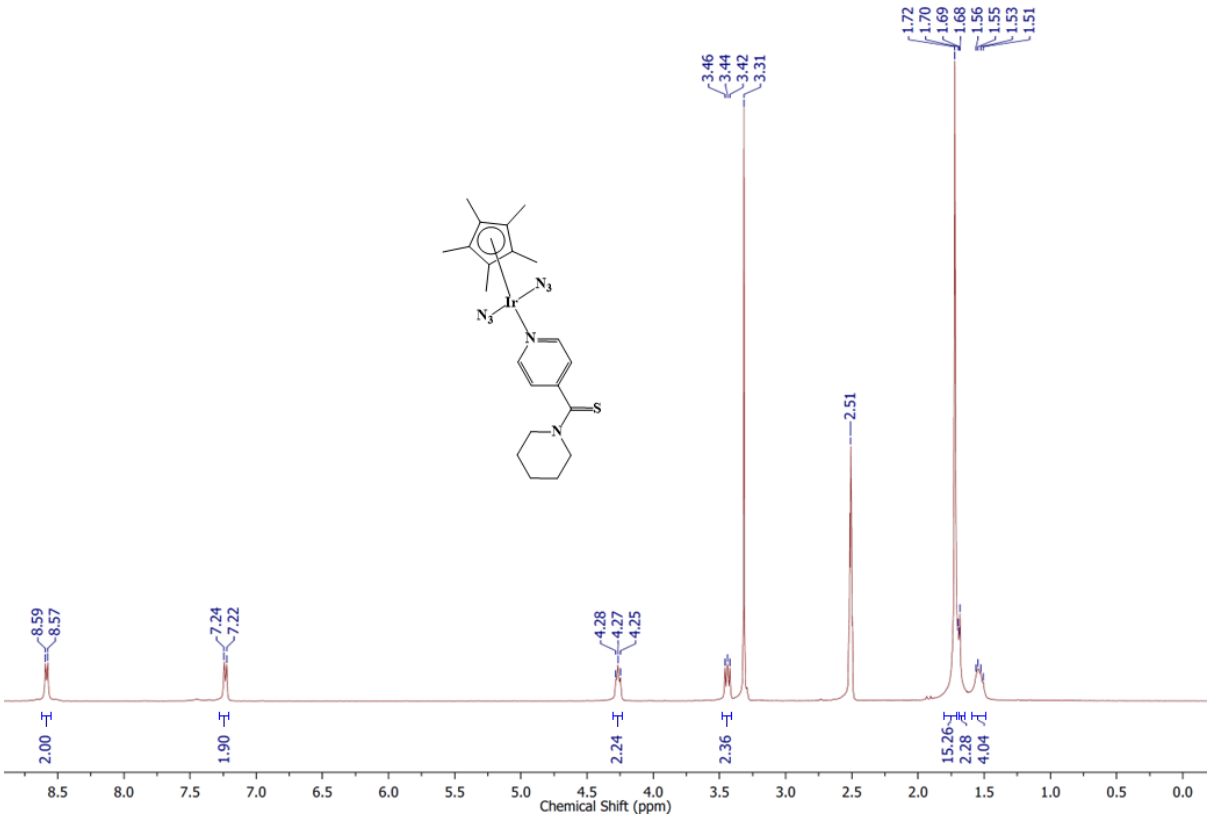

Figure S30: ^{1}H NMR spectrum of complex (**28**) in DMSO-d6

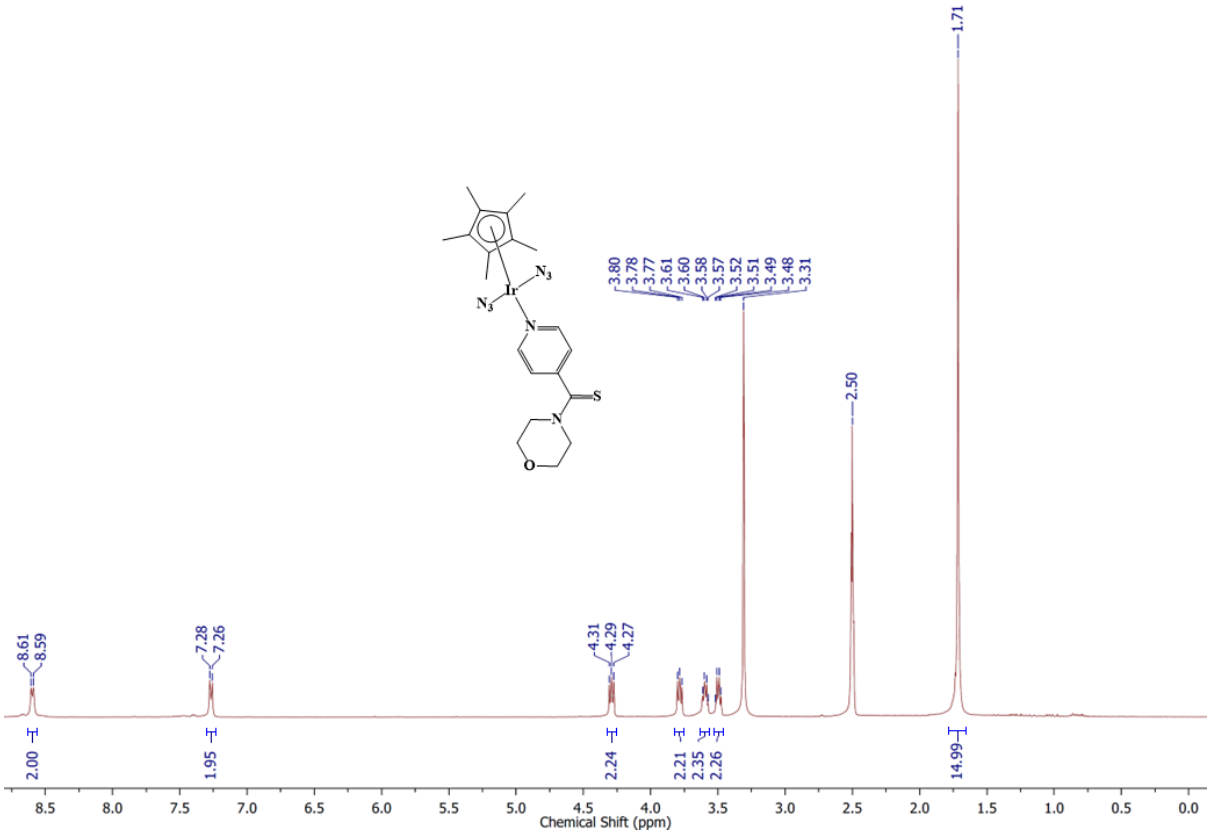

Figure S31: ^{1}H NMR spectrum of complex (**29**) in DMSO-d6

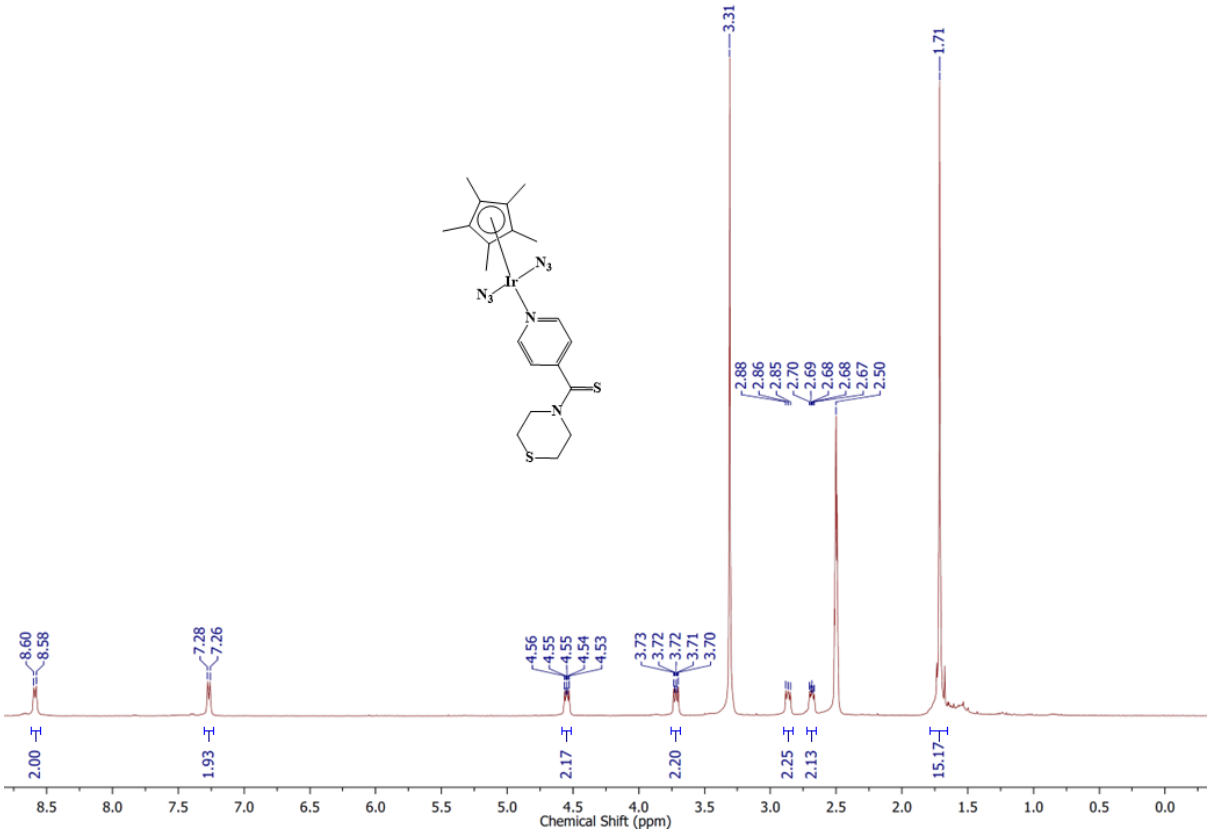

Figure S32: ^{1}H NMR spectrum of complex (**30**) in DMSO-d6

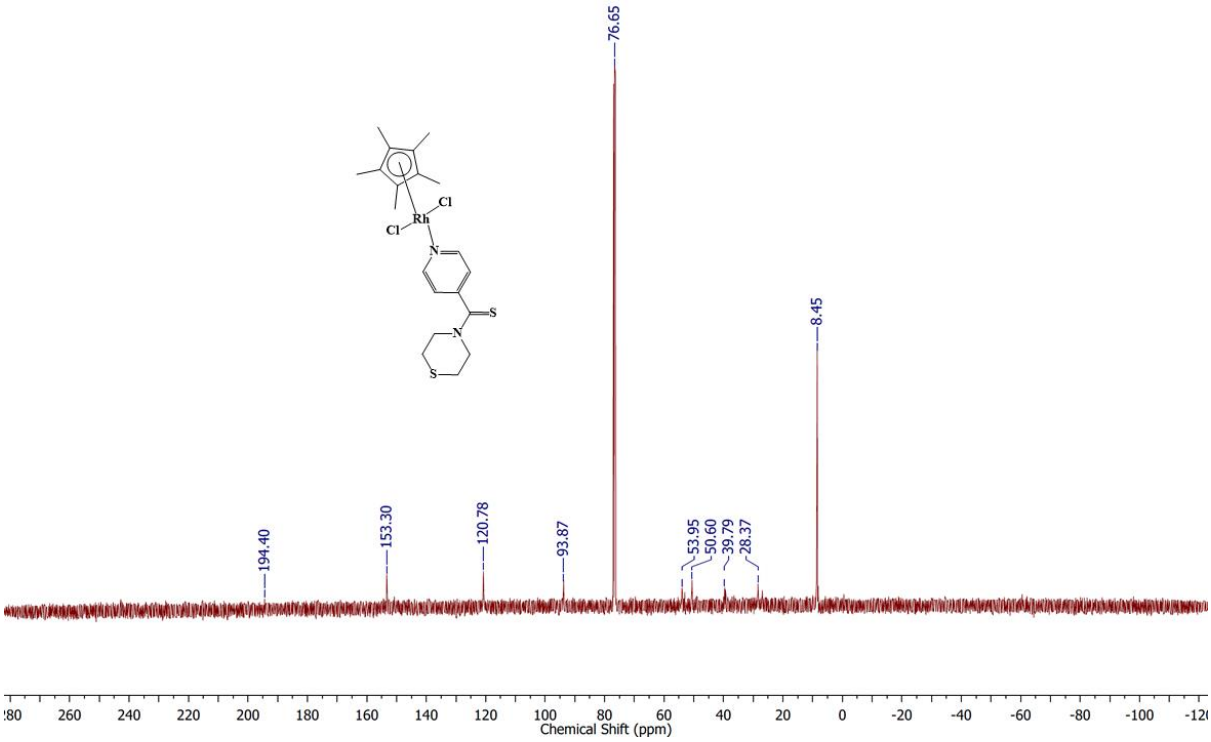

Figure S33: ^{13}C NMR spectrum of complex (**6**) in CDCl3

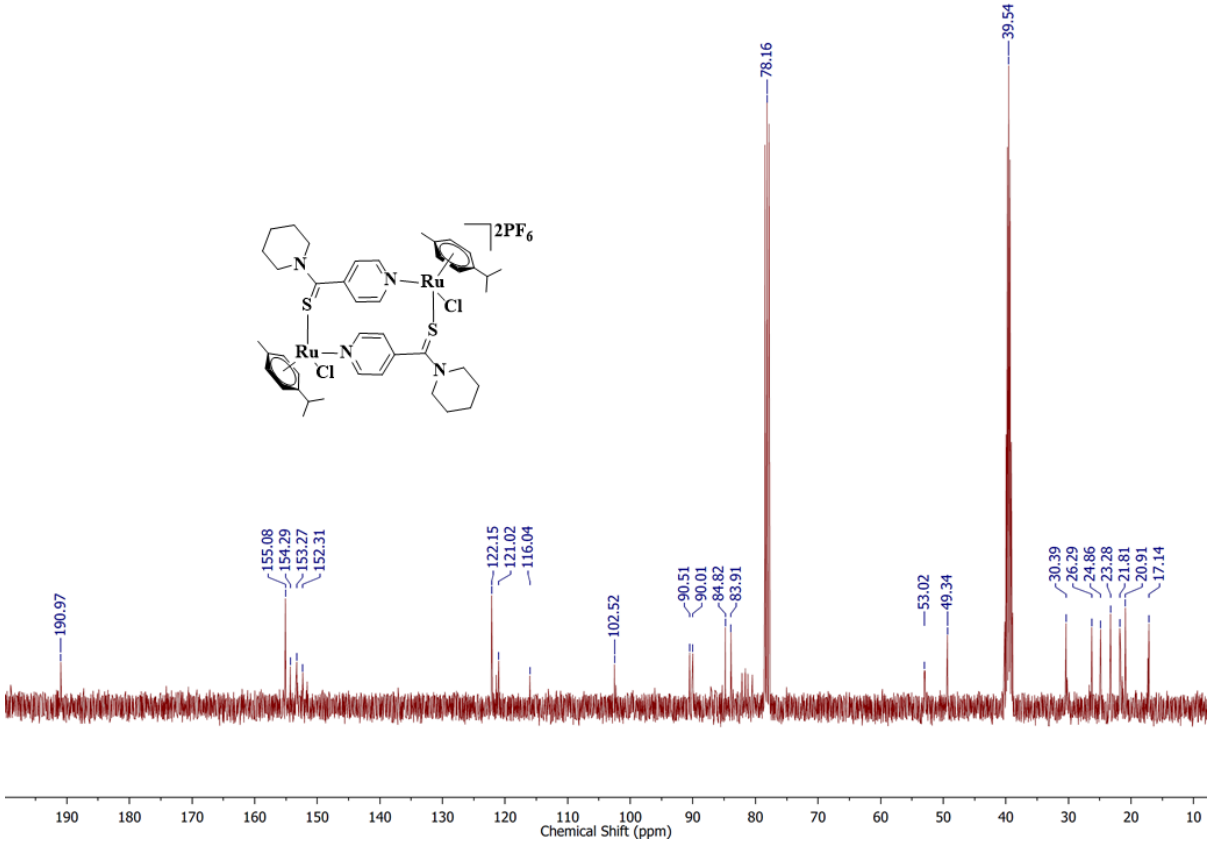

Figure S34: ^{13}C NMR spectrum of complex (**10**) in CDCl3 and DMSO-d6

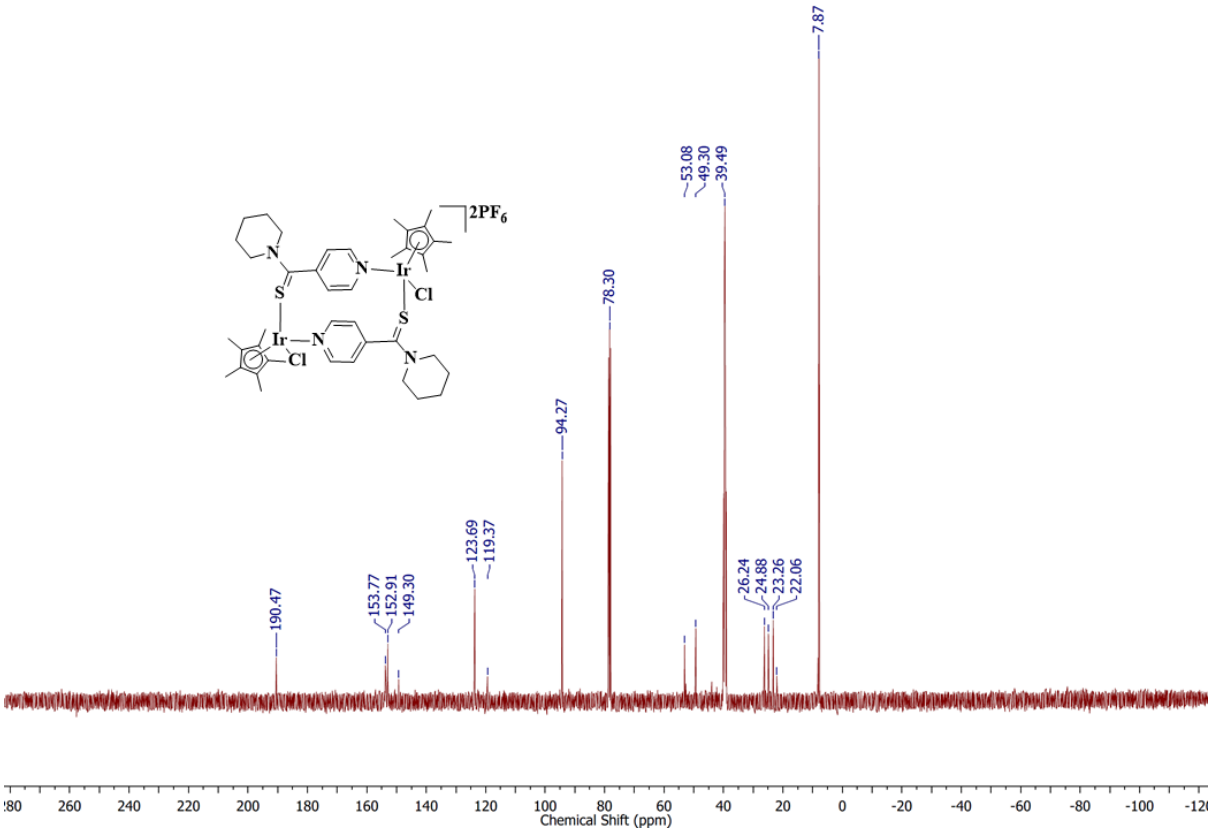

Figure S35: ^{13}C NMR spectrum of complex (**18**) in CDCl3 and DMSO-d6

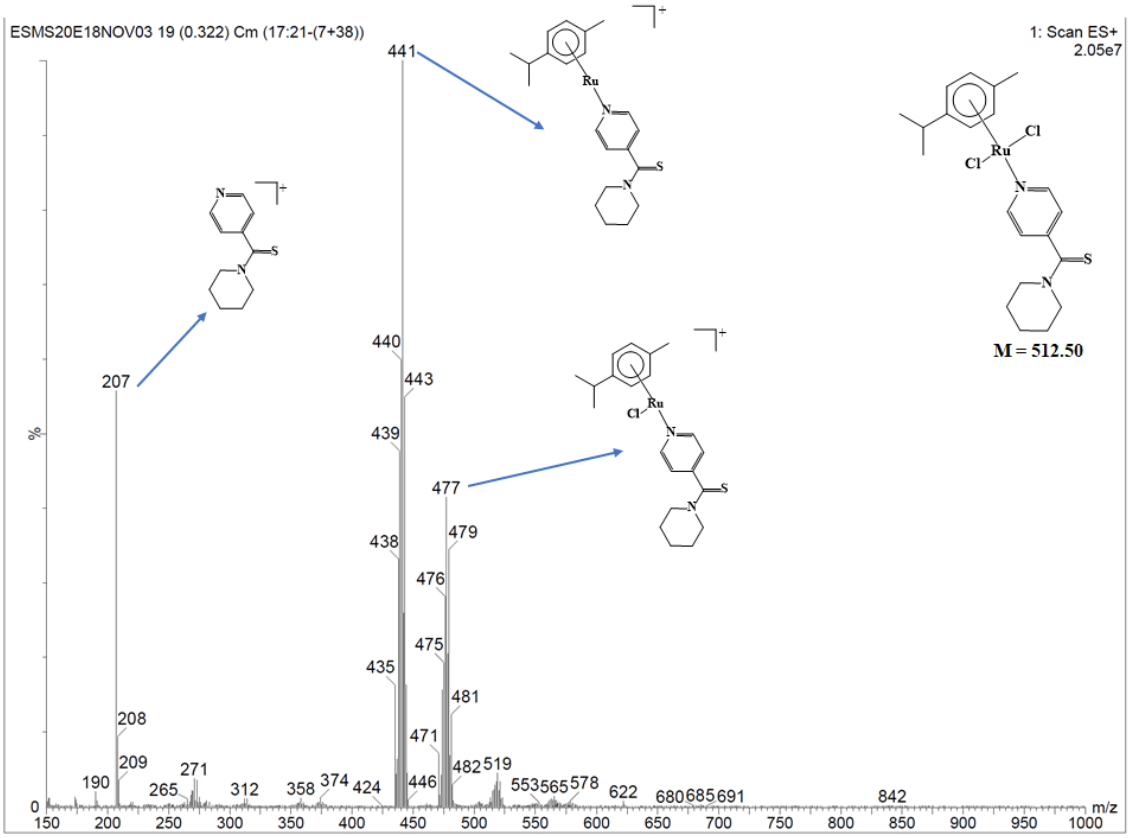

Figure S36: ESI Mass spectrum of complex (**1**) in Acetonitrile

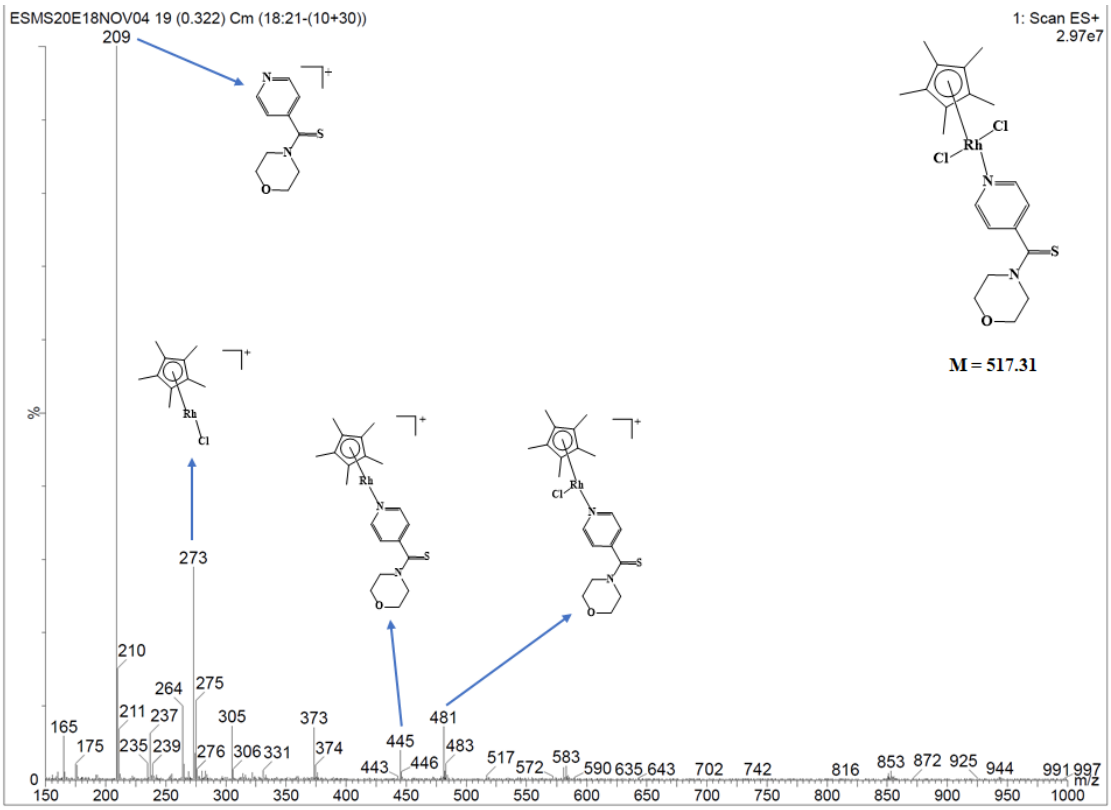

Figure S37: ESI Mass spectrum of complex (**5**) in Acetonitrile

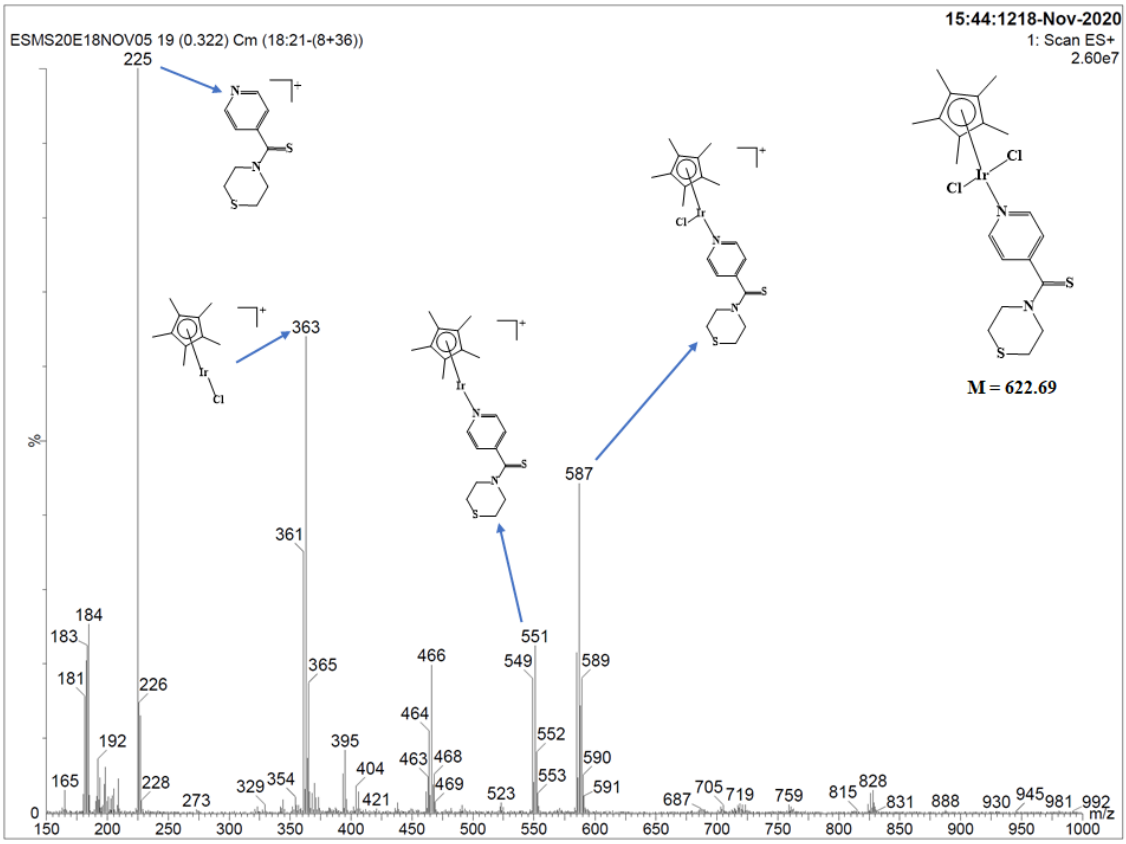

Figure S38: ESI Mass spectrum of complex (**9**) in Acetonitrile

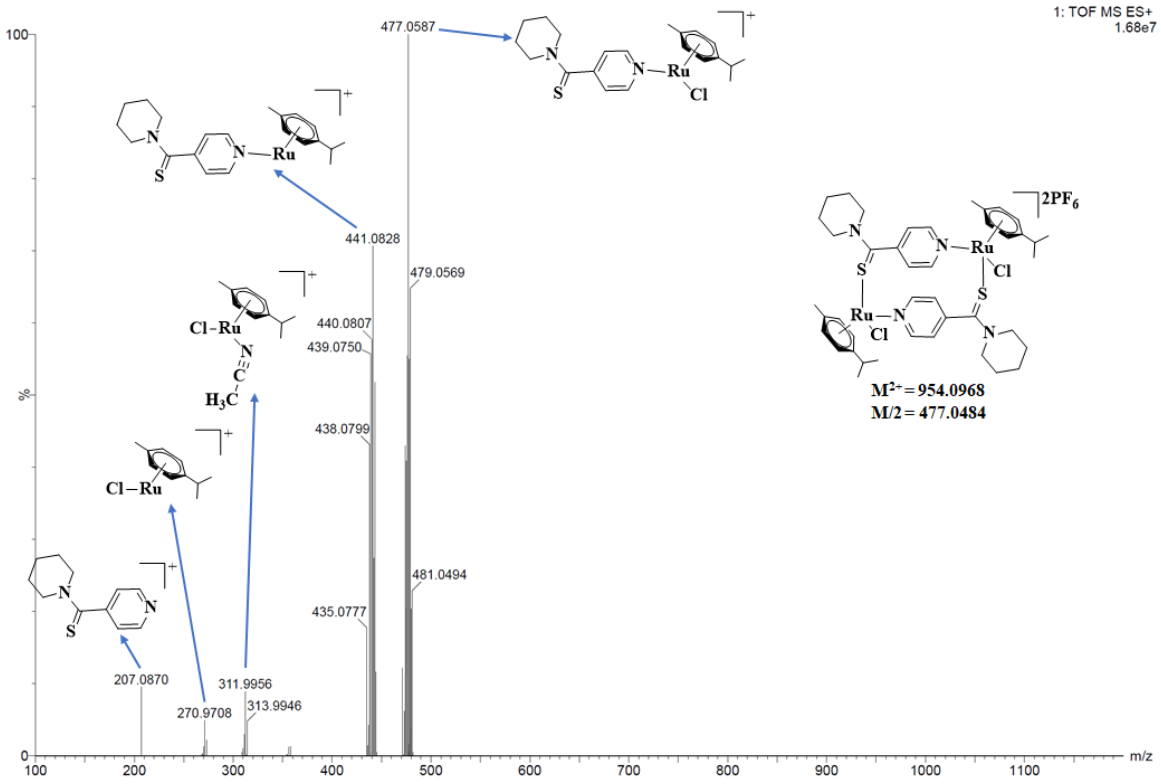

Figure S39: ESI Mass spectrum of complex (**10**) in Acetonitrile

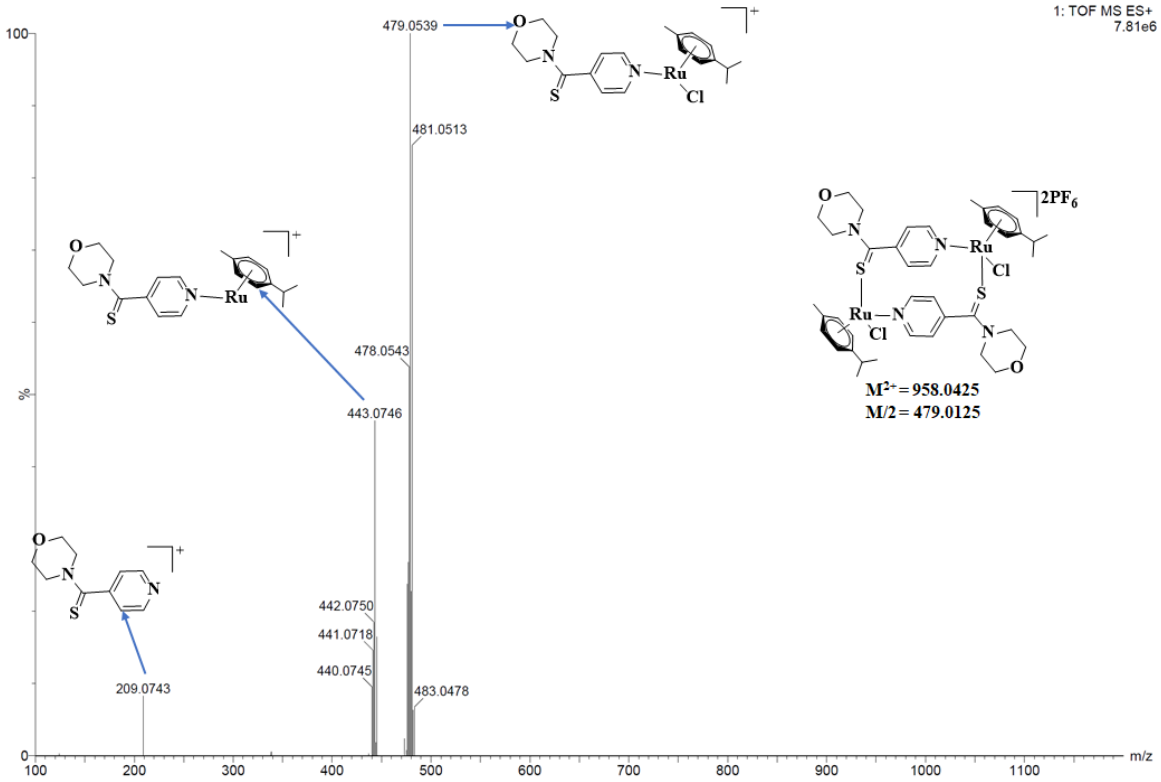

Figure S40: ESI Mass spectrum of complex (**11**) in Acetonitrile

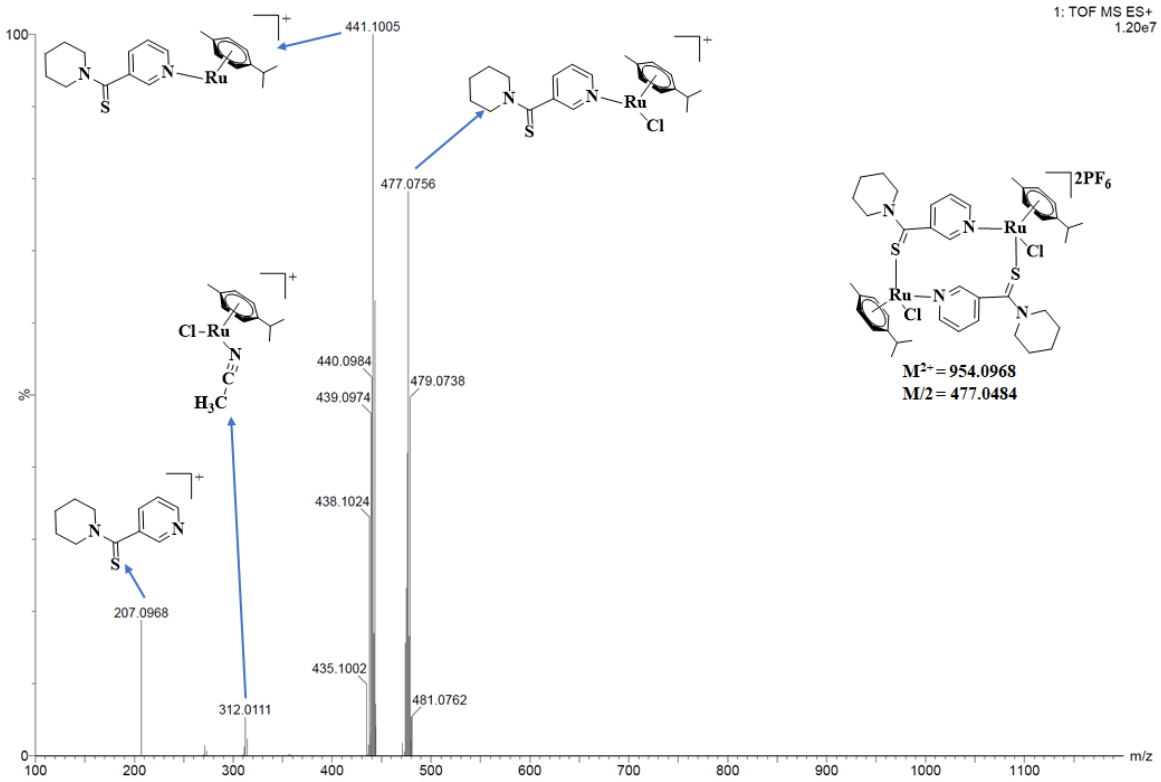

Figure S41: ESI Mass spectrum of complex (**12**) in Acetonitrile

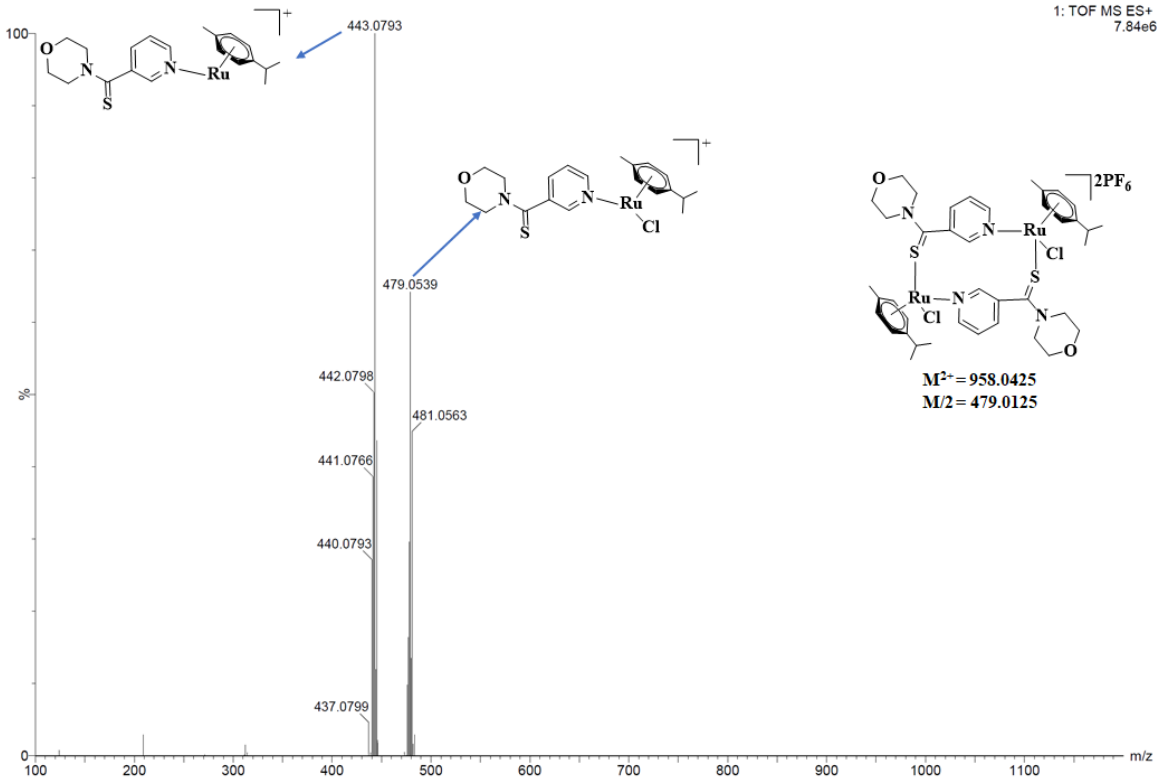

Figure S42: ESI Mass spectrum of complex (**13**) in Acetonitrile

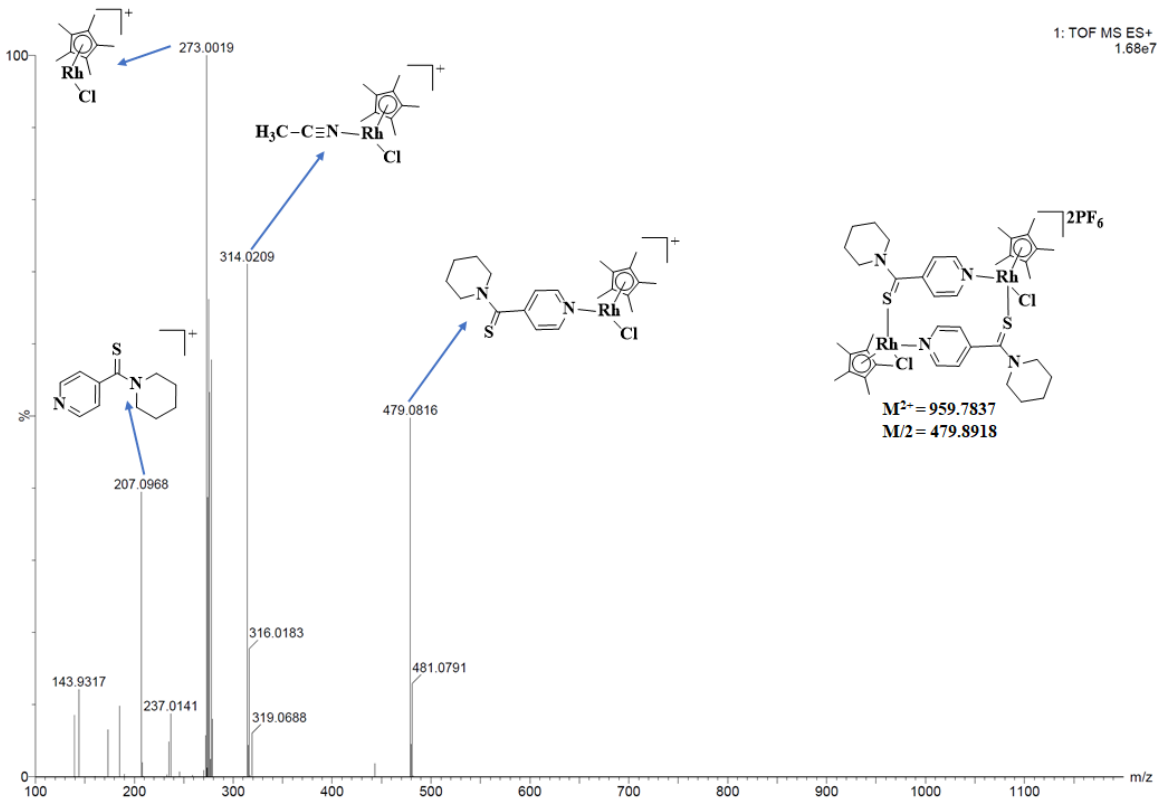

Figure S43: ESI Mass spectrum of complex (**14**) in Acetonitrile

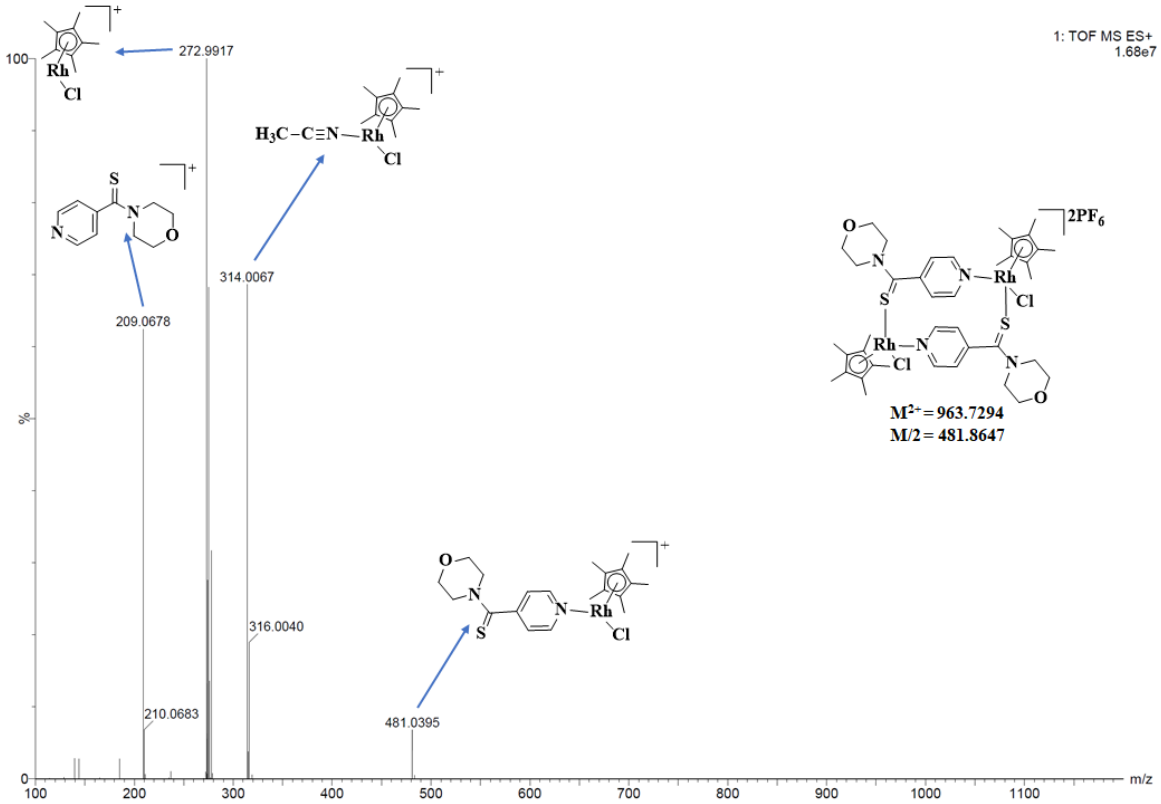

Figure S44: ESI Mass spectrum of complex (**15**) in Acetonitrile

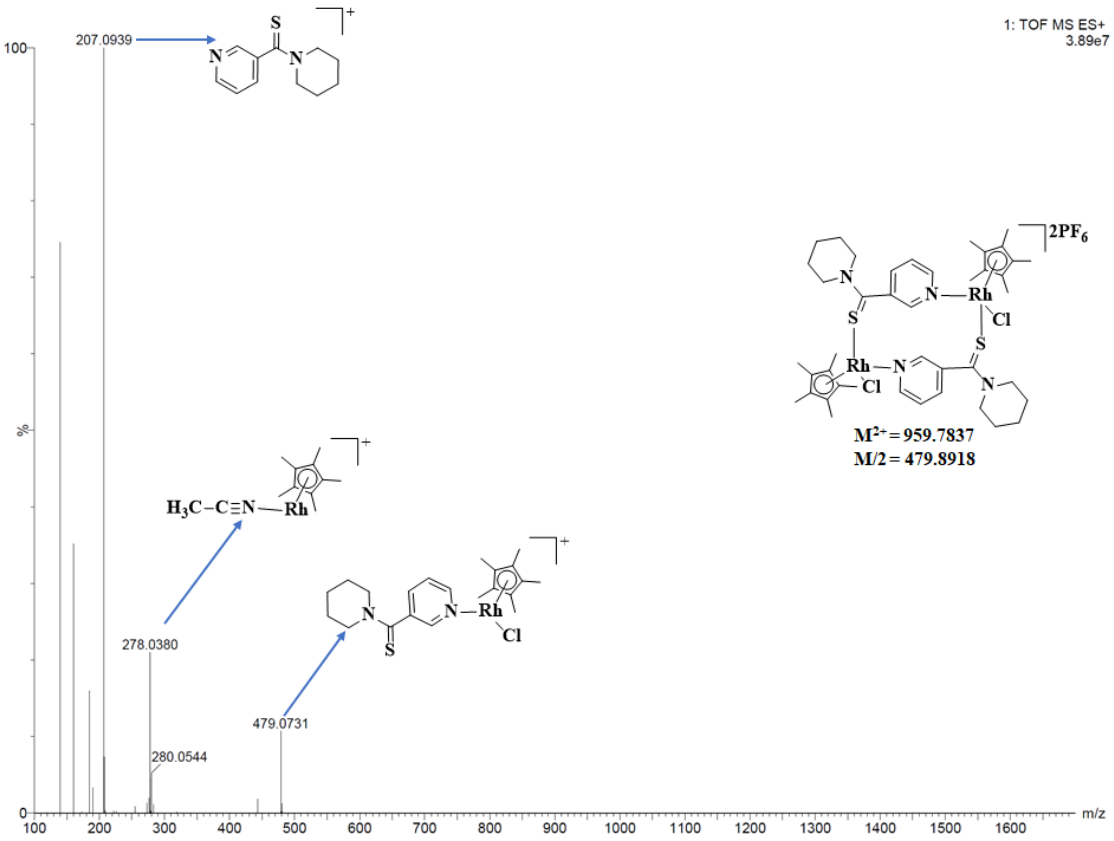

Figure S45: ESI Mass spectrum of complex (**16**) in Acetonitrile

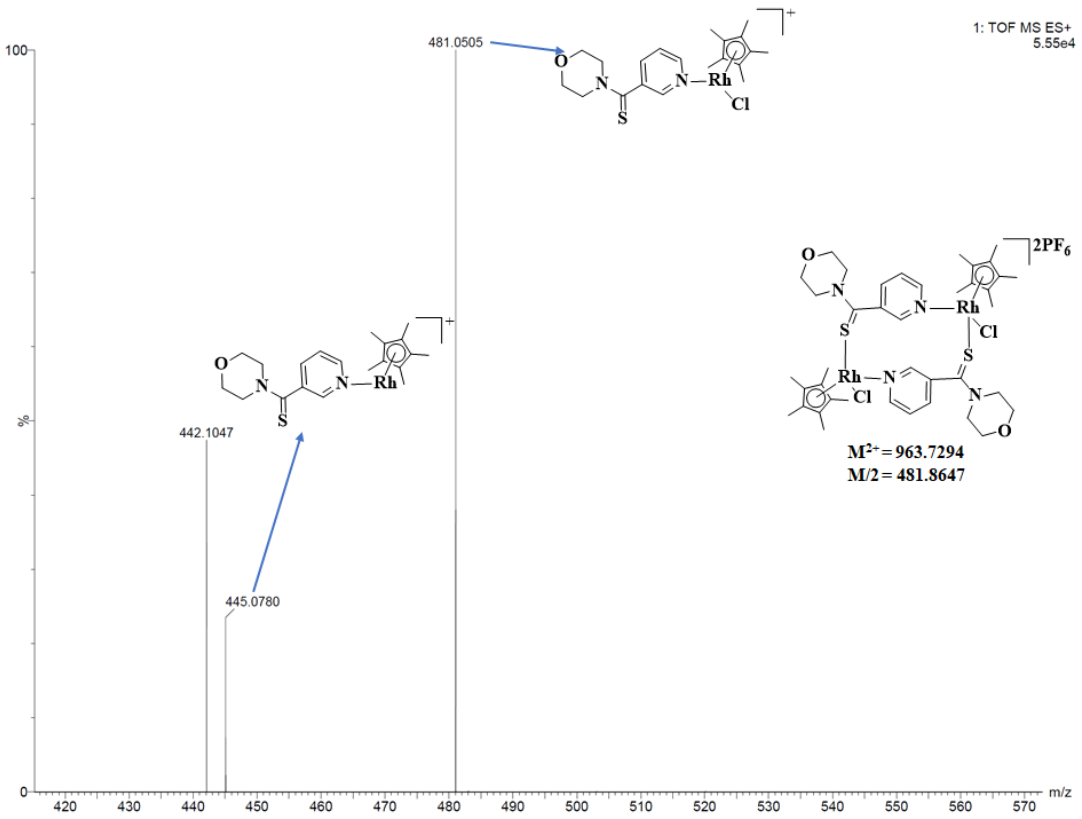

Figure S46: ESI Mass spectrum of complex (**17**) in Acetonitrile

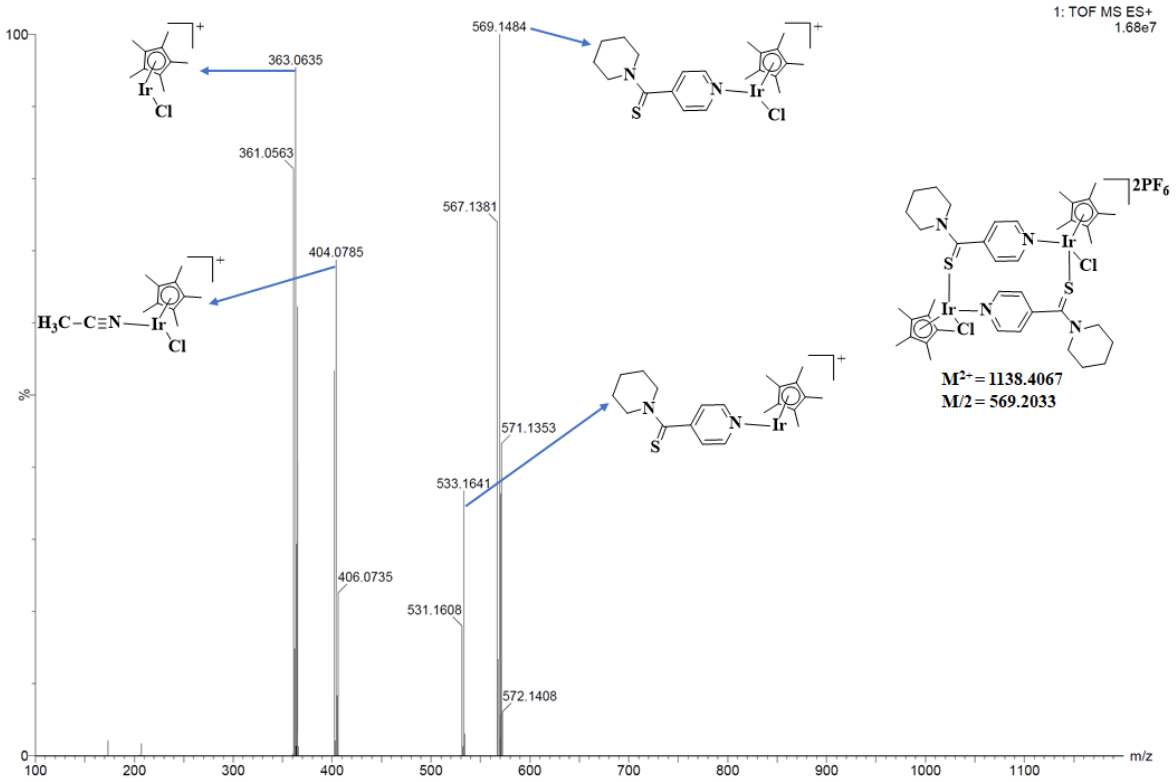

Figure S47: ESI Mass spectrum of complex (**18**) in Acetonitrile

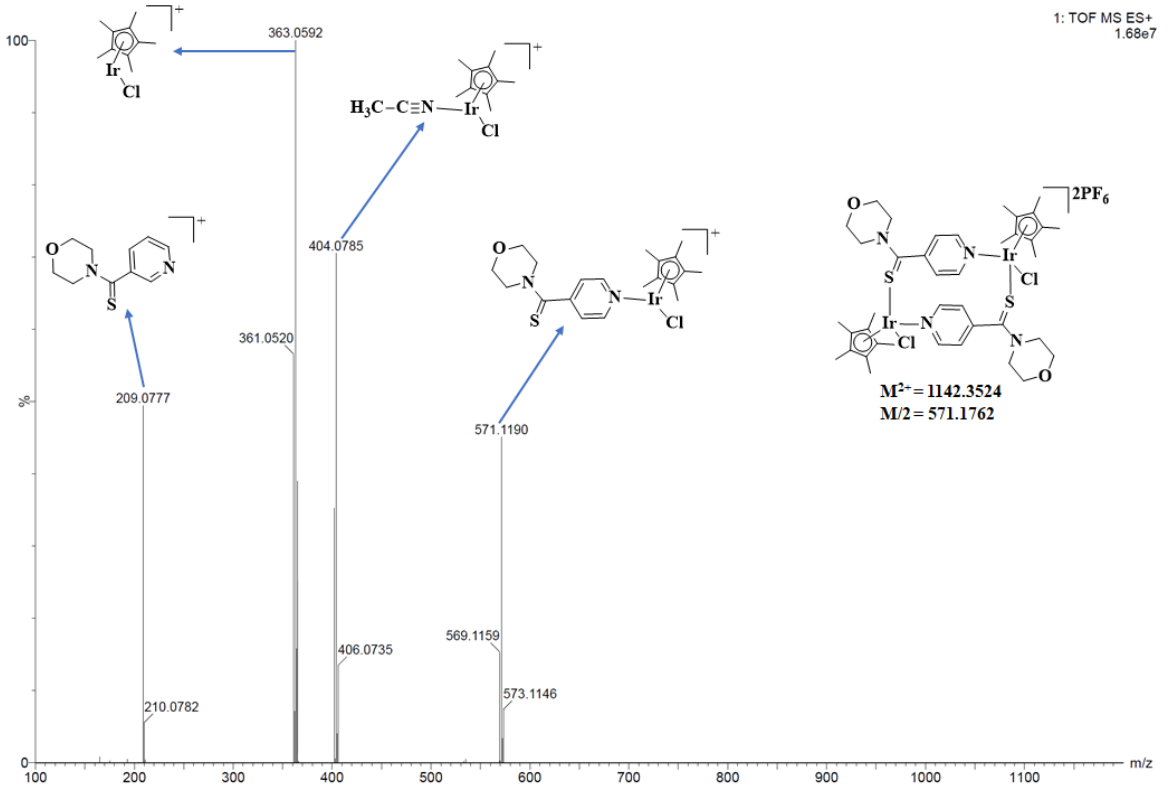

Figure S48: ESI Mass spectrum of complex (**19**) in Acetonitrile

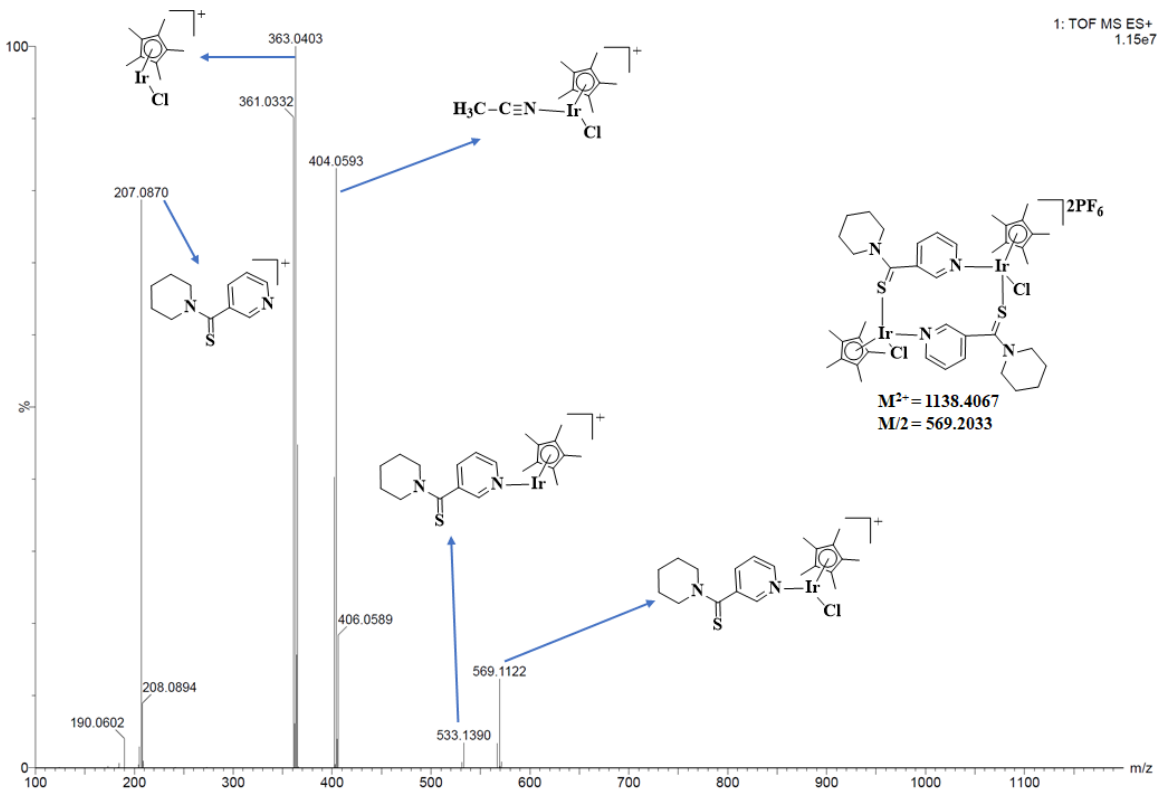

Figure S49: ESI Mass spectrum of complex (**20**) in Acetonitrile

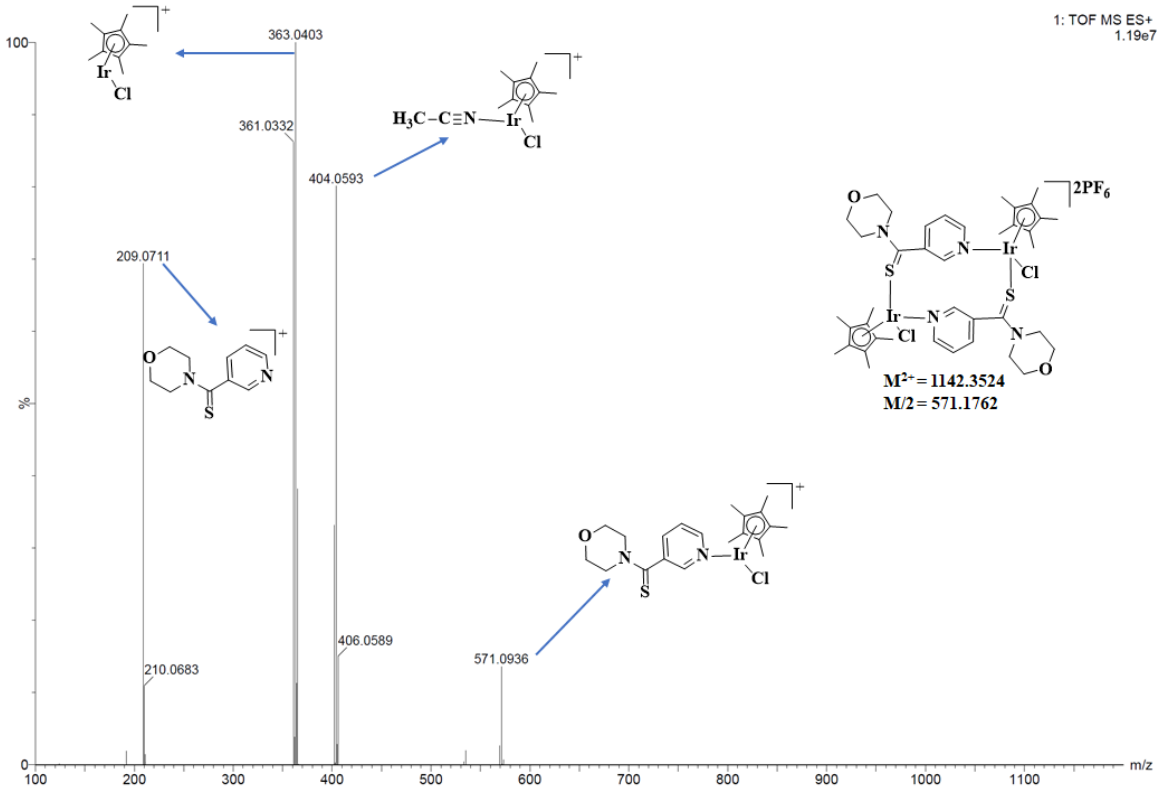

Figure S50: ESI Mass spectrum of complex (**21**) in Acetonitrile

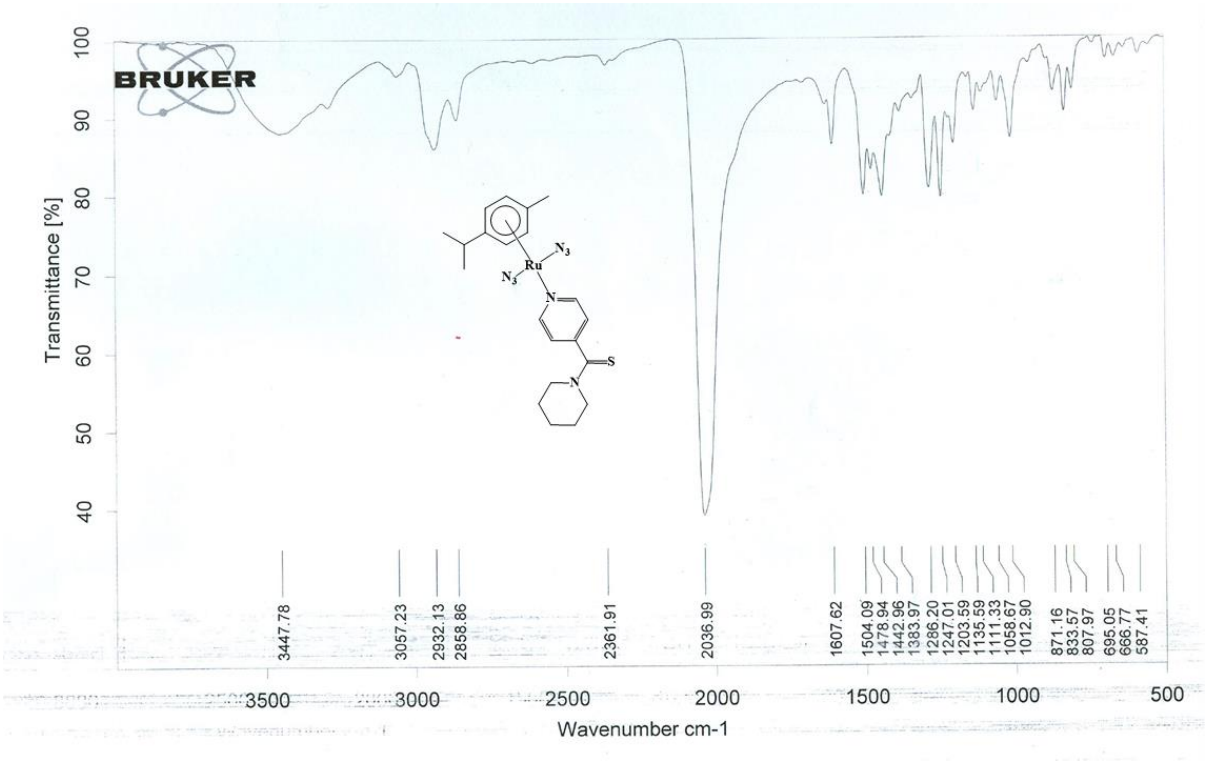

Figure S51: IR spectrum of complex (**22**)

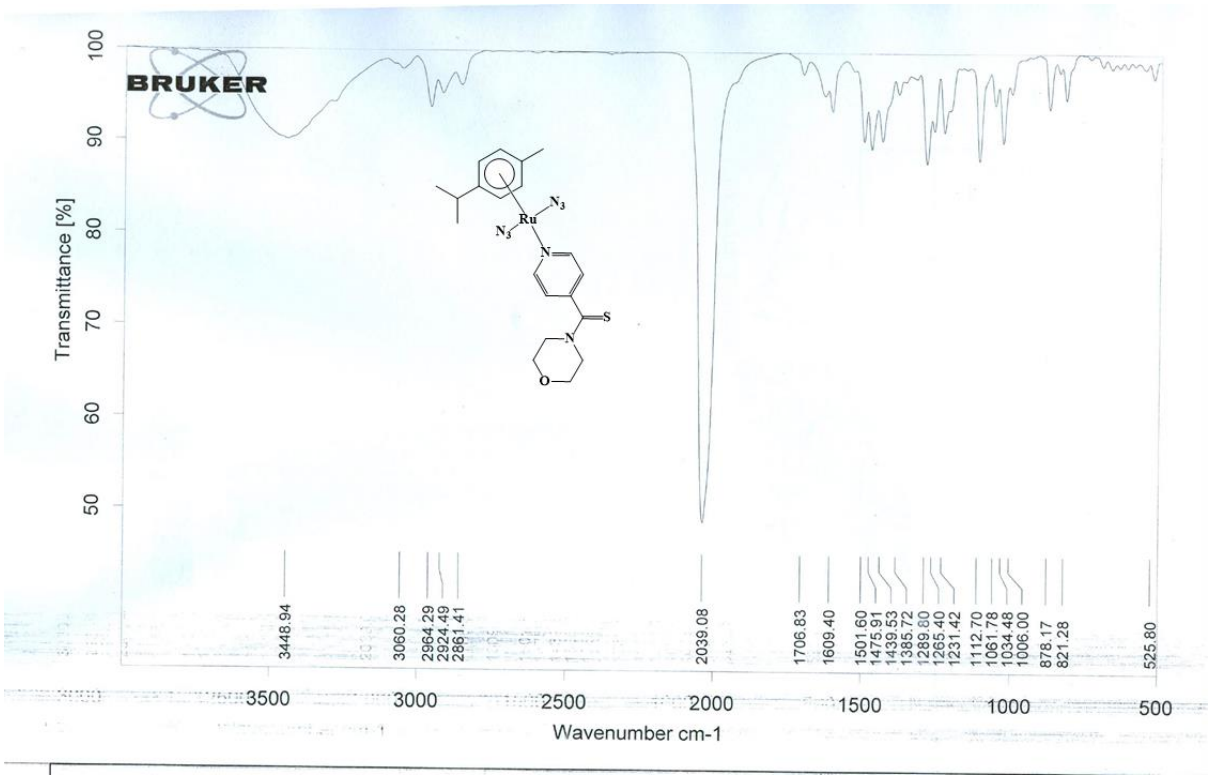

Figure S52: IR spectrum of complex (**23**)

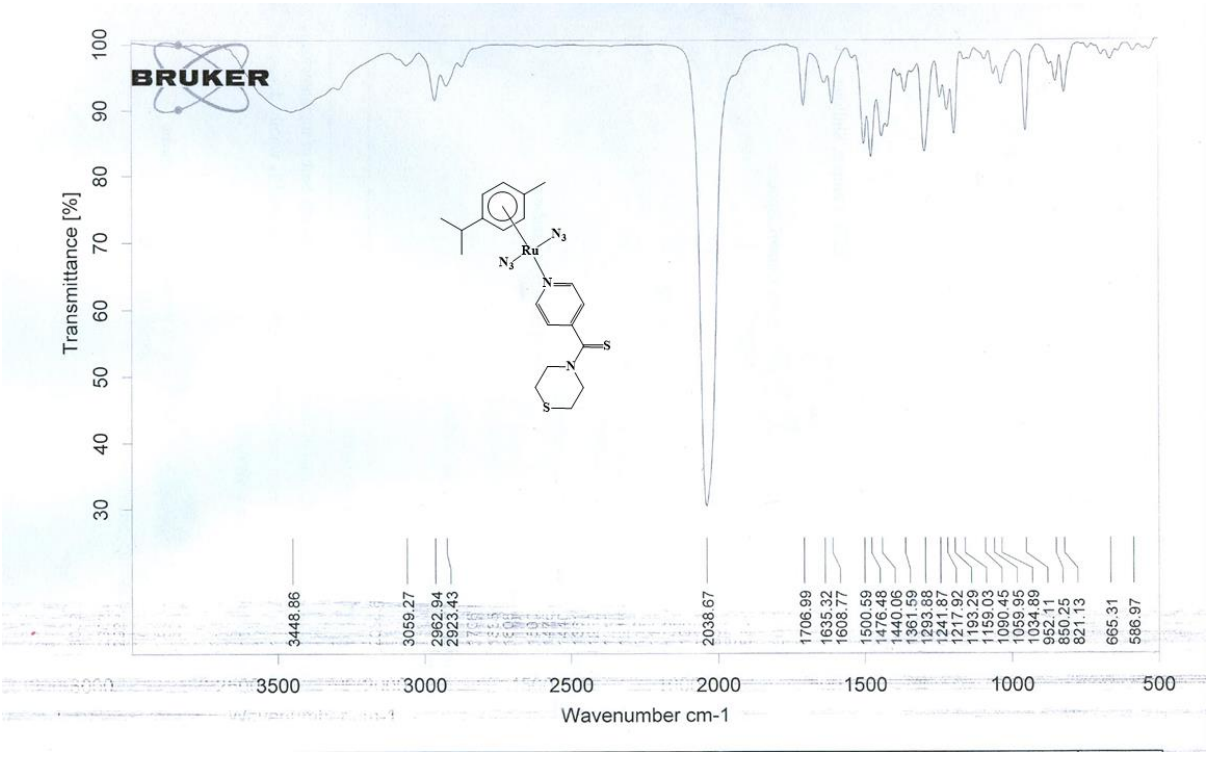

Figure S53: IR spectrum of complex (**24**)

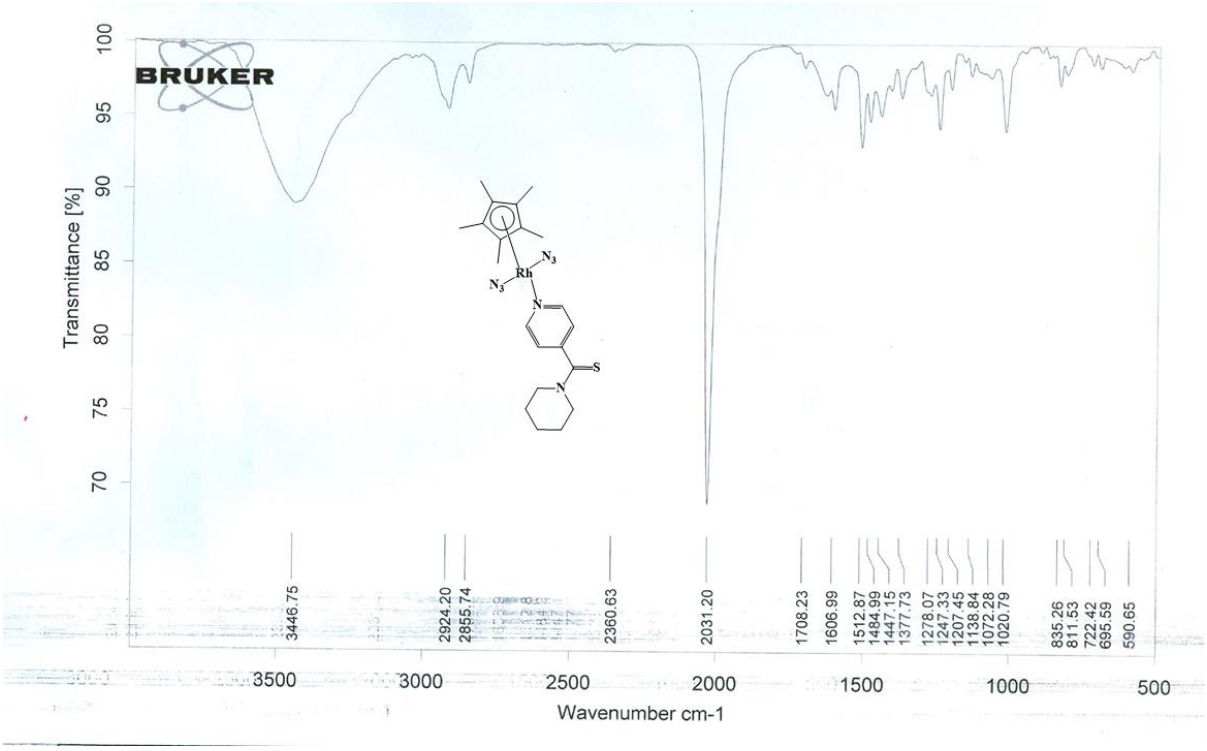

Figure S54: IR spectrum of complex (**25**)

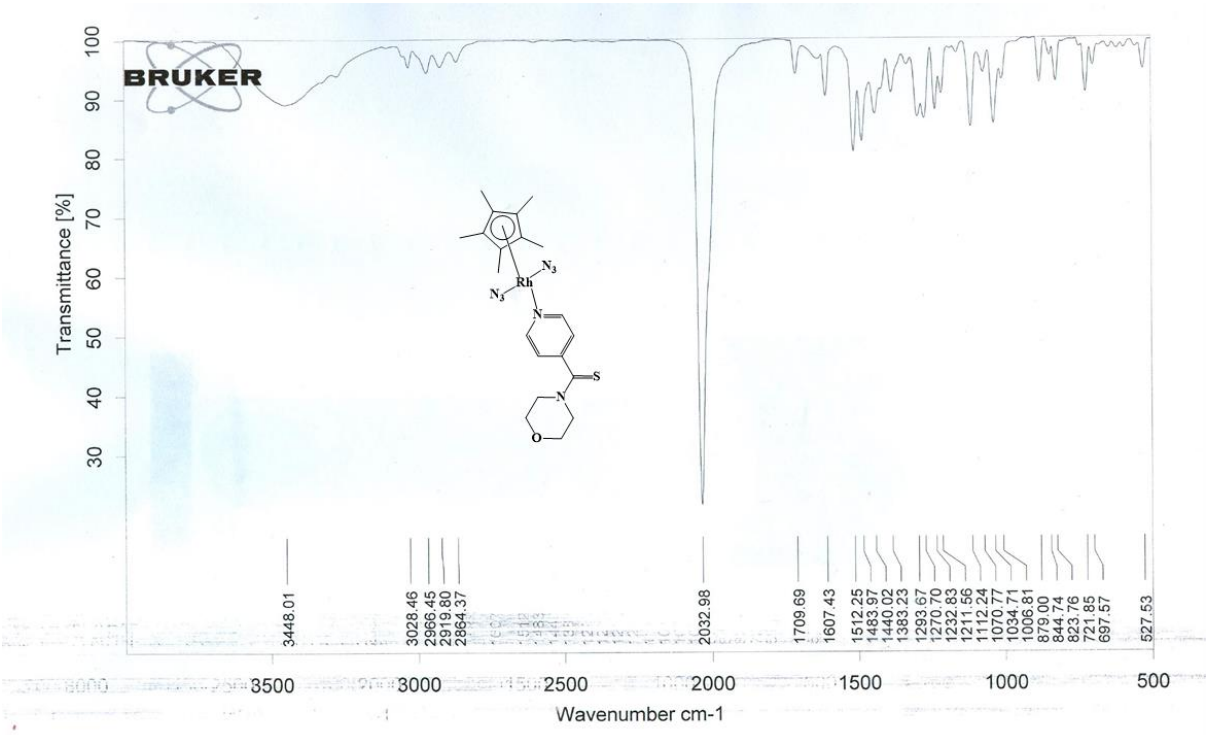

Figure S55: IR spectrum of complex (**26**)

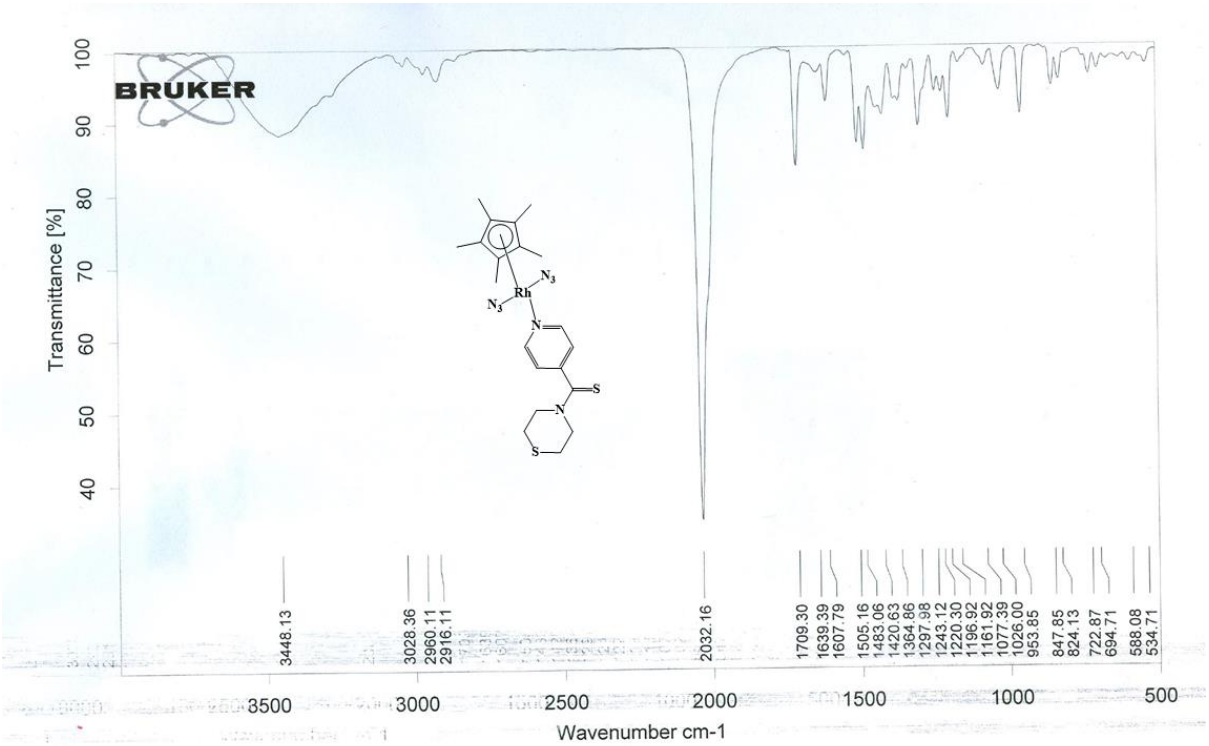

Figure S56: IR spectrum of complex (**27**)

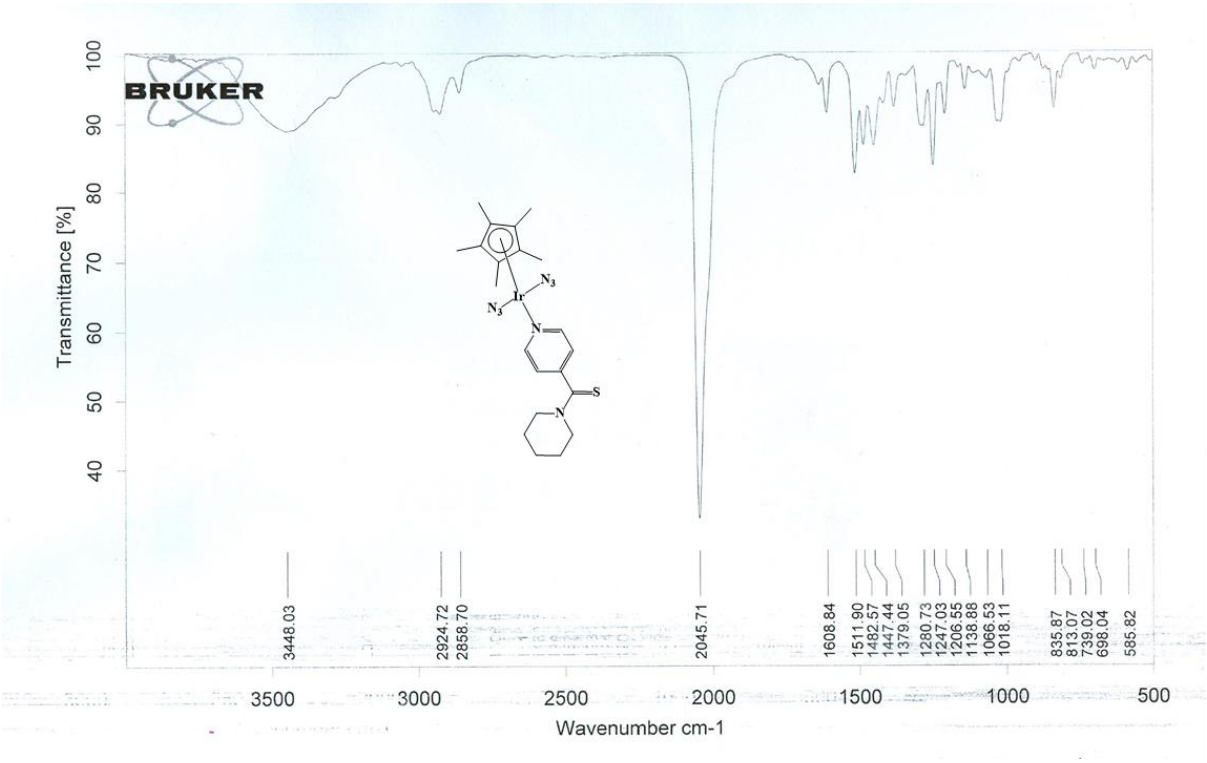

Figure S57: IR spectrum of complex (**28**)

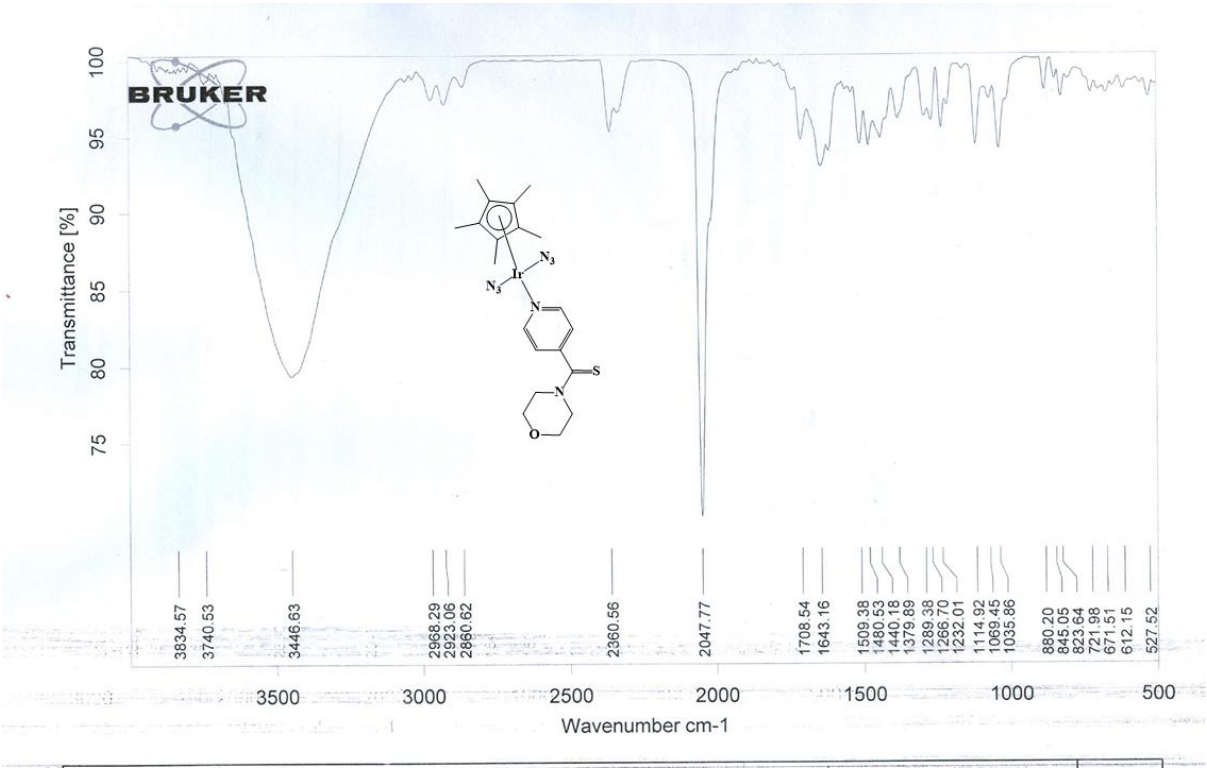

Figure S58: IR spectrum of complex (**29**)

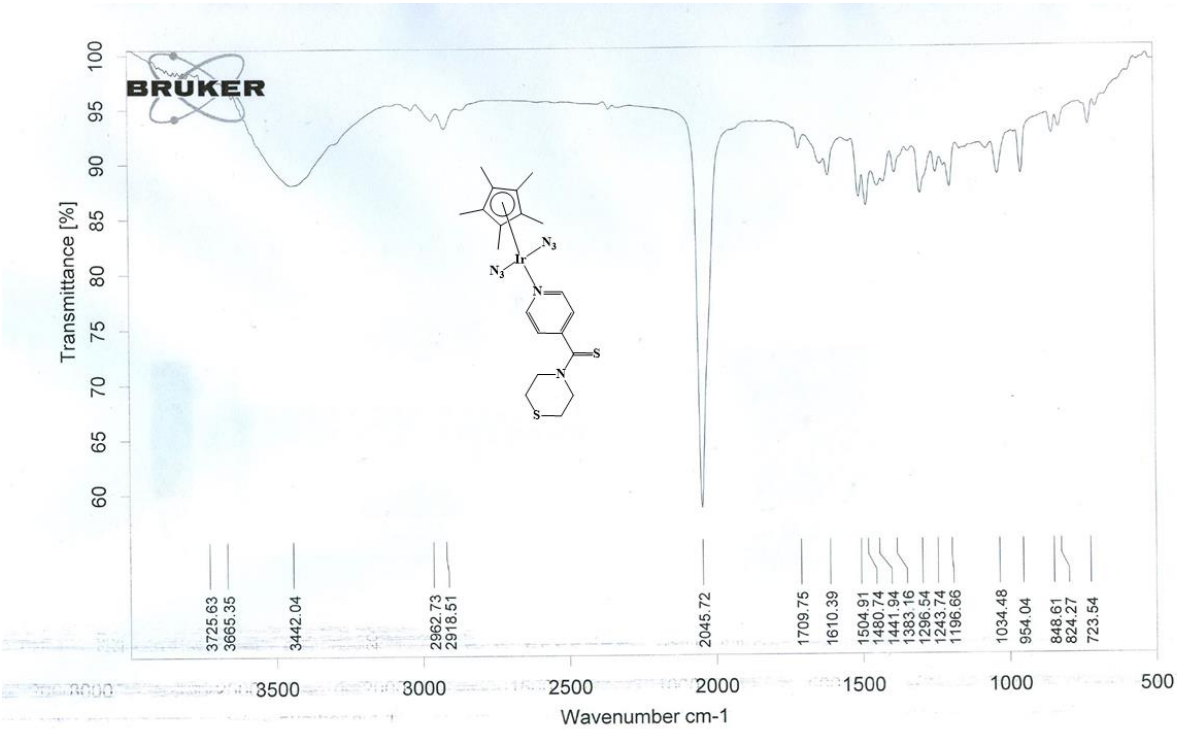

Figure S59: IR spectrum of complex (**30**)

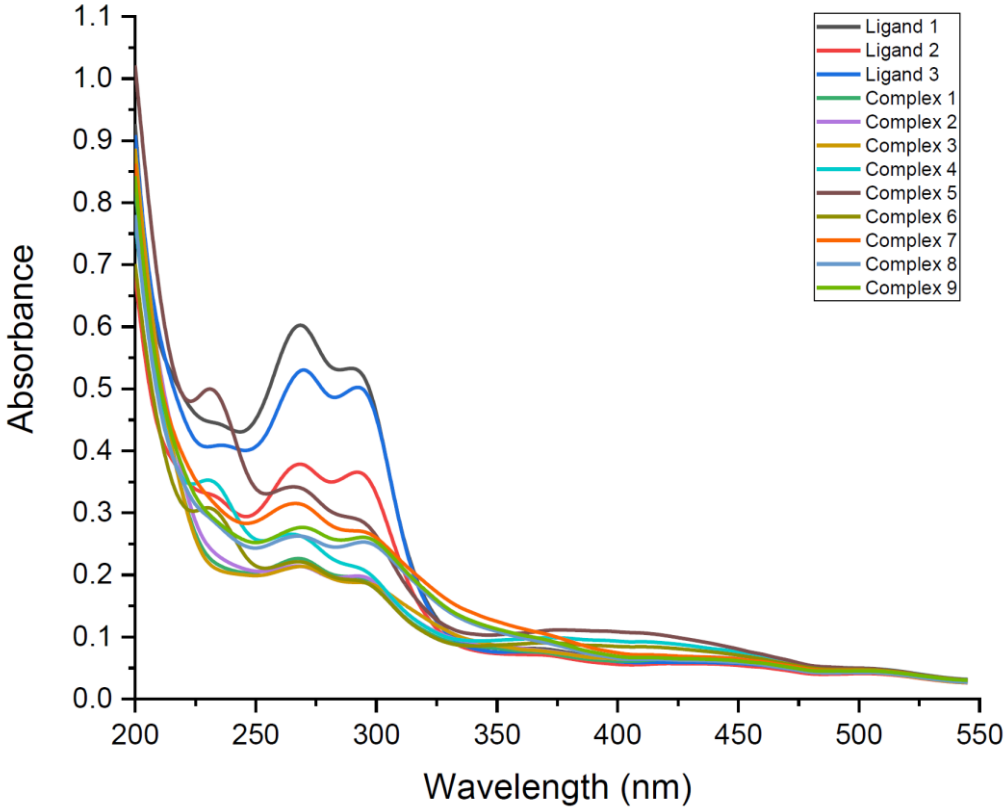

Figure S60: UV-Vis absorption spectra of ligands and mononuclear complexes

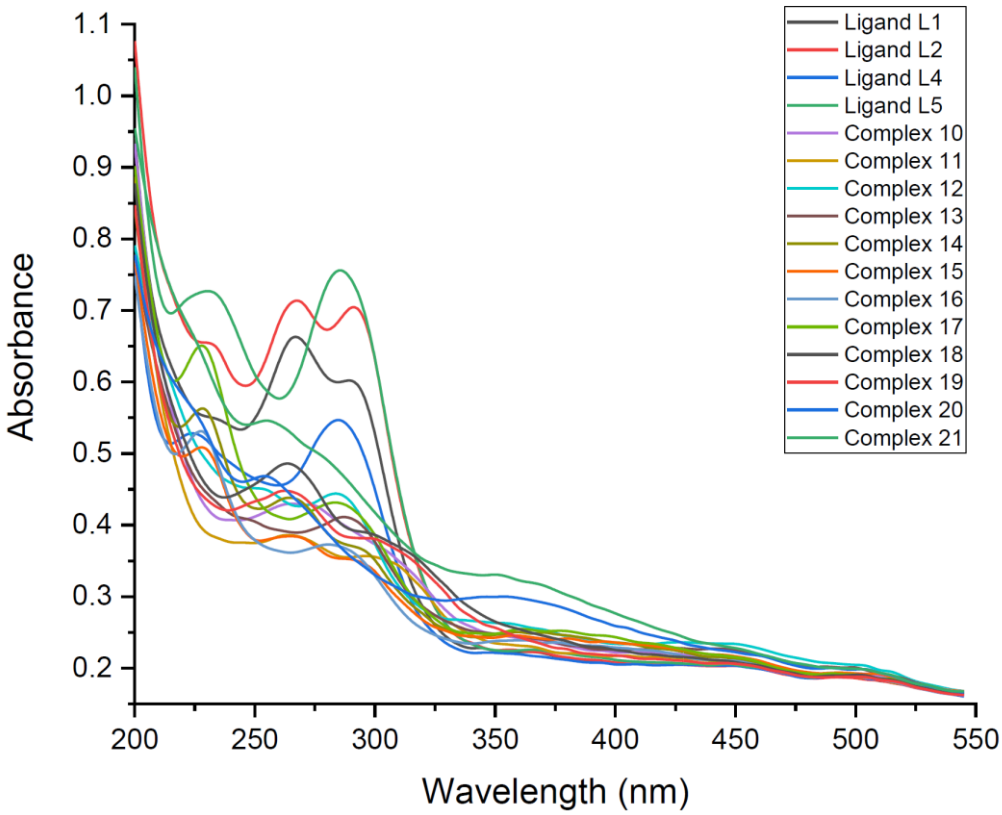

Figure S61: UV-Vis absorption spectra of ligands and dinuclear complexes

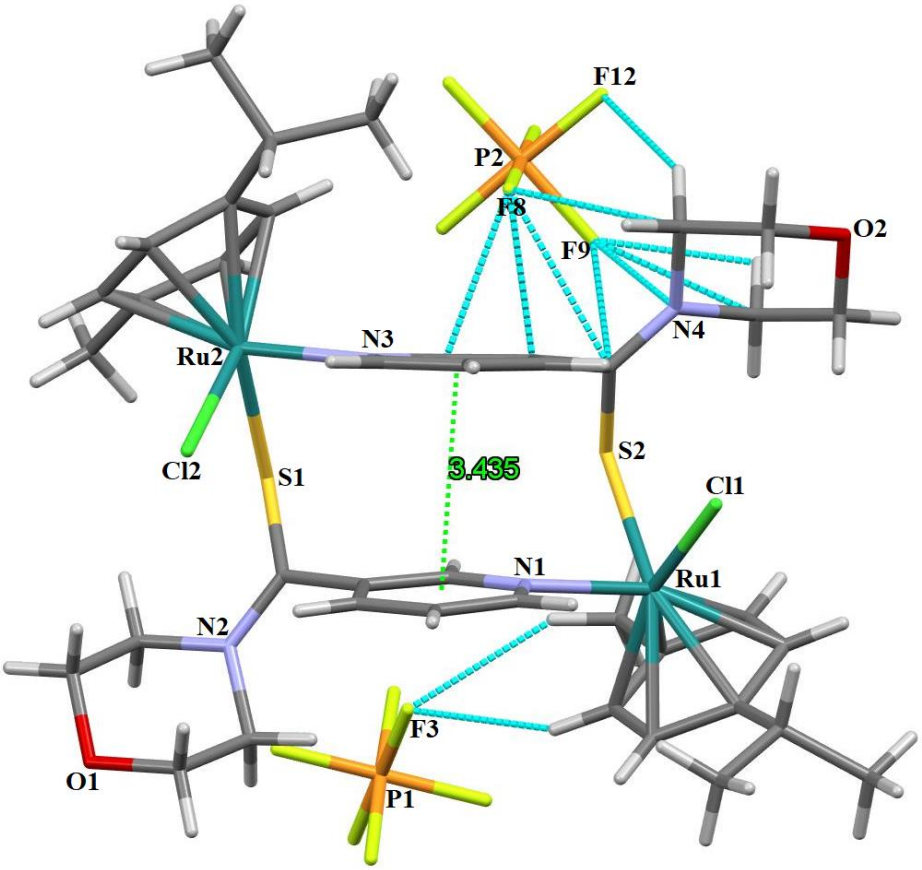

Figure S62: Supramolecular structure of complex **13** showing π-π interaction

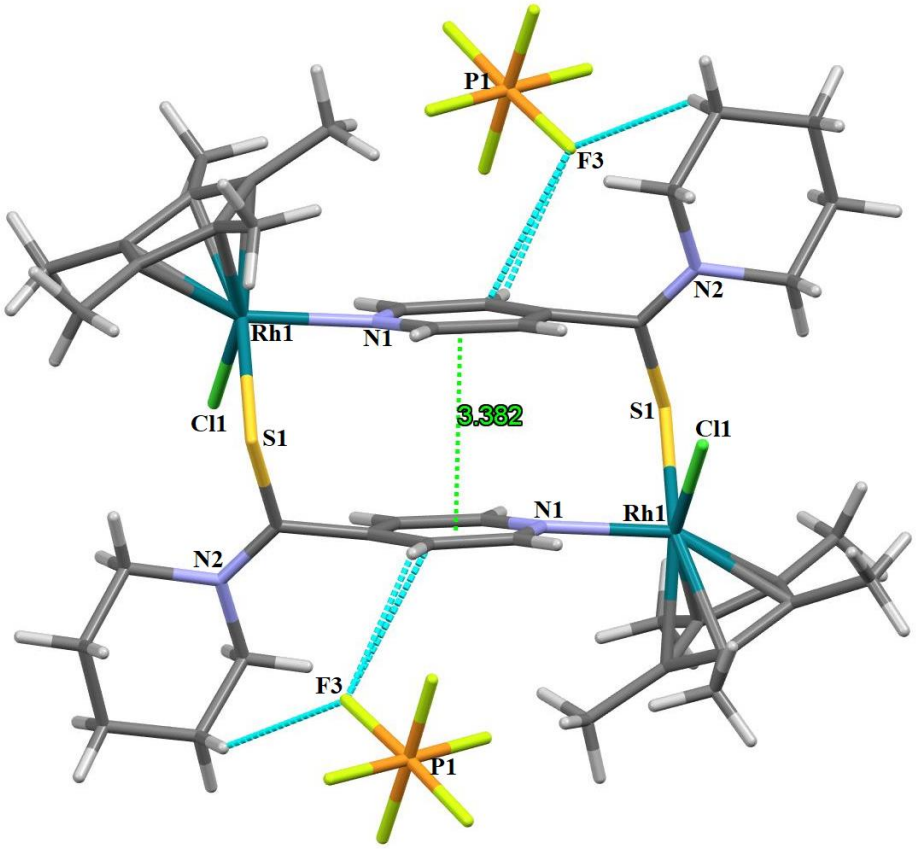

Figure S63: Supramolecular structure of complex **14** showing π-π interaction

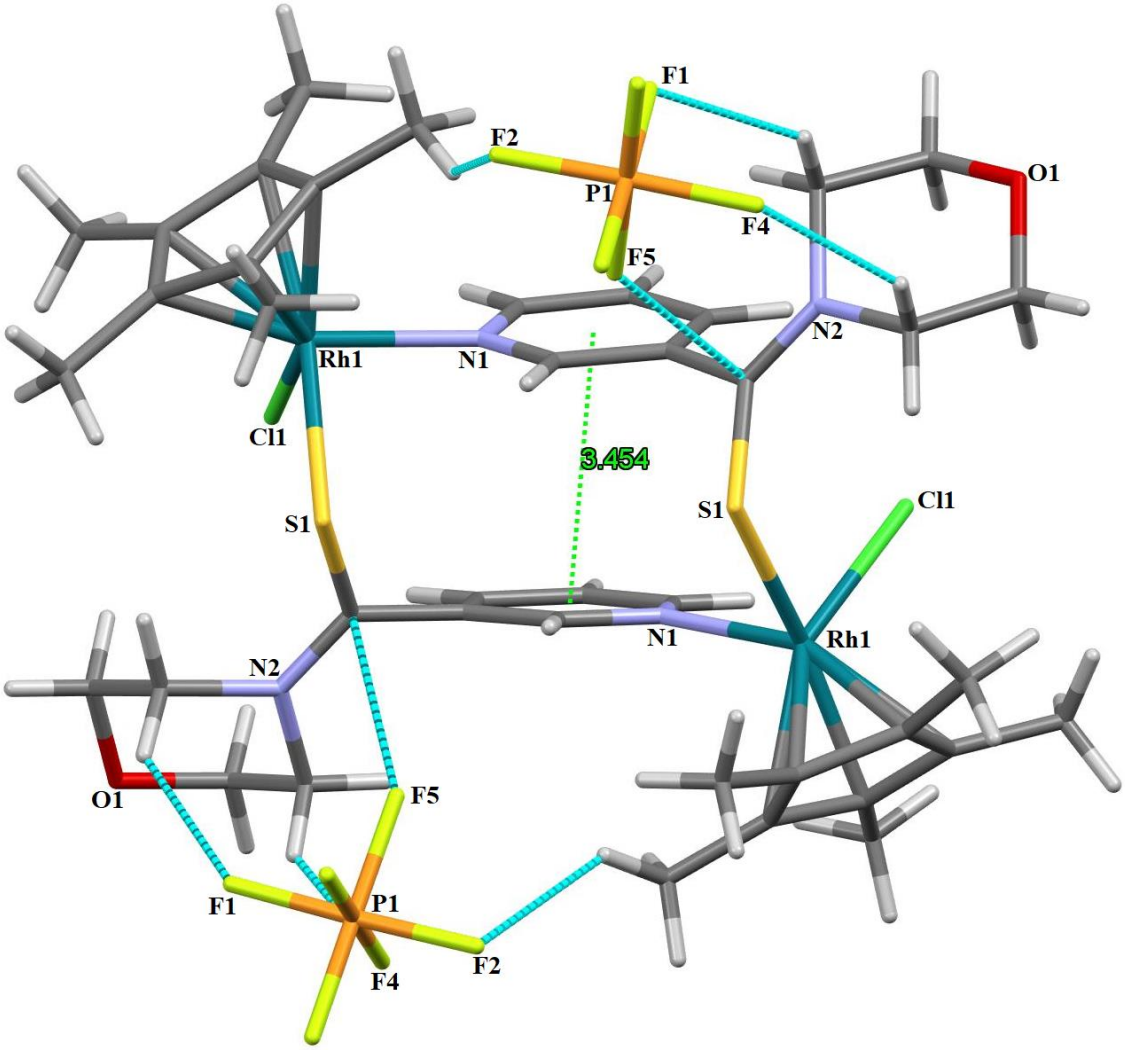

Figure S64: Supramolecular structure of complex **17** showing π-π interaction

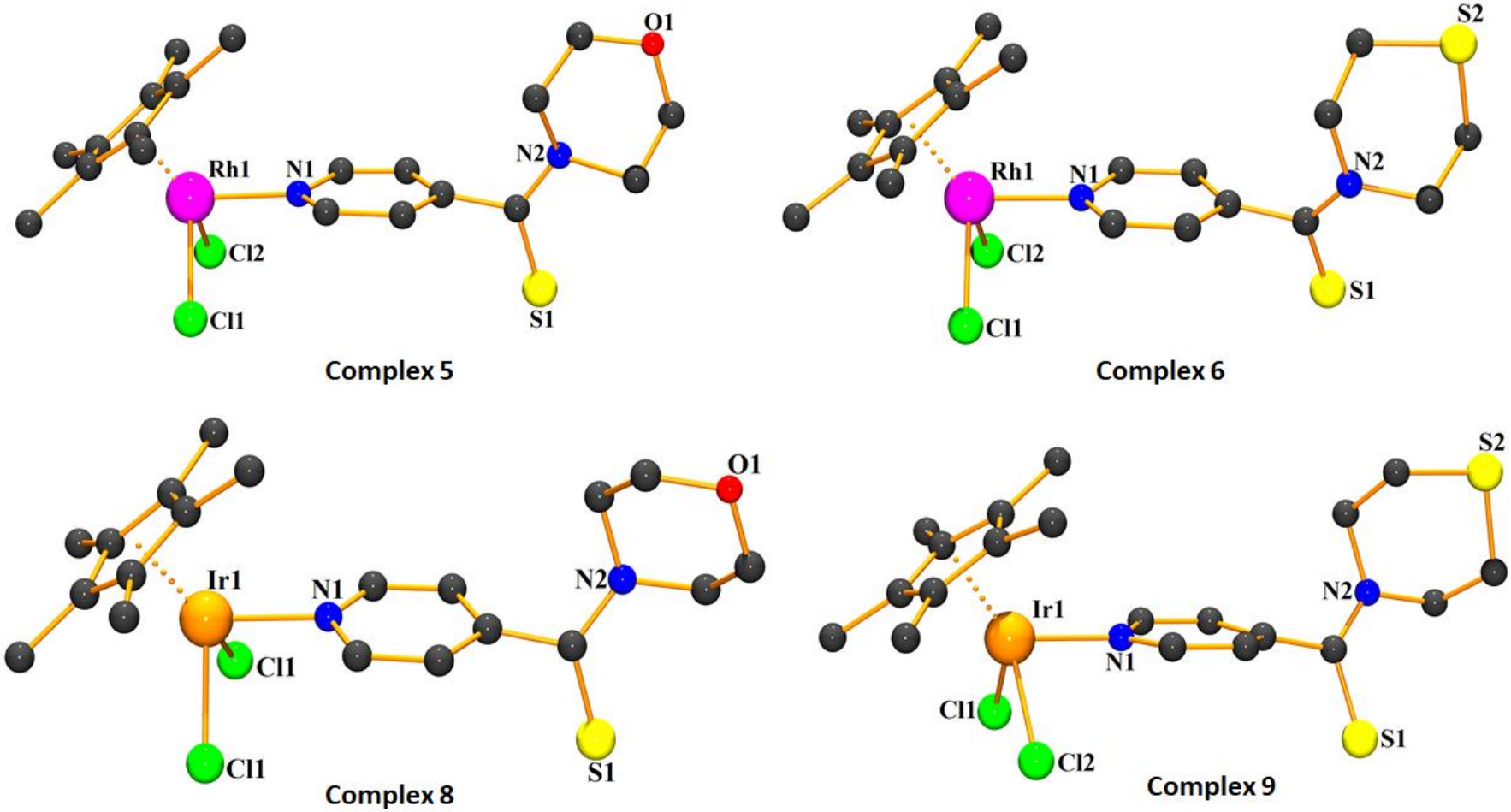

Figure S65: Molecular structure of complexes **5**, **6**, **8** and **9** with a ball and stick representation generated using ORTEP program with 50% thermal ellipsoid probability.

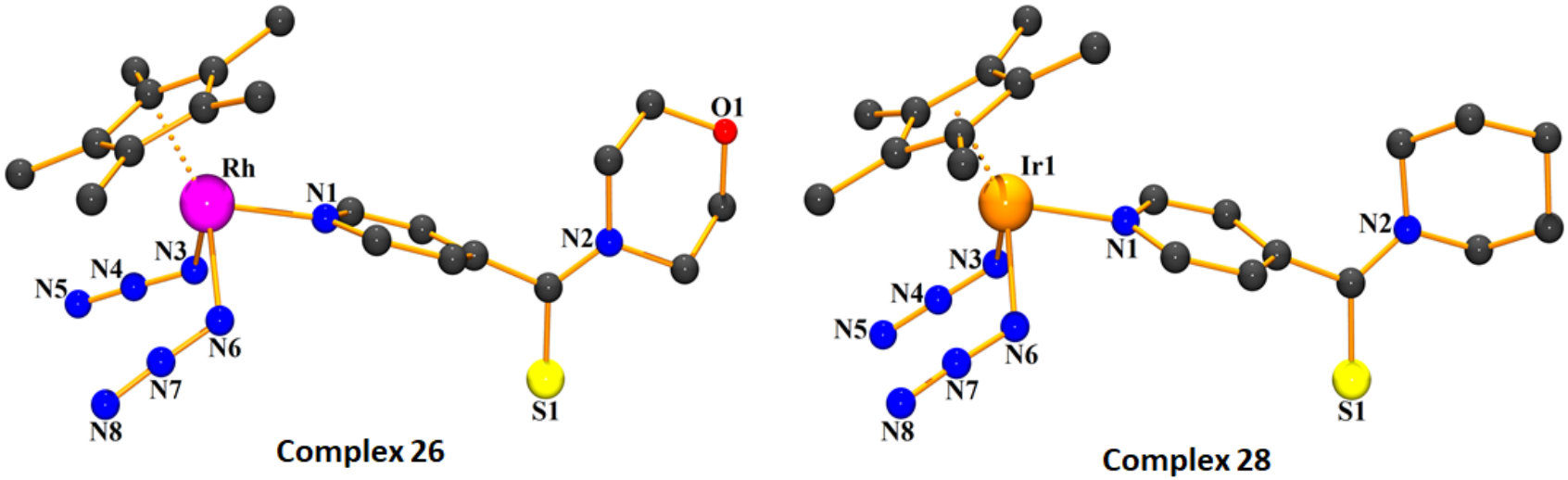

Figure S66: Molecular structure of complexes **26** and **28** with a ball and stick representation generated using ORTEP program with 50% thermal ellipsoid probability.

Table S1: Crystal structure data and refinement of complexes **1**, **2**, **3**, **4**, **5**, **6** and **8**

Complexes	[**1**]	[**2**]	[**3**]	[**4**]	[**5**]	[**6**]	[**8**]
Empirical formula	$C_{21}H_{28}Cl_2N_2RuS$	$C_{20}H_{26}Cl_2N_2ORuS$	$C_{20}H_{28}Cl_2ON_2RuS_2$	$C_{21}H_{29}Cl_2N_2RhS$	$C_{21}H_{29}Cl_4ON_2RhS$	$C_{21}H_{29}Cl_4N_2RhS_2$	$C_{21}H_{29}Cl_4ON_2IrS$
Formula weight	512.48	514.46	548.53	515.33	602.23	648.29	691.52
Temperature (K)	100(2) K	297.04(14)	100(2)	100(2)	291(2)	100(2)	294(2)
Wavelength (Å)	0.71073	0.71073	0.71073	0.71073	0.71073	0.71073	0.71073
Crystal system	monoclinic	monoclinic	monoclinic	monoclinic	Orthorhombic	monoclinic	Orthorhombic
Space group	*P2₁/a*	*P2₁/c*	*P2₁/n*	*P2₁/c*	*Pnma*	*P2₁/c*	*Pnma*
a (Å)/α (°)	12.5100(2)/90	13.3700(7)/90	6.3809(3)/90	8.6547(6)/90	8.8528(7)/90	11.1857(12)/90	8.6022(9)/90
b (Å)/β (°)	14.7339(3)/108.9790(10)	14.7014(7)/114.256(6)	15.1058(6)/91.467(2)	21.2189(15)/99.337(4)	11.3841(16)/90	26.677(3)/90.582(6)	11.3914(10)/90
c (Å)/γ (°)	12.8760(3)/90	12.4251(6)/90	23.3279(10)/90	12.3191(10)/90	26.096(2)/90	8.491(8)/90	26.1587(18)/90
Volume ($Å^3$)	2244.30(8)	2226.6(2)	2247.81(17)	2232.3(3)	2549.8(5)	2533.7(4)	2563.3(4)
Z	4	4	4	4	4	4	4
Density (calc) (g/cm^{-3})	1.517	1.535	1.621	1.533	1.569	1.621	1.792
Absorption coefficient	1.038	1.050	1.135	1.107	1.187	1.273	5.723
F(000)	1048	1048	1120	1056	1224	1256	1352
Crystal size (mm^3)	0.55 x 0.30 x 0.15	0.21 x 0.15 x0.12	0.40 x 0.20 x 0.14	0.18 x 0.13 x 0.11	0.15 x 0.13 x 0.12	0.27 x 0.20 x 0.15	0.25 x 0.23 x 0.21
Theta range for data collection	3.090 to 28.277°	6.472 to 52.744°	1.606 to 28.473	1.919 to 28.441°.	3.358 to 28.966°	1.527 to 26.611°	3.352 to 25.023°
Index ranges	-16<=h<=16, -19<=k<=18, -17<=l<=17	-16<=h<=15, -18<=k<=14, -15<=l<=14	-8<=h<=8, -20<=k<=20, -31<=l<=31	-11<=h<=11, -28<=k<=28, -16<=l<=16	-11<=h<=6, -10<=k<=15, -32<=l<=23	-13<=h<=13, -33<=k<=33, -10<=l<=10	-10<=h<=9, -13<=k<=6, -29<=l<=31
Reflections collected	9829	8636	11032	11027	7038	77503	5319
Independent reflections	5512 [R_{int} = 0.0478]	4516 [R_{int} = 0.0230]	5644 [R_{int} = 0.0113]	5611 [R_{int} = 0.0239]	3097 [R_{int} = 0.0453]	5216 [R_{int} = 0.0693]	2303 [R_{int} = 0.0566]
Completeness to theta = 25.00°	99.7 %	99.09 %	100.0 %	100.0 %	99.4 %	100.0 %	96.5 %
Absorption correction	Semi-empirical from equivalents	Semi-empirical from equivalents	Semi-empirical from equivalents	Semi-empirical from equivalents	Semi-empirical from equivalents	Semi-empirical from equivalents	Semi-empirical from equivalents
Refinement method	Full-matrix least-squares on F^2	Full-matrix least-squares on F^2	Full-matrix least-squares on F2	Full-matrix least-squares on F^2	Full-matrix least-squares on F2	Full-matrix least-squares on F2	Full-matrix least-squares on F2
Data/restraints/parameters	5512/6/247	4516/0/247	5644/0/264	5611/12/286	3097/96/198	5216/116/306	2303/108/205
Goodness-of-fit on F_2	0.999	1.087	1.072	1.034	1.076	1.135	1.086
Final R indices [I>2sigma(I)]	R1 = 0.0429, wR2 = 0.0878	R1 = 0.0318, wR2 = 0.0688	R1 = 0.0210, wR2 = 0.0487	R1 = 0.0369, wR2 = 0.0799	R1 = 0.0487, wR2 = 0.0951	R1 = 0.0715, wR2 = 0.2014	R1 = 0.0511, wR2 = 0.1140
R indices (all data)	R1 = 0.0646, wR2 = 0.0955	R1 = 0.0392, wR2 = 0.0720	R1 = 0.0229, wR2 = 0.0496	R1 = 0.0411, wR2 = 0.0834	R1 = 0.0706, wR2 = 0.1068	R1 = 0.0766, wR2 = 0.2094	R1 = 0.0570, wR2 = 0.1175
Largest diff. peak and hole ($e.Å^{-3}$)	1.408 and -1.452	0.42 and -0.57	0.938 and -0.585	2.102 and -1.644	0.495 and -0.707	2.347 and -2.747	2.806 and -2.865
CCDC No.	2154928	2154929	2154930	2154931	2154932	2154934	2154933

Structures were refined on F_0^2: $wR_2 = [\Sigma[w(F_0^2 - F_c^2)^2] / \Sigma w(F_0^2)^2]^{1/2}$, where $w^{-1} = [\Sigma(F_0^2)+(aP)^2+bP]$ and $P = [\max(F_0^2, 0)+2F_c^2]/3$

Table S2: Crystal structure data and refinement of complexes **9**, **13**, **14**, **17** and **18**

Complexes	[**9**]	[**13**]	[**14**]	[**17**]	[**18**]
Empirical formula	$C_{21}H_{29}Cl_4N_2IrS_2$	$C_{40}H_{52}Cl_2N_4S_2O_2Ru_2P_2F_{12}$	$C_{42}H_{58}Cl_2N_4S_2Rh_2P_2F_{12}$	$C_{43}H_{60}Cl_2N_4S_2O_3Rh_2P_2F_{12}$	$C_{42}H_{58}Cl_2N_4S_2Ir_2P_2F_{12}$
Formula weight	707.58	1247.95	1249.70	1311.73	1428.28
Temperature (K)	100(2)	100(2) K	100(2)	100(2) K	100(2)
Wavelength (Å)	0.71073	0.71073 Å	0.71073	0.71073 Å	0.71073
Crystal system	monoclinic	Triclinic	triclinic	Monoclinic	Monoclinic
Space group	*$P2_1/c$*	P -1	*P-1*	C 2/c	P 21/c
a (Å)/α (°)	11.1464(10)/90	13.6056(7)/82.735(3)	7.959(2)/97.420(19)	22.0955(16)/90	8.2773(2)/90
b (Å)/β (°)	26.663(2)/90.400(5)	14.0473(8)/64.600(3)	12.268(3)/99.95(2)	16.5036(16)/101.726(5)	12.9050(4)/91.1090(10)
c (Å)/γ (°)	8.4706(8)/90	14.1811(8)/71.903(3)	13.193(4)/102.764(16)	14.8446(13)/90	22.8179(10)/90
Volume ($Å^3$)	2517.3(4)	2327.1(2)	1218.6(6)	5300.2(8)	2436.92(14)
Z	4	2	1	4	2
Density (calc) (g/cm^{-3})	1.867	1.781	1.703	1.644	1.946
Absorption coefficient	5.907	1.012	1.021	0.947	5.799
F(000)	1384	1256	632	2656	1392
Crystal size (mm^3)	0.15 x 0.13 x 0.10	0.60 x 0.40 x 0.20	0.09 x 0.08 x 0.08	0.60 x 0.45 x 0.40	0.08 x 0.07 x 0.05
Theta range for data collection	1.527 to 28.487°	1.525 to 28.408°	1.591 to 25.393°	1.552 to 28.464°	1.785 to 28.262°
Index ranges	-14<=h<=14, -35<=k<=35, -11<=l<=11	-18<=h<=18, -18<=k<=18, -18<=l<=18	-9<=h<=9, -14<=k<=14, -15<=l<=15	-29<=h<=29, -22<=k<=22, -19<=l<=19	-10<=h<=10, -14<=k<=15, -30<=l<=29
Reflections collected	79425	23141	4480	25863	10200
Independent reflections	6336 [R_{int} = 0.0525]	11624 [R(int) = 0.0290]	4480 [R(int) = 0.1368]	6652 [R(int) = 0.0120]	5493 [R(int) = 0.0774]
Completeness to theta = 25.00°	100.0 %	100.0 %	100.0 %	99.8 %	97.7 %
Absorption correction	Semi-empirical from equivalents	Semi-empirical from equivalents	Semi-empirical from equivalents	Semi-empirical from equivalents	Semi-empirical from equivalents
Refinement method	Full-matrix least-squares on F^2	Full-matrix least-squares on F^2	Full-matrix least-squares on F^2	Full-matrix least-squares on F2	Full-matrix least-squares on F^2
Data/restraints/parameters	6336/40/284	11624/63/647	4480/54/304	6652/171/399	5493/0/303
Goodness-of-fit on F_2	1.156	1.043	0.931	1.059	0.911
Final R indices [I>2sigma(I)]	R1 = 0.0425, wR2 = 0.0971	R1 = 0.0432, wR2 = 0.0987	R1 = 0.0688, wR2 = 0.1377	R1 = 0.0190, wR2 = 0.0440	R1 = 0.0418, wR2 = 0.0701
R indices (all data)	R1 = 0.0484, wR2 = 0.0998	R1 = 0.0596, wR2 = 0.1052	R1 = 0.1657, wR2 = 0.1859	R1 = 0.0203, wR2 = 0.0448	R1 = 0.0974, wR2 = 0.0808
Largest diff. peak and hole ($e.Å^{-3}$)	3.387 and -2.682	1.129 and -1.013	1.140 and -1.180	0.562 and -0.473	2.794 and -1.261
CCDC No.	2154935	2154936	2154937	2154938	2154939

Structures were refined on F_0^2: $wR_2 = [\Sigma[w(F_0^2 - F_c^2)^2] / \Sigma w(F_0^2)^2]^{1/2}$, where $w^{-1} = [\Sigma(F_0^2)+(aP)^2+bP]$ and $P = [\max(F_0^2, 0)+2F_c^2]/3$

Table S3: Crystal structure data and refinement of complexes **25**, **26**, **28** and **30**

Complexes	[**25**]	[**26**]	[**28**]	[**30**]
Empirical formula	$C_{22}H_{31}N_8RhS$	$C_{21}H_{29}ON_8RhS$	$C_{22}H_{31}N_8IrS$	$C_{20}H_{27}N_8IrS_2$
Formula weight	613.42	615.39	702.71	635.81
Temperature (K)	100(2)	100(2)	100(2)	100(2)
Wavelength (Å)	0.71073	0.71073	0.71073	0.71073
Crystal system	monoclinic	monoclinic	monoclinic	monoclinic
Space group	$P2_1/c$	$P2_1/c$	$P2_1/c$	$P2_1/a$
a (Å)/α (°)	11.2161(9)/90	11.1527(8)/90	11.1957(5)/90	9.0819(4)/90
b (Å)/β (°)	26.7043(18)/91.737(4)	26.4244(17)/91.855(3)	26.6373(14)/91.619(3)	26.5743(13)/90.582(3)
c (Å)/γ (°)	8.8228(7)/90	8.7878(6)/90	8.8859(10)/90	11.1669(6)/90
Volume ($Å^3$)	2641.4(3)	2588.4(3)	2648.9(3)	2694.9(2)
Z	4	4	4	4
Density (calc) (g/cm^{-3})	1.543	1.579	1.762	1.567
Absorption coefficient	0.955	0.978	5.348	5.131
F(000)	1256	1256	1384	1248
Crystal size (mm^3)	0.15 x 0.14 x0.12	0.30 x 0.10 x 0.05	0.15 x 0.03 x 0.02	0.22 x 0.16 x 0.10
Theta range for data collection	1.525 to 28.355°	1.541 to 28.536	1.529 to 25.026°.	0.766 to 28.266°
Index ranges	-14<=h<=14, -35<=k<=35, -11<=l<=11	-14<=h<=14, -35<=k<=35, -11<=l<=11	-13<=h<=13, -31<=k<=31, -10<=l<=10	-12<=h<=11, -34<=k<=35, -14<=l<=14
Reflections collected	13112	83778	9061	10095
Independent reflections	6545 [R_{int} = 0.0161]	6540 [R_{int} = 0.1174]	4586 [R_{int} = 0.0324]	6283 [R_{int} = 0.0658]
Completeness to theta = 25.00°	100.0 %	99.9 %	97.9 %	99.3 %
Absorption correction	Semi-empirical from equivalents	Semi-empirical from equivalents	Semi-empirical from equivalents	Semi-empirical from equivalents
Refinement method	Full-matrix least-squares on F^2	Full-matrix least-squares on F2	Full-matrix least-squares on F^2	Full-matrix least-squares on F2
Data/restraints/parameters	6545/0/313	6540/0/312	4586/9/312	6283/324/310
Goodness-of-fit on F_2	1.098	1.005	1.012	1.287
Final R indices [I>2sigma(I)]	R1 = 0.0347, wR2 = 0.0928	R1 = 0.0346, wR2 = 0.0787	R1 = 0.0266, wR2 = 0.0545	R1 = 0.0570, wR2 = 0.1361
R indices (all data)	R1 = 0.0393, wR2 = 0.0959	R1 = 0.0547, wR2 = 0.0845	R1 = 0.0448, wR2 = 0.0604	R1 = 0.0809, wR2 = 0.1446
Largest diff. peak and hole ($e.Å^{-3}$)	2.425 and -0.811	1.177 and -0.931	2.432 and -0.867	5.056 and -3.570
CCDC No.	2154940	2154941	2154942	2154943

Structures were refined on F_0^2: $wR_2 = [\Sigma[w(F_0^2 - F_c^2)^2] / \Sigma w(F_0^2)^2]^{1/2}$, where $w^{-1} = [\Sigma(F_0^2)+(aP)^2+bP]$ and $P = [\max(F_0^2, 0)+2F_c^2]/3$

Table S4: Selected bond lengths (Å) and bond angles (°) of mononuclear and azido complexes.

Complexes	**1**	**2**	**3**	**4**	**5**	**6**	**8**	**9**
M(1)-CNT	1.661	1.653	1.660	1.770	1.781	1.772	1.799	1.792
M(1)-N(1)	2.113(3)	2.1287(19)	2.1067(12)	2.115(2)	2.124(4)	2.128(6)	2.128(11)	2.111(6)
M(1)-Cl(1)	2.4053(9)	2.4045(7)	2.4193(4)	2.3963(8)	2.4107(10)	2.413(2)	2.413(3)	2.406(4)
M(1)-Cl(2)	2.4085(9)	2.4107(7)	2.4284(4)	2.4063(8)	2.4107(10)	2.422(2)	2.413(3)	2.412(3)
N(1)-M(1)-Cl(1)	86.25(8)	86.04(6)	86.29(3)	88.20(6)	88.64(8)	89.33(18)	89.5(8)	87.4(4)
N(1)-M(1)-Cl(2)	86.88(8)	87.17(6)	87.25(4)	86.53(6)	88.64(8)	87.66(18)	84.3(8)	84.88(19)
Cl(1)-M(1)-Cl(2)	87.35(3)	87.58(3)	86.177(14)	93.03(3)	89.44(6)	88.92(7)	87.37(14)	86.8(2)

Complexes	**25**	**26**	**28**	**30**
M(1)-CNT	1.769	1.768	1.776	1.786
M(1)-N(1)	2.119(2)	2.116(2)	2.103(4)	2.115(7)
M(1)-N(3)	2.122(2)	2.123(2)	2.131(4)	2.09(2)
M(1)-N(6)	2.130(2)	2.129(2)	2.115(4)	2.165(16)
N(1)-M(1)-N(3)	83.92(8)	83.49(8)	82.14(15)	81.4(5)
N(1)-M(1)-N(6)	83.73(8)	83.41(8)	82.31(15)	79.1(12)
N(3)-M(1)-N(6)	86.83(10)	86.44(9)	84.50(16)	81.6(2)

CNT represents the centroid of the *p*-cymene/Cp* ring and (M = Ru, Rh and Ir)

Table S5: Selected bond lengths (Å) and bond angles (°) of binuclear complexes.

Complexes	**13**	**14**	**17**	**18**
M(1)-CNT	1.663	1.776	1.772	1.788
M(2)-CNT	1.692			
M(1)-Cl(1)	2.4111(8)	2.448(3)	2.3936(3)	2.4062(16)
M(2)-Cl(2)	2.4083(8)			
M(1)-N(1)	2.116(3)	2.117(8)	2.1243(11)	2.131(5)
M(2)-N(3)	2.121(3)			
M(1)-S(1)		2.451(3)	2.4237(4)	2.4335(17)
M(1)-S(2)	2.4316(8)			
M(2)-S(1)	2.4190(8)			
Cl(1)-M(1)-N(1)	88.59(8)	88.8(2)	90.34(3)	86.75(15)
N(1)-M(1)-S(1)		92.1(2)	90.39(3)	91.57(15)
Cl(1)-M(1)-S(1)		94.00(11)	92.968(12)	92.11(6)
N(1)-M(1)-S(2)	87.42(8)			
Cl(1)-M(1)-S(2)	92.31(3)			
Cl(2)-M(2)-S(1)	87.64(3)			
N(3)-M(2)-S(1)	89.66(7)			
Cl(2)-M(2)-N(3)	88.06(7)			

CNT represents the centroid of the *p*-cymene/Cp* ring and (M = Ru, Rh and Ir)

Table S6: Antibacterial activity (Agar well) of tested compounds.

S. No.	Compound Names	Zone of inhibition (Diameter in mm) at conc. 200 µg			
		E. coli	***P. aeruginosa***	***S. aureus***	***B. thuringiensis***
1	Complex 1	-	-	17±1	-
2	Complex 2	-	-	18±1	16±1
3	Complex 3	-	-	-	16±1
4	Complex 4	-	-	-	15±1
5	Complex 6	-	-	-	18±1
6	Complex 7	-	-	20±1	16±1
7	Complex 8	-	18±1	18±1	21±1
8	Complex 9	-	18±1	18±1	17±1
9	Complex 14	-	-	21±1	19±1
10	Complex 15	-	-	22±1	20±1
11	Complex 16	-	-	21±1	19±1
12	Complex 17	-	-	22±1	22±1
13	Complex 18	-	-	21±1	20±1
14	Complex 19	-	-	22±1	22±1
15	Complex 20	-	-	22±1	20±1
16	Complex 21	-	-	22±1	22±1
17	Kanamycin (+ve control)	22±1	21±1	23±1	22±1

E. coli = *Escherichia coli*; *P. aeruginosa* = *Pseudomonas aeruginosa*; *S. aureus* = *Staphylococcus aureus*; *B. thuringiensis* = *Bacillus thuringiensis*, NI: No Inhibition and Data are means (n = 3) ± Standard deviation of three replicates.

Table S7: DPPH radical scavenging activity of tested compounds.

Compound	% DRSA	Standard Error
AA	100	0
Ligand 1	4.5	±0.7
Ligand 2	6.1	±1.1
Ligand 4	9.25	±0.04
Ligand 5	11.60	±0.22
Complex 2	6.5	±0.1
Complex 3	2.5	±0.2
Complex 7	16.9	±0.1
Complex 8	35.6	±1.1
Complex 9	22.1	±3.3
Complex 10	17.59	±0.16
Complex 11	24.47	±0.14
Complex 12	15.46	±0.18
Complex 13	16.04	±0.32
Complex 15	5.51	±0.09
Complex 16	1.39	±0.17
Complex 17	9.51	±0.16
Complex 18	22.88	±0.08
Complex 19	19.68	±0.23
Complex 20	17.46	±0.17
Complex 21	19.48	±0.44

*AA: Ascorbic acid